Vysoké učení technické v Brně
Fakulta strojního inženýrství
Ústav konstruování

Brno University of Technology
Faculty of Mechanical Engineering
Institute of Machine and Industrial Design

MAGNETORHEOLOGICAL SUSPENSION DAMPER FOR SPACE APPLICATION

Ing. Michal Kubík
Autor práce
Author

Doc. Ing. Ivan Mazůrek, CSc.
Vedoucí práce
Supervisor

Dizertační práce
Dissertation Thesis

Brno 2017

STATEMENT

I hereby declare that I have written the PhD thesis Magnetorheological suspension damper for space application on my own according to advice of my supervisor Doc. Ing. Ivan Mazůrek, CSc. and using the sources listed in references.

Brno, _____ .....

Michal Kubík

BIBLIOGRAPHICAL REFERENCE

KUBÍK, M. Magnetorheological suspension damper for space application. PhD thesis. Brno University of Technology, Faculty of Mechanical Engineering, Institute of Machine and Industrial Design. Supervisor: Doc. Ing. Ivan Mazůrek, CSc.

ACKNOWLEDGEMENT

I would like to thank my supervisor Doc. Ing. Ivan Mazůrek, CSc. and whole department of condition monitoring for their support and advice during my doctoral study. Special thanks must go to my wife and parents for their support during my Ph.D. study.

ABSTRACT

The present thesis deals with the development of the MR suspension damper for space application. Some important requirements for semi-active control damper for space application are a hermetic separation of operating fluids from the rest of the launch vehicle and short response time of damping element. Those requirements meet magnetorheological damper with bellows unit, according to state of the art. Magnetic circuit of the MR damper was made from ferrite material which allows to rapidly decrease the response time of the MR damper. Hermeticity was ensured using a bellows unit. Design of this type of damper exhibits a lot of design limitations. The developed MR damper with ferrite magnetic circuit achieved response time 4.1 ms and dynamic force range 8. During the design of the MR damper for space application, a new method for design of semi-actively control MR damper with short response time were searched. Specifically, the method for elimination of eddy currents in magnetic circuit of MR damper, magnetostatic and transient magnetic model, CFD model of bypass gap, hydraulic model of MR damper and their experimental verification. The presented methods allow for the design new MR damper for space application lighter, with short response time and with higher dynamic force range.

KEYWORDS

Magnetorheological damper, magnetorheological fluid, short response time, MR damper, elimination eddy currents, bypass gap of MR damper

ABSTRAKT

Dizertační se práce se zabývala vývojem magnetoreologického (MR) tlumiče odpružení pro kosmonautiku. Dle současného stavu poznání jsou důležitými parametry pro semi-aktivně řízený tlumič pro kosmonautiku hermetické oddělení pracovní kapaliny od zbytku nosiče a krátká časová odezva tlumícího elementu. Těmto požadavkům vyhovuje magnetoreologický tlumič s vlnovcovou jednotkou. Magnetický obvod MR tlumiče pro kosmonautiku byl vyroben z feritového materiálu, který umožnil výrazně snížit časovou odezvu. Hermetičnost byla zajištěna použitím vlnovcové jednotky. Konstrukce takového typu tlumiče ovšem přináší celou řadu problémů. Vyvinutý MR tlumič s feritovým magnetickým obvodem dosahoval časové odezvy 4.1 ms a dynamického rozsahu 8. Během konstrukčních prací na MR tlumiči pro kosmonautiku byly hledány nové metody pro konstrukci semi-aktivně řízeného MR tlumiče s krátkou časovou odezvou. Konkrétně se jednalo o metodu eliminace vířivých proudů v magnetickém obvodu MR tlumiče, magnetostatický a transietní magnetický model, CFD model obtokové štěrbiny, hydraulický model MR tlumiče a jejich experimentální verifikace. Tyto nové metody umožní konstrukci MR tlumiče pro kosmonautiku lehčí, s nižší časovou odezvou a vyšším dynamickým rozsahem.

KLÍČOVÁ SLOVA

Magnetoreologický tlumič, magnetoreologická kapalina, krátká časová odezva, MR tlumič, eliminace vířivých proudů, obtoková štěrbina MR tlumiče

CONTENT

1 INTRODUCTION

In recent years, an average 87 launches of launch vehicles were carried out. The communication or the researcher satellites were launched most often. Vibration and shock loads during the shipment may cause destruction of optics, electronics, and other sensitive equipment of the satellites. To compensate for the hard dynamic environment, satellites must be designed to high dynamic level [1], which rapidly increases the cost and weight of satellite components. An interesting method is to reduce dynamic loads using a vibration isolation system which is between the launch vehicle propulsion and the payload. From the point of view efficiency isolation, weight or cost, the semi-active control vibration isolation system appears a suitable option. The decrease of the dynamic load to the frequencies up 25 Hz is important for most design of satellites. It is necessary to have a damper that can quickly change its damping force (response time of the damper) for effective semi-active control. Specifically, for frequency 25 Hz, the response time 4 ms is needed. Until recently, the design of this type of damper was unknown. In 2013, Strecker at al. published the design of the magnetorheological (MR) damper with response time 1.5 ms. The MR damper works with magnetorheological fluid.

The MR fluid is composed of microscale ferro-magnetic particles, non-magnetic carrier oil, and additives [2]. In the presence of magnetic field, the MR fluid changes the rheological properties, especially apparent viscosity: from low value (fluid) to high value (pseudo-solid). The first mention of MR fluid comes from Rabinov and Winslow [3] in the 1940s. However, new generations of MR fluids and MR devices were intensely developed in the 1990s. Kordonsky et al. [4] published the application of MR fluids for various technical devices, or Gorodkin et al. [5] patented a magnetorheological valve. At the turn of the 20th and 21st centuries, a wide range of application of MR fluids appeared in a variety of technical devices. The most successful application of MR fluid was a magnetorheological (MR) damper. The company Lord developed the MR damper for the suspension of the truck or bus seats [6]. Cadillac or Ferrari offered MR dampers for suspension of their cars [7].

Figure 1 MR dampers (left) automotive [8], (middle) cable stay bridges [9], (right) damper for earthquake hazard mitigation [10]

MR dampers were also used in civil engineering structures for mitigation of damages caused by earthquake [10] or for cable stay bridges (Franjo Tudjman Bridge in Dubrovnik) [9] in Figure 1. The issue of decreasing the response time of damping

force of MR damper was intensively examined at the beginning of the 21st century. It was found that inductance of the coil, response time of MR fluid, and eddy currents generated in the magnetic circuit influence the response time of MR damper [11]. Strecker at al. [11] from Brno University of Technology published their finding that the response time of damping force of MR damper can by reduced by a suitable choice of the magnetic circuit material and by a suitable current controller.

The MR damper with short response time opens up new possibilities of using the MR damper for progressive vibration isolation systems, such as the vibration isolation system of the launch vehicle. However, the published design of MR damper by Strecker at al. is not suitable for space application. The design process of MR damper with short response time suffers from a number of limitations. It will be necessary to solve lot of technical problems or to propose completely new methods for the design of MR damper with short response time. The design of demonstrator of semi-active control of the magnetorheological damper for space application is main aim of present thesis.

2 STATE OF THE ART

2.1 Vibration isolation systems

Mechanical vibrations are generated due to the imbalance of rotating and reciprocating components (rotors, electric motors, combustion engines), impact forces, pressure loadings at surfaces due to the winds or acoustic noises, etc. [12]. These vibrations are undesirable in most devices; therefore, a vibration isolation system is used for their elimination. These systems are usually composed of the springs that accumulate energy, and the dampers that dissipate the energy from system [13]. Vibration isolation systems are located between the source of vibration and the isolated devices. Washing machines [14], seats of trucker [15] of airplane engine are examples of typical application (Figure 2) of vibration isolation system. The target parameter, which is used to quantify the performance of the vibration isolation system, is the transmissibility (usually acceleration transmissibility) between the source and the isolated device. The acceleration transmissibility is given by the ratio of accelerations of isolated device and the source of vibration. In the next sections, vibration isolation systems are divided according to the control of damping element.

Figure 2 Vibration isolation systems (launch vehicle, seats of trucker [15], washing machine [14], airplane engine [16])

2.1.1 Passive vibration isolation system

In this system, damping is given from the "factory" and cannot be changed during the lifetime of vibration isolation system [17]. The material (silentblock) or viscous a damping (hydraulic damper) can be used. If the damper is manufactured with a high value of damping (Figure 3, right, passive), the acceleration transmissibility is relatively low in the vicinity of resonance frequency but the acceleration transmissibility decreases slowly at higher frequencies. If the damper is manufactured with a low value of damping (Figure 3, left, passive), the acceleration transmissibility is considerable in the vicinity of the resonance frequency. However, a decrease of acceleration transmissibility occurs at higher frequencies. The setup of damping level in passive vibration isolation system is a trade-off between the acceleration transmissibility at resonant frequency and the acceleration transmissibility at higher frequencies [18]. These types of dampers are used in numerous car suspensions or in train bogies because they are cheap and reliable.

2.1.2 Adaptive control of vibration isolation system

A level of damping can be changed in adaptive vibration isolation system; this change of damping level is relatively slow (tens of seconds). The adaptive systems are commonly used in bogies of rail vehicle [19, 20] or in car suspensions [21]. The adaptive control function of damper can be described on the car suspension. Use of adjusters on the damper can set the level of damping in the halted car. The advanced dampers are adjustable during the ride by the driver. Specifically, in the car, different driving modes (sport, comfort ...) can be chosen. Some dampers allow for the change of damping level during the car cornering. This type of dampers is offered e.g. by the company ZF Sachs as a hydraulic CDC shock absorber [21]. Some car makers also offer magnetorheological shock absorbers from the company BWI [8].

2.1.3 Semi-active control of vibration isolation system

The semi-active control of vibration isolation system is a real-time control of damping element by a control algorithm, which switches a damping level at the appropriate time. The ECU (electronic control unit) and sensors (acceleration sensor, etc.) are necessary for semi-active control. An appropriately selected control algorithm has an influence on the performance of vibration isolation system. One of the most commonly used control algorithms to minimize the acceleration transmissibility is Skyhook [22]. The name ‘‘Skyhook’’ derived from the fact that a passive damper hooked to an imaginary inertial reference point [23].

The algorithm Skyhook has many versions which vary according to the properties of the damper. Krasnicki [24] proposed a so called on/off type skyhook control strategy in 1980. The on/off algorithm Skyhook is frequently used because it provides a bi-state control of damping level where this level switches between the minimum (Off) and the maximum (On) damping force. The acceleration transmissibility of this type of control is shown in Figure 3 (SA-2). Another type of algorithm – a continuous algorithm Skyhook - is also frequently used. In this case, the damping element must allow for a continuous change of damping level. The acceleration transmissibility of this type of control can be seen in Figure 3 (SA-1). However, there is a number of other algorithms, e.g. the on/off balance control, which also include the influence of the spring.

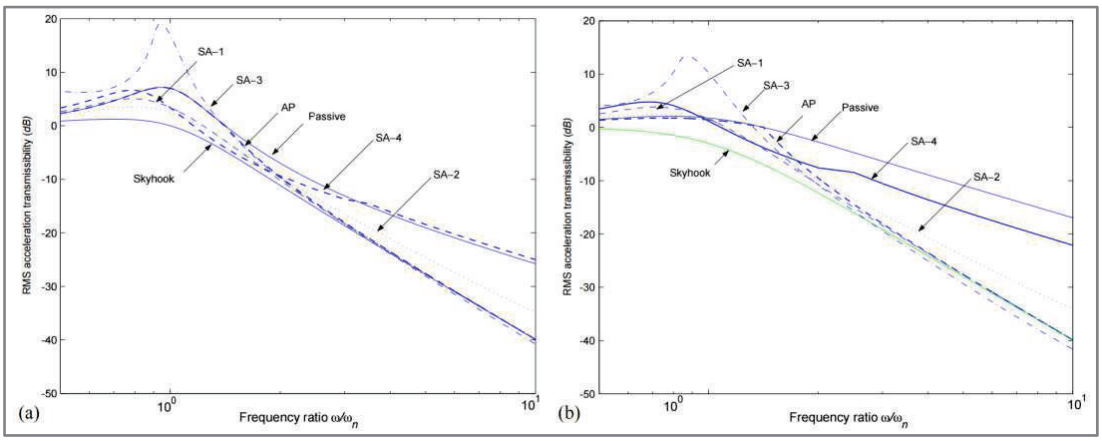

Figure 3 Comparison of transfer ratio a) low damping b) moderate damping [23]; SA-2 on/off skyhook control, SA-1 continuous skyhook control, skyhook with zero off damping force

An important parameter of the damper for semi-active control is the time needed for the rise or drop of damping force on the control signal (the response time of damper) [25]. A long response time limits the control of vibration isolation system at higher frequencies (performance decrease). Eslaminasab [26] deals with the influence of damper response time of vibration isolation system on the acceleration transmissibility using a mathematical model. The acceleration transmissibility with the response time of 1 ms is close to an ideal system [26]. A small reduction of the response time (e.g. from 2 ms to 1 ms) has a significant impact on transmissibility. Therefore, the damper with short response time and Skyhook control algorithm seems to be the best vibration isolation system based on the damping principle. The design of electro-hydraulic damper has the lowest response time of about 15 ms [19]. An interesting candidate for the use in these systems is a magnetorheological damper which provides a lower response time than the electro-hydraulic damper.

2.2 Vibration isolation system for space application

Satellites are very important products used for many purposes, such as communications, navigation, or weather forecasts. Similarly to other products, the satellite must be designed, manufactured, tested and shipped. However, the shipment of satellite is more complicated than that of all other products [1]. Vibration and shock loads during the shipment may cause destruction of optics, electronics, and other sensitive equipment. To compensate for the hard dynamic environment, payloads must be designed to high dynamic level [1], which rapidly increases the cost and weight of payload components. An interesting alternative is to reduce dynamic loads using a vibration isolation system which is between the launch vehicle propulsion and the payload [27]. Nowadays, the payload is connected to the launch vehicle by passive cone adapter made of composite or similar materials [28] (Figure 4).

Figure 4 Launch vehicle composite cone adapter [29]

This version is reliable and relatively cheap. Another significant advantage is its relatively low weight. However, for some types of payload, the elimination

of vibration by composite cone of launch vehicle is insufficient. Therefore, a lot of companies are developing progressive vibration isolation systems. The company Moog developed the soft ride system. This technology is based on the damping flexure element (Figure 5). Stiffness and the damping are sized to mission-specific requirements [1].

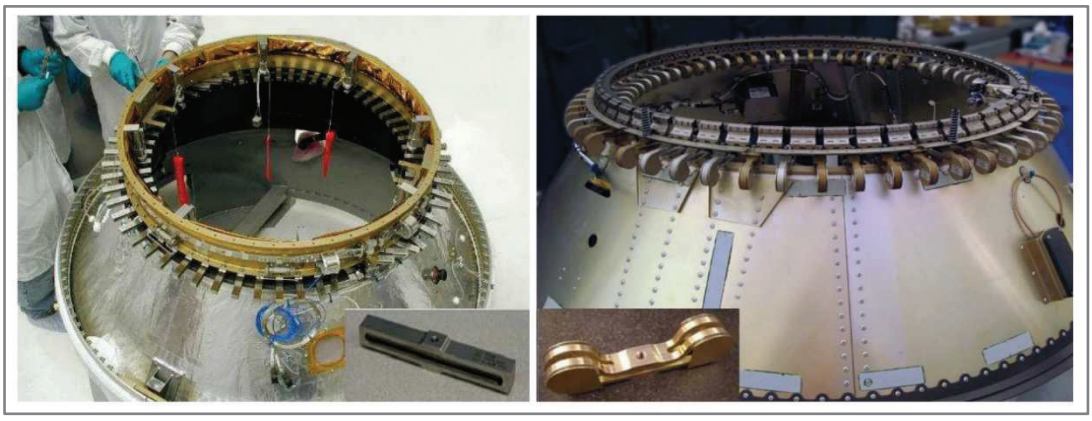

Figure 5 The soft ride system UniFlex (left), soft ride system OmniFlex (right) [1]

The company Honeywell developed the passive vibration isolation system ELVIS (Evolved Launch Vibration Isolation System) based on patented hydraulic D-Struts [30, 31] (Figure 6). The ELVIS provides a better isolation and damping to protect the sensitive equipment during the launch than the launch vehicle composite cone or soft ride system. The D-Strut system was originally developed for satellite reaction wheel in Hubble Space Telescope [32]. ELVIS is composed of several damping and spring struts and adapters for system connectivity [33].

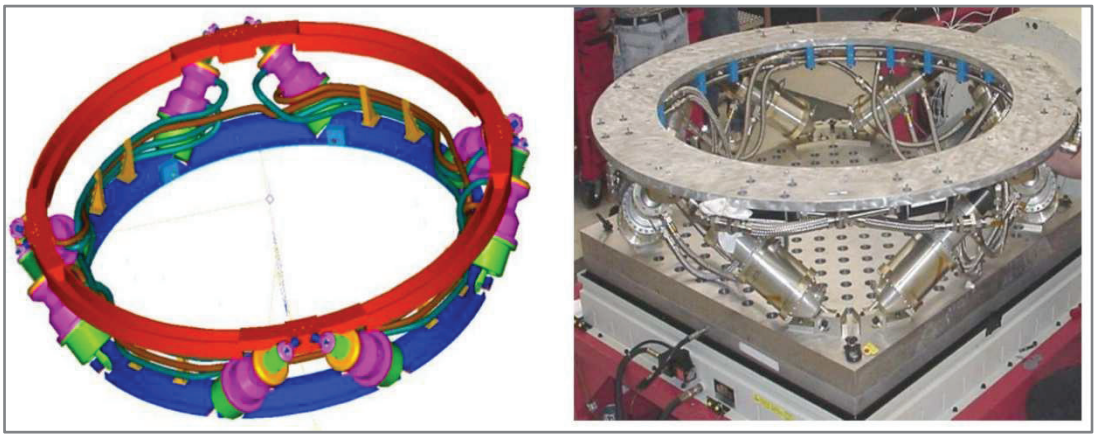

Figure 6 Vibration isolation system ELVIS [34], [33]

2.2.1 D-Strut system

The D-Strut is composed of metal bellows (Figure 7 408, 412), flanges (Figure 7 404, 406) and damping annulus (Figure 7 409). The primary and the secondary bellows are connected via the fluid path of damping annulus where hydraulic oil flows while primary bellows are compressed (the damper C_A). The primary and secondary bellows substantially provide the radial stiffness K_A and volumetric stiffness K_B. Typically, the primary and secondary bellows are selected such that the

volumetric stiffness K_B is in the range of from K_A to ten times K_A [35]. This configuration is a three-parameter vibration isolation system (a relaxation isolator [36] or an elastically connected damper [17]).

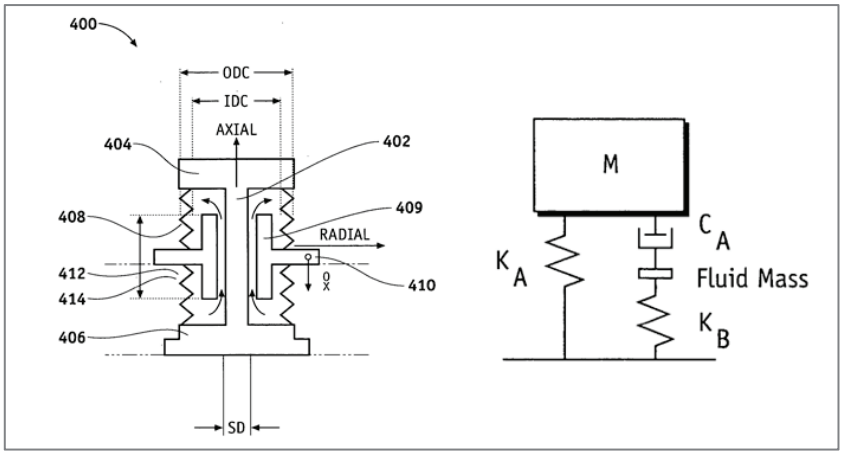

Figure 7 D-strut (left), three parameter isolation system (right) [31]

A two-parameter system has a single spring in the parallel with the damper. In addition, three-parameter system has another spring which is connected to with the damper in series. Figure 8 shows the difference between these two systems [37]. The main advantage of three-parameter vibration isolation system in comparison with two-parameter vibration isolation system is its lower acceleration transmissibility at isolation frequencies with the same damping level (Figure 8).

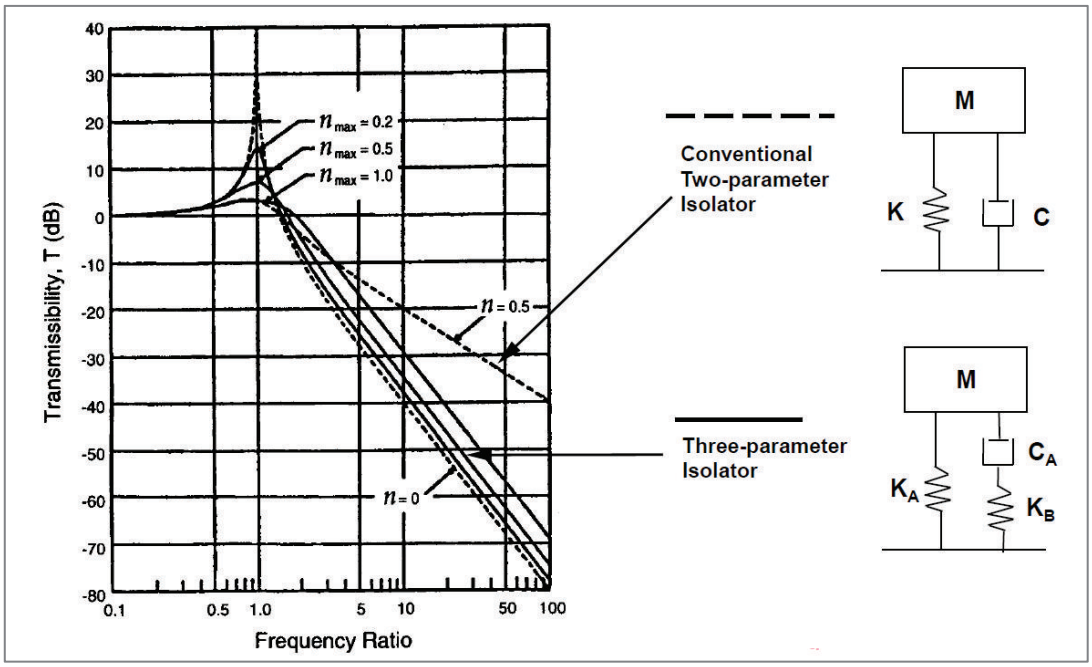

Figure 8 Comparison of two-parameter (dotted line) and three-parameter (solid line) system [37]

The design of the first generation of passive three-parameter vibration isolation system D-Strut is shown in Figure 9 [37]. This system is composed of two primary bellows, two secondary bellows, annulus, piston, flanges, and fluid.

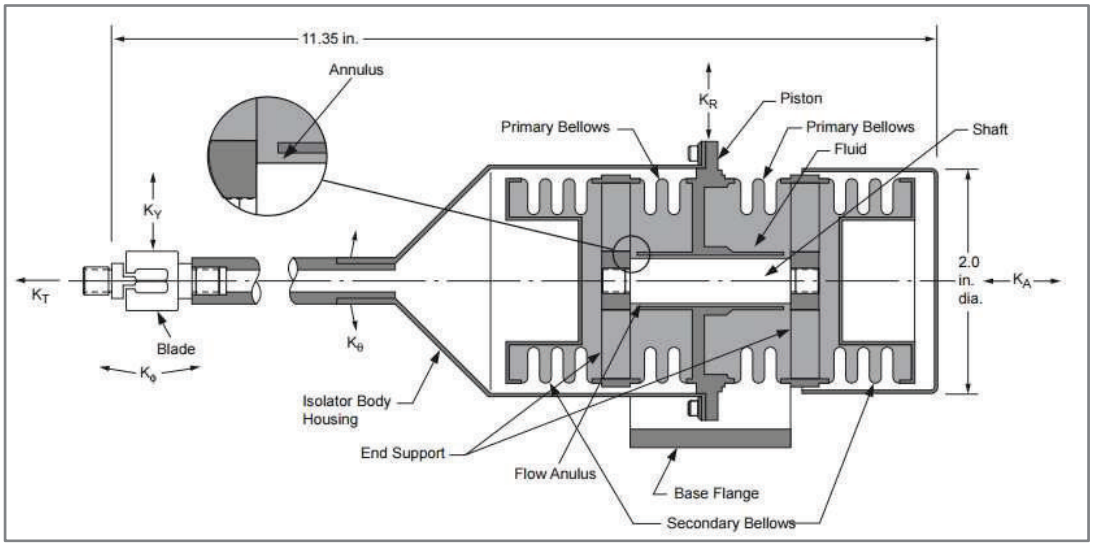

Figure 9 Three-parameter vibration isolation system D-Strut [37]

The next step in the development of this technology was the active control of hybrid D-Strut (Figure 10). This system contains a voice coil, payload accelerometer, and a base accelerometer for the control of voice coil. The hybrid D-Strut represents an active control of three-parameter vibration isolation system and provides a lower transmission of vibration than the passive D-strut. However, there is a risk of destabilization of vibration isolation system by inadequate control [32].

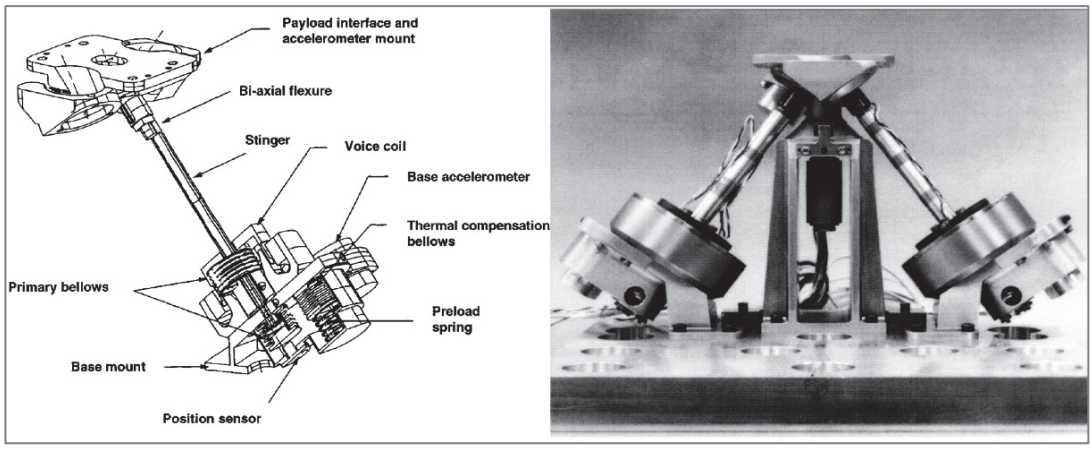

Figure 10 Three-parameter hybrid D-Strut vibration isolation system with voice coil [32]

A future research step will be to use a semi-active control damper in vibration isolation system. An interesting candidate is the use of magnetorheological technology.

2.2 Magnetorheological fluid

Magnetorheological (MR) fluid is a suspension of micro-scale, non-colloidal ferromagnetic particles in a non-conductive carrier fluid and additives [38]. The MR fluid exhibits a rapid change of rheological behaviour under an external magnetic field. Ferromagnetic particles in MR fluid form chain-like structures in the direction of magnetic field which rapidly increases yield stress of MR fluid (Figure 11). The

value of yield stress is strongly dependent on the level of applied magnetic field. An evolution of yield stress in the MR fluid with external magnetic field is a basic feature of MR technology and is usually called the Magnetorheological (MR) effect [39].

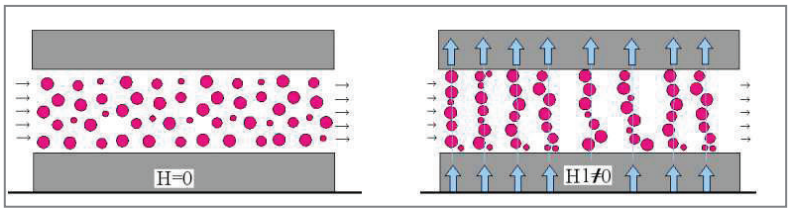

Figure 11 Magnetorheological effect [40]

The type of MR fluid and the level of magnetic field affect the yield stress of MR fluid. These fluids differ from each other by particles size, particles material, volume of particles, carrier fluid, or additives. The particles size is typically in the range from 1 μm to 10 μm [38]. A commonly used material of particles is the reduced carbonyl iron powder (CIP) because it exhibits good magnetic properties (high magnetic saturation B = 2.1 T) and low magnetic remanence [2, 38]. The low magnetic remanence improves dispersibility of particles in the carrier fluid which should have low viscosity, excellent lubricity, chemical compatibility with material particles and good antioxidant properties [2]. This can be find in PAO (polyalphaolefin) [38], a commonly used material. The additives in MR fluid have an impact on particle settling, friction, wear or durability. Main limiting factors of MR fluid are magnetic saturation and abrasiveness. The typical rheological and magnetic properties of commercially available MR fluids are listened in Tab. 1.

Tab. 1 Typical properties of MR fluid

Property of MR fluid	Typical value
Viscosity	0.04-0.8 Pa.s (40 °C)
Density	2200 – 3600 kg/m^3
Solid content by weight	from 72 % to 86 %
Saturated yield stress	30 - 60 kPa
Operating temperature	-40 to 130 °C
Relative permeability	from 3 to 10

In the MR controllable devices, typical operating modes have been identified during the years of their application. The MR fluid operates in flow, shear and squeeze modes (Figure 12); each operating mode has its advantages and disadvantages.

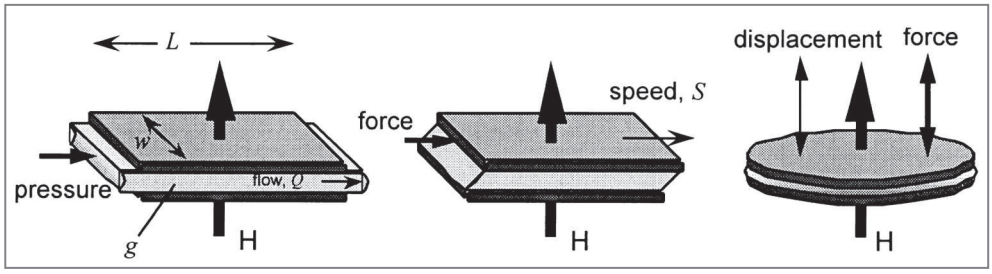

Figure 12 Operating modes; flow (left), shear (in the middle), squeeze (right) [39]

In the flow operating mode, the MR fluid flows between the two stationary parallel plates (Figure 12, left). The magnetic field controls the hydraulic resistance. The flow operating mode is commonly used in automotive industry [41], in civil engineering [10], or in prosthetics [42]. In the shear operating mode, the MR fluid flows between the parallel plates which are in relative movement (Figure 12, middle). In this operating mode, rotary dampers or clutches work [43]. The squeeze operating mode (Figure 12, right) is the last one to describe. In this mode, the parallel plates compress the MR fluid. This mode is used in the devices with high force and small stroke, e.g. tn technical practice, it is used in the MR silentblock [44].

In the space vibration isolation system, the damper stroke is usually in millimeters. Based on this information, the flow operating mode of MR damper is the most appropriate for space vibration isolation system.

2.3 Magnetorheological damper

A magnetorheological (MR) damper or valve is a device which uses a strong and rapid change of yield stress of MR fluid in the direction of magnetic field. The MR damper is composed of piston, bearing and seal, floating piston or diaphragm (with accumulator), and MR fluid [10]. The piston consists of magnetic circuit and electromagnetic coil. There is a gap in the magnetic circuit which is flooded with MR fluid (an annular orifice in the piston usually called the active zone). The piston divides the MR fluid volume between the compression chamber and the rebound chamber. The active zone of the piston unit allows for a flow of MR fluid between the chambers in the piston rod motion. During the flow of MR fluid in the active zone, it is possible to control the value of yield stress (hydraulic resistance) by electric current in the coil. This causes a rapid increase in damping force. The MR damper is mechanically simpler than the traditional design of the hydraulic shock absorber because it does not contain mechanical moving parts (Figure 13). For this reason, the MR damper is noise-free.

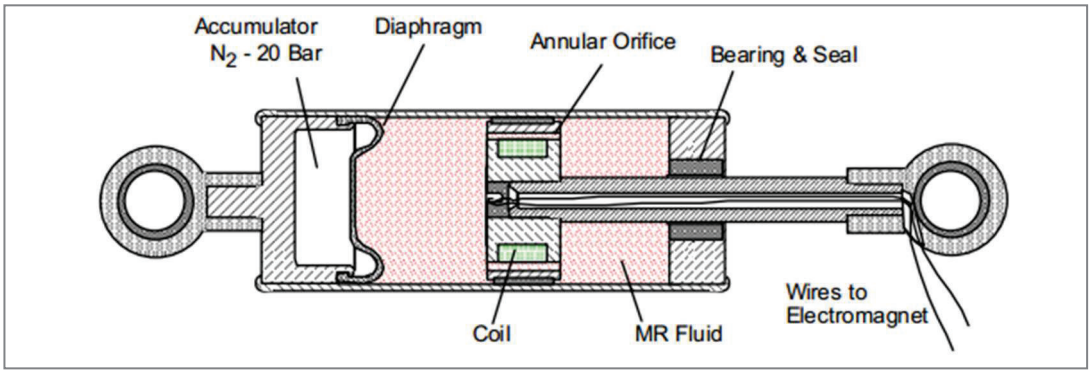

Figure 13 Magnetorheological damper [45]

One of the important characteristics describing the MR damper behaviour is the force-velocity dependency (F-v). The MR damper has an infinite number of F-v dependencies that differ in the supplied current on the coil. For this reason, the F-v dependency of MR damper is often presented as a maximum current in the coil (On-state) and a zero current in the coil (Off-state). A typical damping force of conventional MR damper in On-state has a steep slope at low piston velocity and a gentle slope at high piston velocity (Figure 14, right, blue line) [46]. From this

perspective, the MR damper is similar to the friction damper. The undesired jump in damping force might degrade the comfort in vehicle or other applications [46, 47].

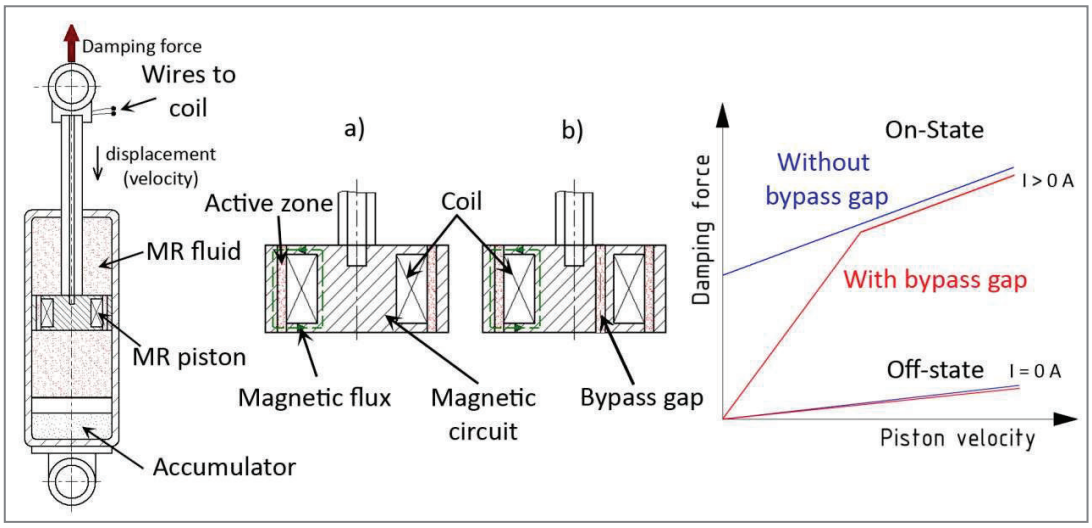

Figure 14 The scheme of the MR damper (left); a) conventional piston unit of MR damper, b) piston unit with bypass gap; F-v dependency (right) in off and on-state without bypass gap (blue) and with bypass gap (red) [47]

A parallel connection of bypass gap to the active zone in the on-state of MR damper decreases the damping force at low piston velocity (Figure 14, right, black line) [47]. The MR fluid can flow through the bypass gap, no matter what the magnetic field is applied in the active zone (On-state). It is assumed that the magnetic field does not affect the bypass gap. The piston with bypass gap can be seen in Figure 14 b).

An important parameter influencing the efficiency of MR damper in the adaptive or semi-active control is a dynamic force range (in some publication set-up ratio). This is defined as a ratio between the damping force in On-state $F_{ON}(v, H)$ (resisting force) and the damping force in Off-state $F_{OFF}(v)$ (uncontrollable force) for the given piston velocity v and the given magnetic flux H as follows [10]:

$$\mathrm{D(v,H)} = \frac{\mathrm{F_{ON}(v,H)}}{\mathrm{F_{OFF}(v)}} = \frac{\mathrm{F_{\tau}(v,H)+F_{uc}(v)}}{\mathrm{F_{uc}(v)}} = 1 + \frac{\mathrm{F_{\tau}(v,H)}}{\mathrm{F_{\eta}(v)+F_f}} \qquad (2.1)$$

The damping force in On-state $F_{ON}(v,H)$ consists of controllable damping force $F_{\tau}(v,H)$ and uncontrollable force $F_{uc}(v)$. The uncontrollable force consists of friction force F_f and viscous force $F_{\eta}(v)$. The friction force is caused by friction of rod guide, wiper seal, and rod seal. A dynamic force range can be significantly influenced by the design of MR damper (friction of seal, geometry, etc.). The higher the value of dynamic force range, the higher the quality of semi-active control [48, 49].

The response time of MR damper also influences the efficiency of semi-active control. The response time of MR damper is the time needed for the rise to 63.3 % (in some publication 95%) of steady state damping force on the control current [25] (Figure 15).

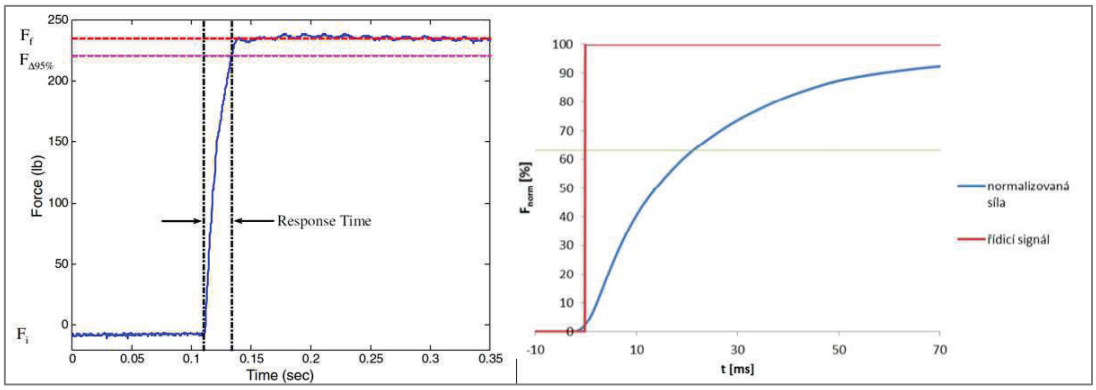

Figure 15 Response time as 95 % of steady-state (left)[10]; The response time as 63.3 % of steady-state (right) [11]

The lower is the value of response time, the higher is the quality of semi-active control that can be achieved [26]. The response time of MR damper is influenced by:

- response time of MR fluid,
- inductance of MR damper coil (response time of exciting current),
- eddy current in coil core (response time of magnetic field in the active zone).

The response time of MR fluid was estimated in the range of 0.45-0.6 ms by Gonclaves at al. [50]. It is obvious that the response time of MR fluid is much shorter than the response time of MR damper (20 ms). Many researchers [11, 51] deal with the response time of exciting current on the coil. With the use of a suitable current controller, it is possible to decrease the response time of exciting current under 0.5 ms [11]. The functional principle of current controller is described in [38]. The most important effect on the response time of MR damper can be observed with eddy currents in the magnetic circuit (the response time of magnetic field in the active zone). Strecker et al. [11] and Maas at al. [52] proposed to use the ferrite material of the magnetic circuit which is magnetically conductive and electrically non-conductive. Strecker et al. [11] measured the response time of MR damper with Epcos ferrite N87 material on the magnetic circuit. The measured response time was about 1.5 ms depending on the piston velocity (Figure 16). However, the ferrite materials exhibit a lower machinability and fragile behaviour. The tensile strength of ferrite material is much lower than that of steel. Another drawback is a three times lower saturation of magnetic field than that of steel, which significantly affects the dynamic force range. The material selection and geometry design affect the dynamic force range and the response time of MR damper.

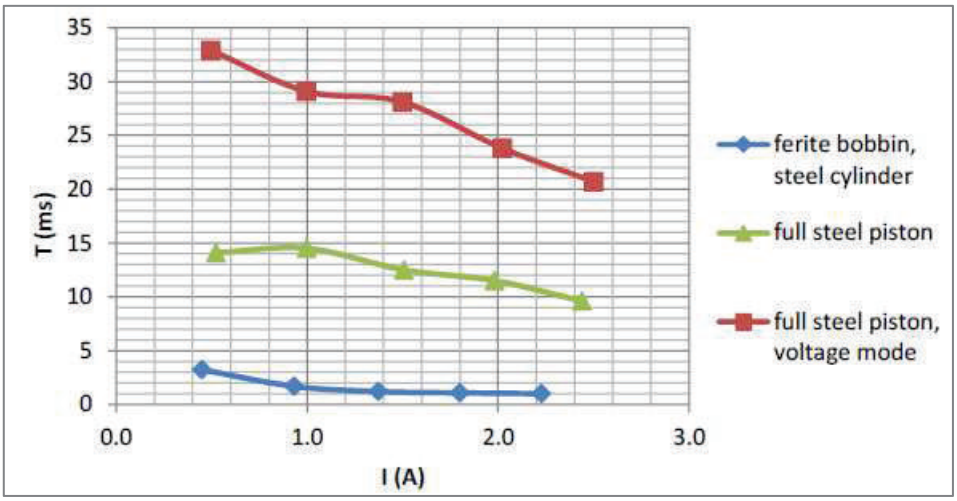

Figure 16 The dependency of response time on the control current for different materials of magnetic circuit [11]; voltage mode and low carbon steel magnetic circuit (red), current mode and low carbon steel magnetic circuit (green), current model of a ferrite bobbin and low carbon steel cylinder (blue)

2.4 Methods for the design semi-active control MR damper

The main goal of this chapter is to describe the methods for design of the semi-active control MR damper. The dynamic force range and the response time of MR damper influence the efficiency of semi-active control. The following chapters are divided as follows: mechanical, magnetic, magnetorheological, and hydraulic sections. The influence of each section on the dynamic force range and the response time is discussed.

2.4.1 Mechanical section

A method of how to separate (to seal) the MR fluid from the environment is the fundamental part of mechanical section. A sealing method has an influence on the dynamic force range of MR damper because it causes an increase on Off-state forces.

2.4.1.1 Separation of MR fluid from the environment

Many design types of seals used in the hydraulic damper differ in a number of factors such as durability, leakage risk, friction losses, or wear [17]. The high-pressure resistance (up to 5 MPa in the traditional damper design) and minimum Coulomb friction losses are the basic requirements for all types of seals. The Coulomb friction losses decrease the dynamic force range. Interestingly, there are only a few references in the literature related to the methods or tests of the MR damper seal [53, 54]. This chapter is divided into: rubber blade seal, metal bellows, and magnetic seal.

Rubber blade seal

A choice of sealing design is influenced by the application and the type of sealing media. Piston rod seals used in hydraulic dampers are different from the piston rod seals in a hydraulic cylinder. Hydraulic systems (cylinder or pump) require a maximum system tightness (small leakage); however, the Coulomb friction losses are insignificant. In the hydraulic damper, it is important to minimize Coulomb friction losses.

A selection of piston rod seal for the MR damper is more complicated because the MR fluid contains tiny abrasive particles. The issue of the Coulomb friction losses of the piston rod seal becomes more important in the case of semi-active control MR damper. Coulomb friction losses significantly decrease the dynamic force range. In the design of MR damper, the piston rod seal is placed next to the piston rod guide. So far, according to the available information, no publication has been devoted to the design of the piston seal operating in the MR fluid; only a few patents can be found. The patent of company Delphi (BWI group) [55] describe two types of piston rod seal. The first type, a single-edged piston rod seal (Figure 17, left, 30), is in contact with MR fluid while the second type, a double-edged rod seal (Figure 17, left, 26), is placed behind the piston rod guide (Figure 17, left, 32). The carrier fluid of MR fluid lubricates the piston rod guide and seals. The MR damper contains a porous material (porosity of about 250 nm) which allows for leakage of carrier fluid of MR fluid to the piston rod guide (the patent of company Delphi [56]). This is an elegant way how to ensure lubrication throughout the lifetime of the MR damper (Figure 17, right, 38).

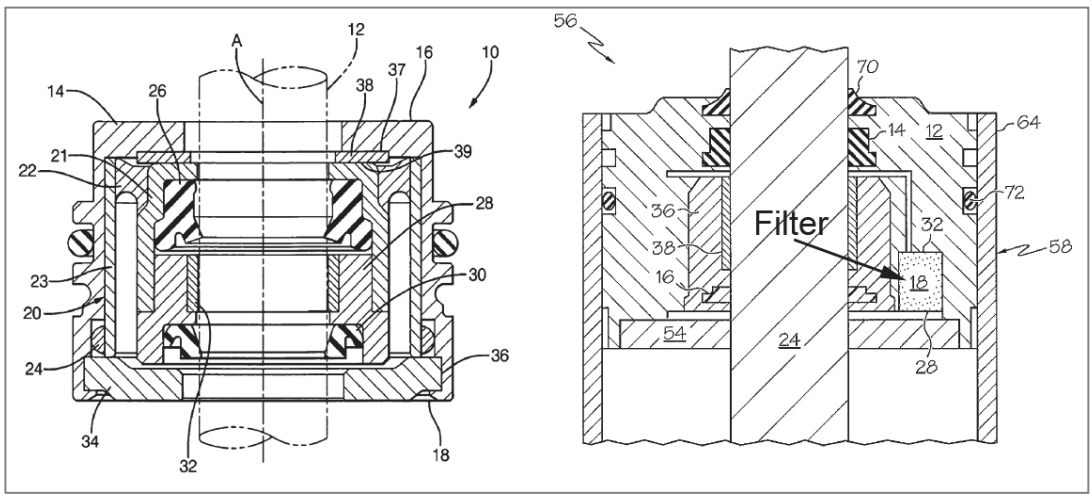

Figure 17 An Arrangement of piston rod seal (left) [55]; lubrication of piston rod guide by filter [56]

Wear of material of piston rod seal (polyurethane) was studied by Iyengar [53], being tested in: hydraulic oil, in carrier fluid of MR fluid (base oil 1), in carrier fluid of MR fluid which contains a thixotropic agent, and in MR fluid. The volume wear of sealing material is higher in the MR fluid than in the hydraulic oil. The material with the lowest wear volume in hydraulic oil does not exhibit the lowest wear volume in the MR fluid. It cannot be simply assumed that the optimal sealing material for the hydraulic fluid will be optimal for the MR fluid (Figure 18). The wear volume in MR fluid is significantly influenced by the temperature (Figure 18). It should be noted that there is no publication referring to the durability of piston rod seal operating in the MR fluid.

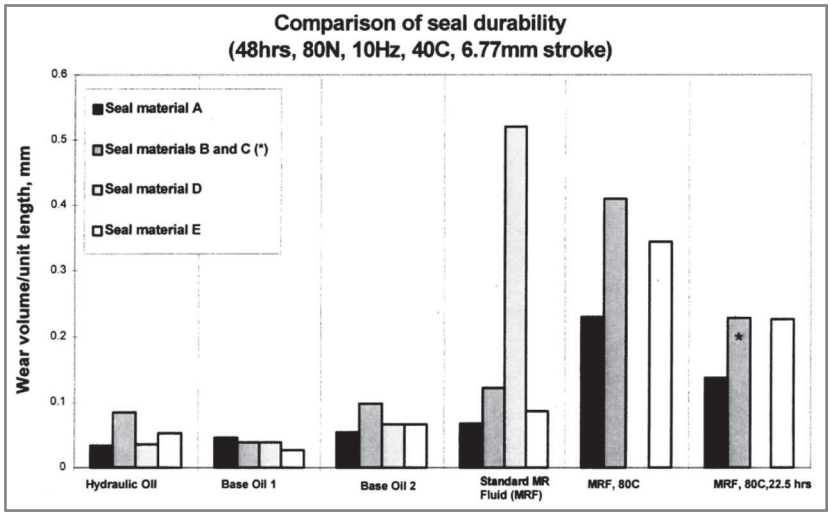

Figure 18 Comparison of wear volume of different materials in different fluids [53]

Metal bellows

Bellows are flexible shell components usually made of stainless steel by welding or forming (Figure 20). A design of damper with bellows, which eliminate Coulomb friction losses of piston rod sealing, exists [57]. The hydraulic damper with bellows was used for the bridge Millennium Footbridge in London (Figure 19) or in the above-mentioned design of the D-strut.

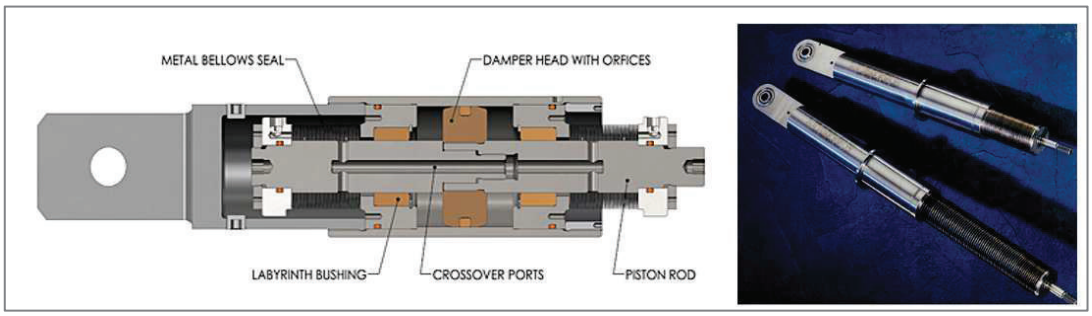

Figure 19 The hydraulic damper with bellows; design for Millennium Footbridge in London [57]

By compressing primary bellows, the hydraulic fluid flows through crossover ports to the secondary bellows. The flow of fluid creates a damping force so the seal movement is not needed. An important advantage of this type of seal is no leakage of the hydraulic fluid and no friction losses.

Figure 20 Metal bellows [58]

However, a disadvantage of the bellows is a relatively low stiffness which creates an inflation due to internal pressure. This may lead to a complete elimination of fluid flowing due to the bellows flexibility. Other disadvantages are a high price and a relatively small stroke.

Magnetic seal

The MR damper works with magnetic fluid which can be used for sealing. The magnetic fluid seal is composed of magnetic circuit, sealing shaft, and magnetic fluid (Figure 21). The design of magnetic shaft seal with ferrofluid was published in [59], [60]. This type of seal uses the ferromagnetic fluid which contains nanoparticles (single-domain particle); this seal variant has a low pressure drop (maximum of 1 bar).

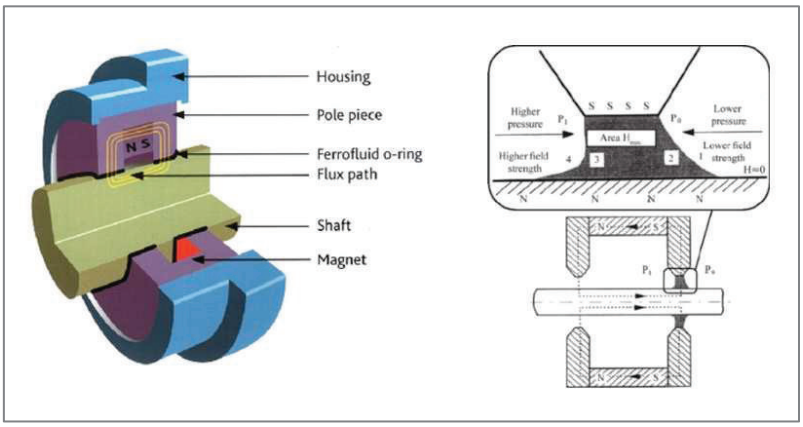

Figure 21 The ferromagnetic shaft seal (left) [60], location magnetic fluid in magnetic fluid seal (right)

Some authors use a magnetorheological fluid instead of ferrofluid. The MR fluid contains micrometric particles (multi-domain) which create a mutual magnetic interaction between; this causes the higher pressure drops. Kordonski et al. [61] and Matuszewski et al. [60] dealt with the design of magnetorheological shaft seal. A disadvantage of this concept is a considerable loss of moment due to the "tearing" of the particle chains during rotation. According to the available information, the concept of a magnetorheological seal for sliding motion is not mentioned in the literature. This could be a challenging field for future research.

2.4.2 Magnetic section

The magnetic design of MR damper affects the response time and the dynamic force range of MR damper. Magnetic models are significant for the study of influence of geometry and material selection on the response time and the dynamic force range of MR damper. The published magnetic models are described in the chapter below. Magnetic and electric properties magnetic circuit material have an impact on the dynamic force range and the response time of MR damper. Eddy currents in the magnetic circuit result in a longer response time of MR damper. The methods for elimination of eddy currents are described in the following section.

2.4.2.1 Methods for elimination of eddy currents in magnetic circuit

Eddy currents are loops of electrical currents induced by changing of magnetic field. Eddy currents flow in loops perpendicular to the magnetic field; they can be inducted by time-varying of the magnetic field [62]. Eddy currents create the magnetic field opposite to the magnetic field in the magnetic circuit. A superposition method sums these fields; therefore, the resulting field is lower. This has a major effect on the increase in the response time of magnetorheological damper. The electromotive force U is created due to a rapid change of the magnetic flux Φ (fast regulation).

$$U = \frac{d\Phi}{dt} \tag{2.2}$$

The magnitude of the eddy current can be calculated from the Ohm law and the electrical resistance of the material of magnetic circuit because the eddy currents are similar to the electric current from their physical nature.

$$I = \frac{U}{R} \tag{2.3}$$

According to the above, the elimination of eddy currents is possible by:

- use of the material with high electric resistivity (increase R),
- appropriate geometric adjustment of the magnetic circuit, which increases the electric resistance in the direction of flow of eddy currents (increase R),
- minimizing the magnetic flux (decrease U).

These points are described in greater detail in the next sections.

Elimination of eddy currents by using the material with high electrical resistance

The most commonly used ferromagnetic materials are low carbon steel, Fe-Co, Fe-Ni, Fe-Si alloys, pure iron, or ferrite materials. Magnetic and electric properties of ferromagnetic iron alloys are fundamentally influenced by the chemical composition. The electrical resistance of iron alloys can be significantly increased by Si or Al (Figure 22). The higher the content of Si in silicon steel, the higher the electric resistance and the lower the magnetic saturation (Figure 22 middle). The maximum relative permeability of Fe-Si is at 6.5 % of Si (Figure 22 right).

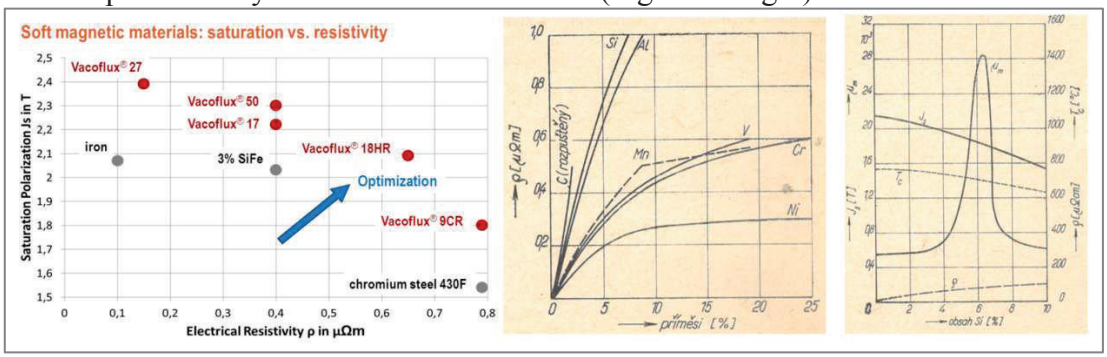

Figure 22 The saturation polarization dependency of electrical resistivity of different Fe-Co alloys (left), influence of chemical composition on the electric resistivity of Fe (middle), influence of Si on the magnetic saturation and electric resistivity of silicon steel (right) [63]

Fe-Co alloys are also frequently used because they have excellent magnetic properties; however, they are very expensive (1kg cost 250 $). The magnetic saturation of Fe-Co is 10% greater than that of pure iron, between 30 % and 50 % of Co content. A dependency of magnetic saturation and electric resistivity of Fe-Co alloys with different content of Co can be seen in Figure 22 (left). Another major alloy is Fe-Ni; the magnetic properties of Fe-Ni are similar to pure iron to the 10 % of Ni. Fe-Ni is almost non-magnetic with content of 30 % of Ni and Fe-Ni with content of 50% of Ni achieved 75 % of magnetic saturation of pure iron. The maximum relative permeability can be achieved with 80 % of Ni [63]. However, the relative permeability significantly decreases after the mechanical load. In recent years, composite materials have also been used (soft magnetic composite - SMC) [64], [65]. These materials are manufactured by compression (up to 980 MPa) from pure iron powder with insulation surface layer and by heating of about 700 °C in a special atmosphere [64]. SMCs have a high magnetic saturation (1.6 T) and a low electric resistivity (roughly 10 Ω.m) [66]. The price for 1 kg is about 40 $. A disadvantage of this material is a rather low relative permeability (roughly 400) [67]. The most recently used group of magnetic materials are soft ferrites. These materials have a high electric resistivity (roughly 10^{-2} Ω.cm) and a low magnetic saturation (0.5 T) but they exhibit a rapid decrease in magnetic saturation with the increase in temperature [68].

Elimination of eddy currents by geometric adjustment of magnetic circuit

The second option of how to eliminate eddy currents is the increase of electric resistivity by a suitable geometrical adjustment of magnetic circuit. The electric resistance increases in the direction of flow eddy currents. A relatively frequent geometric adjustment is the use of the magnetic circuit made of laminated sheets; this method is frequently applied in electric motors or in transformers (Figure 23). In the laminated version, the eddy currents flow only in a single sheet; therefore, the magnetic flux in the magnetic circuit decreases. The lamination method is not applicable in the case of complicated geometry of magnetic circuit.

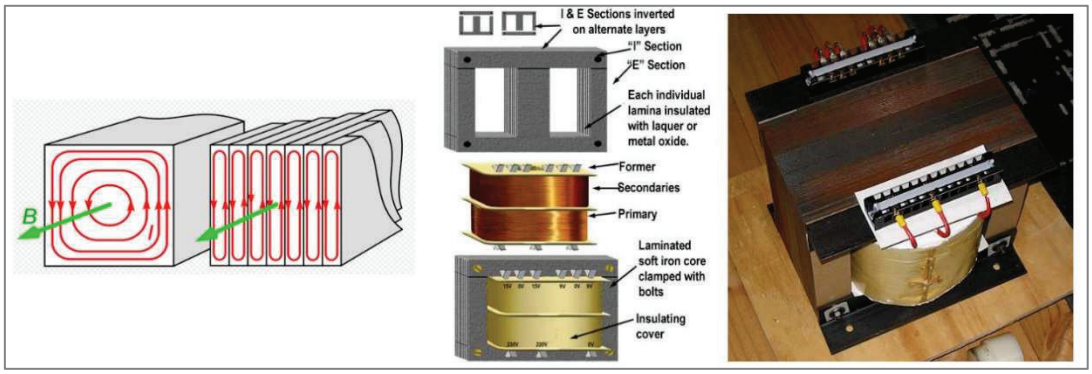

Figure 23 Magnetic flux (green) and eddy currents (red) (left)[69], the laminated magnetic circuit (middle, right)[70]

The lamination method for magnetic circuit of magnetorheological damper was used by Oliver and Kruckemeyer [71] (Figure 24) and Goldasz [38]. These designs of MR damper are similar to the design of electric motor. Laminated sheets form a series of individual magnetic poles with gaps in – between so the eddy currents cannot flow

between the poles. This method provides a short response time of MR damper but it is very expensive and also its assembly is very complicated.

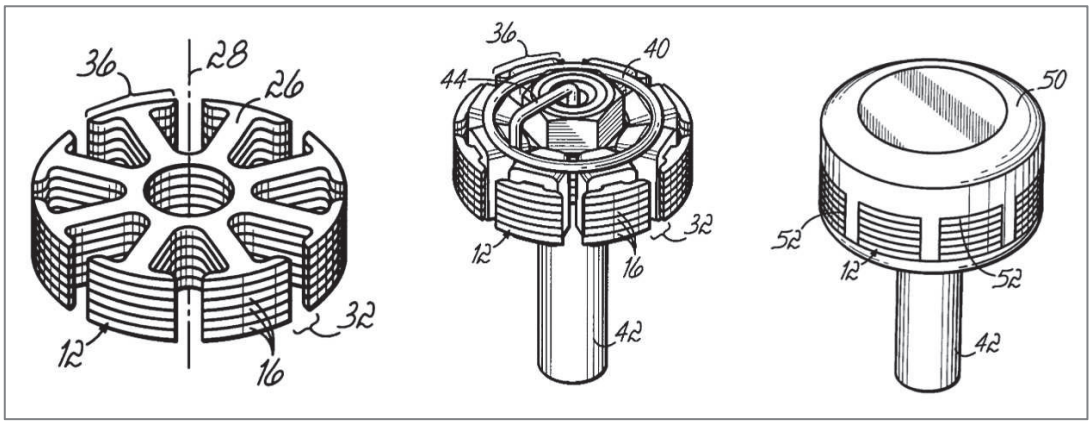

Figure 24 Laminated magnetic circuit of MR damper [71]

Elimination of eddy currents by minimizing the magnetic flux

The electromotive force is given by the magnetic flux and the time of change of magnetic flux. The higher the magnetic flux, the higher the eddy currents in the magnetic circuit. A method of how to decrease the eddy currents is a decrease in the magnetic flux. A multi-coil configuration decreases the magnetic flux because this design of MR damper uses the coils with a lower number of turns (Figure 25). A multi-coil configuration is well described in [38, 72]. The second option is increase a height of active zone (gap). However, the increase of height gap decreases the dynamic force range.

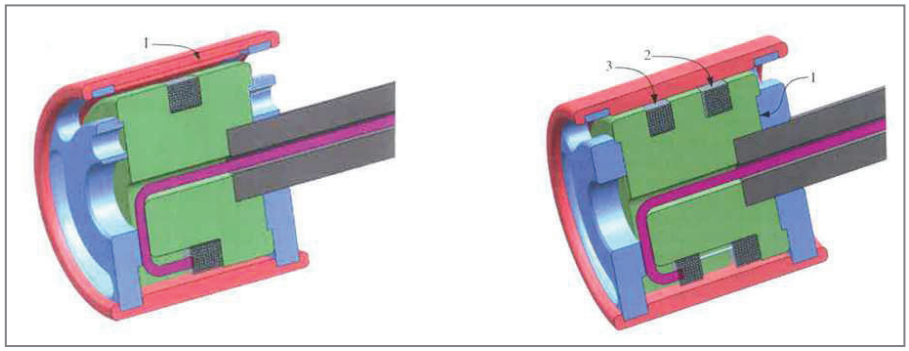

Figure 25 Single-coil configuration (left), multi-coil configuration (right) [38]

2.4.2.2 Magnetic models

Magnetostatic and transient magnetic models are important models for the MR damper design. A dynamic force range of MR damper can be estimated by the magnetostatic model and the post-yield hydraulic model. A transient magnetic model is used for simulation of the response time of magnetic field of MR damper.

The magnetostatic model is important for the dimensional design of magnetic circuit of MR damper due to maximization of magnetic flux in the active zone. This model is also important for the coil design. Analytical and numerical magnetostatic models were published e.g. by Nguyen [73] who described a simplified analytical magnetostatic model of MR damper. However, the calculation of this model is complicated because of non-linear material behaviour (B-H curve). For this reason,

a lot of authors use the FEM magnetostatic model; these authors usually employed the software Ansys/Emag [74, 75] or FEMM [76–78]. In most publications, a simplified 2D axisymmetric model is used. A very important output of this model is the intensity of the magnetic field in the active zone. This value is used in the hydraulic models because of influence on the yield stress of MR fluid. Unfortunately, this model is difficult to experimentally verify because it is not possible to measure the magnetic flux density in the active zone with MR fluid. The second problem is an accurate B-H curve of material.

The transient magnetic model is fundamental for determination of the response time of magnetic field in the active zone for the step rise of control current. Neverteless, this model is not commonly used for the design process of MR damper. According to the available literature, the transient magnetic model was published by Takesue [79] and Zheng [80]. Zheng [80] used the software Comsol, while Takesue [79] did not refer to the software used for his study.

2.4.3 Magnetorheological section

2.4.3.1 In-use-thickening of MR fluid

Carlson [81] published his finding that if the MR fluid in the MR damper is subjected to high stress and a high shear rate over a long time period in MR damper, the off-state force increases progressively (Figure 26). This effect is probably caused by spalling of the friable surface layer from the surface of the carbonyl iron particles. These small pieces are of nanometric size, which has the impact on the viscosity of MR fluid. When the viscosity (off-state force) of MR fluid increases, the dynamic force range of MR damper decreases.

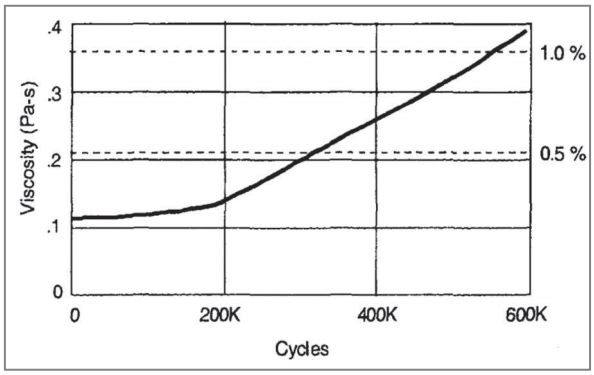

Figure 26 The increase of viscosity due to in-use-thickening

Carlson [81] published the equation for the expected lifetime of MR fluid (LDE - lifetime dissipated energy), which is based on the in-use-thickening effect. The LDE is simply a total mechanical energy dissipated per unit volume of MR fluid over the lifetime of devices.

$$LDE = \frac{1}{V} . \int_0^{life} P \, . \, dt \tag{2.4}$$

Where V is the volume of MR fluid [m^3], P is the mechanical power [W], converted to heat of MR device. LDE of commercial available MR fluid is about 10^7 J/cm^3. The

volume of MR fluid in MR devices is an important parameter which influences the lifetime and dynamic force range of the device.

2.4.4. Hydraulic section

A hydraulic section contains three areas of interest referring to the F-v dependency which has an influence on the dynamic force range (Figure 27). The off-state, pre-yield, and post-yield regime are described below. In each regime, the hydraulic model is present.

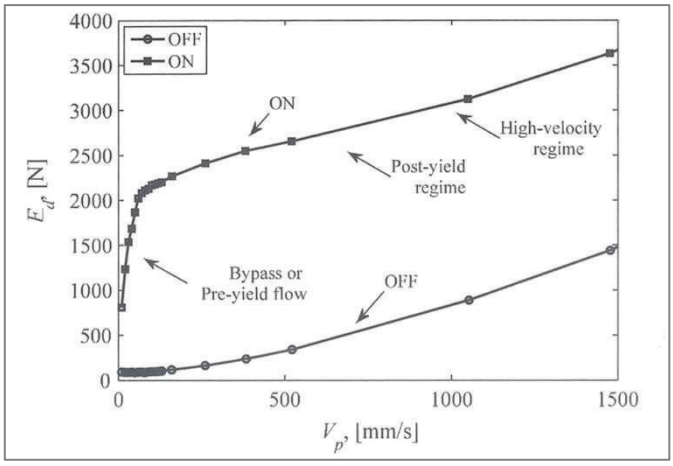

Figure 27 The F-v dependency of MR damper [38]

2.4.4.1 Pre-yield regime

In the following section, only a bypass gap of the MR damper will be described. This gap is parallelly connected to the active zone of MR damper and causes a decrease in damping force (F-v dependency) at low piston velocities. Foister [82] patented the bypass gap in MR damper (Figure 28) in 2009.

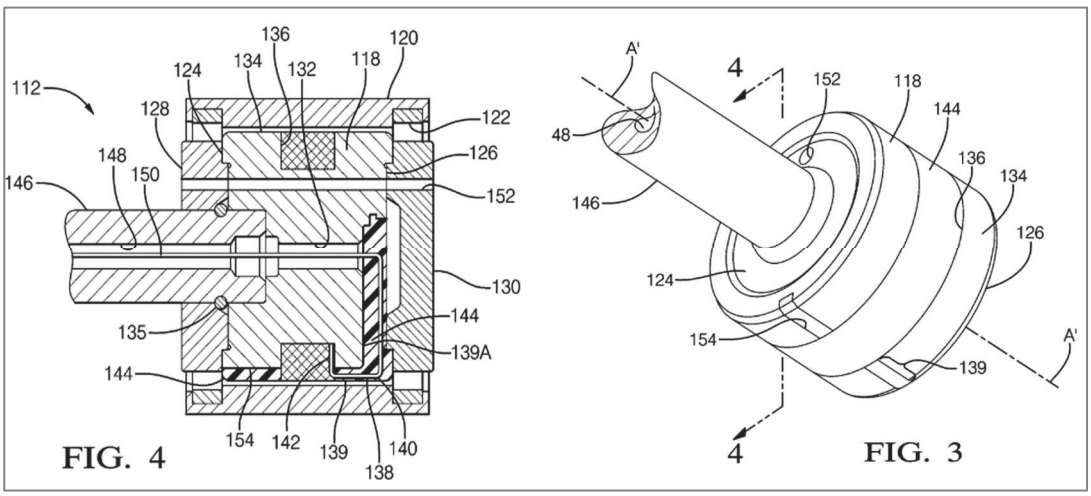

Figure 28 Patents of bypass gap by Foister [82]

Lisenker [83] also patented the bypass gap in MR damper and the company Delphi (BWI group) owns both patents. Sohn [46] described the problem of design of bypass gap in MR damper. In his opinion, the MR damper without bypass gap causes undesirable hardness in vehicle application, which may degrade the ride

comfort. A suitable design of bypass gap is important for performance of MR damper. Sohn [46] published a simple analytical hydraulic model of the bypass gap but this model is inaccurate due to simplifications.

Goldasz [38] reported that the pressure drop of bypass gap can be described by Darcy-Weisbach equation. In this equation, it is necessary to estimate the friction factor from the steady-state CFD model. The CFD simulation was solved as 2D axisymmetric, and the k-ε turbulent model was used. The other models of bypass gap were not found in the literature.

2.4.4.2 Post-yield regime

A post-yield regime is the regime where the shear stress in the active zone is higher than the yield stress of MRF. A hydraulic model of this regime is important for design of MR damper due to specific damping force requirements. This model is based on the non-Newtonian behavior of MR fluid in the magnetic field. This behavior is usually described by the Bingham model with adjustable yield stress by the magnetic field. The shear stress in MR fluid is described by:

$$\tau = \tau_0(H)\,\mathrm{sgn}(\dot{\gamma}) + \eta\dot{\gamma}, \qquad |\tau| \geq |\tau_0(H)|, \tag{2.5}$$

$$\dot{\gamma} = 0, \qquad |\tau(H)| \leq |\tau_0(H)|, \tag{2.6}$$

where H is magnetic flux intensity (A/m), $\dot{\gamma}$ is shear rate (1/s), η is magnetic field independent of post-yield plastic viscosity (Pa. s), τ is shear stress in MR fluid (Pa) and τ_o is yield stress in MR fluid (Pa). The Bingham model did not include shear thinning at high shear rates [2]. This behavior was described by Herschel–Bulkley model. However, the Bingham model is sufficiently accurate for the design phase of MR damper [38]. The three most commonly used hydraulic models of the post-yield regime of MR damper are the following:

- 3D or 2D rotationally symmetric CFD hydraulic model of MR damper,
- analytical axisymmetric model of MR damper,
- analytical model of parallel plates.

All presented models are steady-state. The 2D rotationally symmetric CFD hydraulic model of MR damper was published by Sternberg [84] (Figure 29) and Zekeriya [85]. This model is very accurate because it contains exact geometry, entrance and exit losses, or exact value of yield stress in each area. The connection of CFD and magnetostatic model is an important advantage, which allows to determine a different yield stress in each area. However, the solution is time-consuming and the result significantly depends on the chosen boundaries.

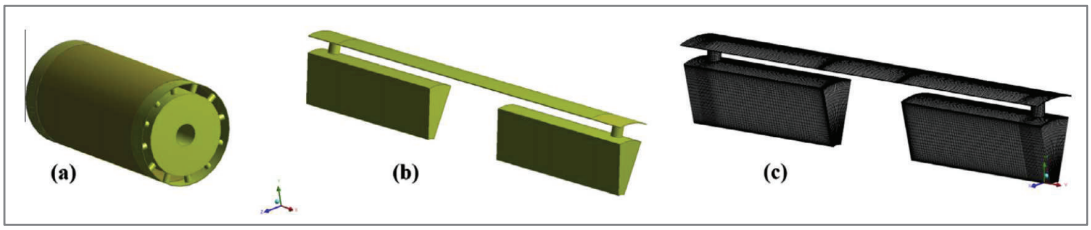

Figure 29 The 2D rotationally symmetric CFD model [84]

The analytical axisymmetric model of MR damper is based on Navier-Stokes equation. A detailed description of the model is referred to in [10]. This model is too complicated for the design phase of MR damper; therefore, it is simplified to the model of parallel plates. The hydraulic model based on parallel plates is often used for the design phase of MR damper (Figure 30).

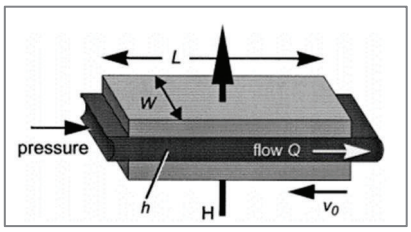

Figure 30 Model of parallel plates [10]

Yang in [10] published the post-yield hydraulic model of MR damper which is based on parallel plates geometry. The resisting force F_{ON} in Yang´s hydraulic model consists of friction force F_f, viscous force F_η and controllable force F_τ :

$$F_{ON} = F_\tau + F_\eta + F_f \tag{2.7}$$

$$F_{ON} = \left(2.07 + \frac{12Q\eta}{12Q\eta+0.4wh^2\tau_0}\right)\frac{\tau_0 LA_p}{h} sgn(v_0) + \left(1 + \frac{whv_0}{2Q}\right)\frac{12Q\eta LA_p}{wh^3} + F_f, \tag{2.8}$$

where *h, w, l* are geometries of the active zone (Figure 30) [m], Q is volumetric flow rate [m^3/s], η is post-yield plastic viscosity [Pa.s], τ_0 yield stress of MR fluid [Pa] and A_p is the area of piston without piston rod [mm^2].

2.4.4.3 Off-state regime

The off-state regime consists of viscous and Coulomb friction losses of MR damper. The Coulomb friction of piston rod seal causes the Coulomb friction losses of MR damper. The piston rod Coulomb friction force of MR damper in automotive industry is about 70 N; this value is dependent on the internal pressure. The post-yield plastic viscosity (in some publications referred to as dynamic viscosity) and geometry of active zone influences the viscous losses. The MR fluid without magnetic field is usually modeled as Newtonian fluid. Yang in [10] published a hydraulic model of the off-state regime based on the equation in chapter 2.4.4.2.

$$F_{OFF} = F_\eta + F_f \tag{2.9}$$

$$F_{OFF} = \left(1 + \frac{whv_0}{2Q}\right)\frac{12Q\eta LA_p}{wh^3} + F_f, \tag{2.10}$$

where *h, w, l* are geometries of the active zone (Figure 30) [m], Q is volumetric flow rate [m^3/s], η is post-yield plastic viscosity [Pa. s], τ_0 yield stress of MR fluid [Pa] and A_p is the area of piston without piston rod [mm^2]. The value of off-state damping force significantly affects the dynamic force range. A small reduction in this force significantly increases the dynamic range. For this reason, the viscosity of MR fluid and the type of piston rod seal are very important parameters of design process.

Finally, the remanent magnetization of magnetic circuit also affects the off-state regime.

3 ANALYSIS AND CONCLUSION OF LITERATURE REVIEW

The most commonly used vibration isolation system for space applications is a composite cone [29]. This is an economic and reliable variant of vibration isolation system. However, the elimination of vibrations and shocks by composite cone are insufficient for many types of payload by composite cone. For this reason, more progressive vibration isolation systems are still under development. The company Honeywell developed a vibration isolation system based on Steward platform (ELVIS) [33, 34]. A patented passive D-Strut, which has a springing and damping function, [37] was used in this system. The system D-strut was used to deliver the Hubble's telescope to the orbit [32]. The main disadvantage of ELVIS vibration isolation system is a weight higher than that of composite cone. For this reason, the methods to increase the efficiency of vibration isolation system are still under development to justify the higher weight. Active vibration isolation systems are high-energy consuming. There is also a risk of destruction of the vibration isolation system by an inadequate control. From the point of views of efficiency and weight of vibration isolation system, the semi-active control seems to be the most appropriate.

However, the efficiency of semi-active control is influenced by the response time of damping element [26] and the dynamic force range [49, 86]. According to the information from ESA, it is important to control the frequencies up to 25 Hz for a wide range of payloads. For the effective semi-active control, ten regulation interventions per period are necessary. The required response time of damping element for ESA shall be about 4 ms. An important requirement for space application is a hermetic separation of operating fluids from the rest of the launch vehicle. The damper with a common design of piston rod seal is inapplicable because there is a risk of damping fluid leakage. A challenging method is the use of metal bellows [57, 58]. The sealing system with bellows was also used in Honeywell D-Strut [37]. An important issue is a choice of the technology for semi-active control damping element. Electro-hydraulic dampers achieved the lowest values of the response time, i.e. about 15 ms [19], but this is too long for space application. The magnetorheological technology seems to a be better candidate for semi-active control damping element.

A design of MR damper was dealt with by many authors [10, 44, 75, 87]. However, the design of MR damper was primarily focused on the possibility of change (by electric current) of damping level (adaptive mode). There was no requirement for the time needed for the rise of damping force (response time of MR damper). The response times of available designs of MR damper are between 20 ms and 200 ms. The response time of MR damper is similar to that of electro-hydraulic dampers. However, Strecker [11] published the method of how to decrease the response time of MR damper to 1.5 ms.

In the chapter 2.4, the methods were described in terms of the influence on the dynamic force range and the response time of MR damper. These methods were divided into several sections: mechanical, magnetic, magnetorheological, and hydraulic.

The methods of separation of MR fluid from the environment have a significant influence on the mechanical section. In general, three methods can be found: piston rod seal, bellows, and magnetic seal. Friction losses of piston rod

decrease the dynamic force range and always leads to a leakage. From this perspective, they are inappropriate for space applications. Bellows provides hermetic sealing of fluid from the environment and provide zero friction losses. Main disadvantages of bellows are a limited stroke and a problematic design. An inappropriate design (low volumetric stiffness) of bellows geometry may worsen the damper function due to the bellows inflation. The last group is a magnetic seal. The MR fluid can be used as a sealing medium in the magnetic seal [61]. This method has a great potential but has not been sufficiently explored yet. However, similarly to the rubber sealing, there is a leakage risk related to this method of sealing. The greatest potential for space application has a bellows.

The magnetic section has a significant impact on the response time and the dynamic force range of MR damper. A selection of material with high magnetic saturation (Fe-Co, pure iron) increases the dynamic force range. However, these materials have a low electric resistivity, which negatively influences the response time. The lamination method of magnetic circuit significantly increases the electric resistance in the direction of eddy currents flow. However, for the geometry of magnetic circuit of MR damper, this method is difficult to use. One option of how to achieve 4 ms of the response time is the use of ferrite magnetic material or SMC. The ferrite material has a high electric resistance but a low magnetic saturation (500 mT). The latter dramatically reduces the dynamic force range of MR damper compared to the use of low carbon steel. A selection of material for magnetic circuit is always trade-off between the dynamic force range and the response time of MR damper. For this reason, the magnetic models would help to choose a proper material of magnetic circuit for the specific dynamic range and the response time. The transient magnetic model of MR damper is published only in [79] or [80]. The methodology of this model is not clear. The construction and experimental verification of magnetic model is one of sub-goals of this thesis. However, the alfa-omega is to find the material or geometry of magnetic circuit which provides a high dynamic range and short response time of MR damper; this is one of the most important parts of the present thesis.

In-use-thickening of MR fluid has an effect on the dynamic force range in the magnetorheological section. The off-state force increases when the MR fluid in the MR damper is subjected to high stress and a high shear rate over a long-time period. The cause of this viscosity increase is spalling of surface layer from MR fluid particles [81]. The dynamic force range decreases with load time. For space applications, this effect is irrelevant because the load time of MR fluid is very short (journey into the orbit takes around 5 min).

The hydraulic section has an effect on the dynamic force range. The important areas referring to the F-v dependency are the following: pre-yield regime, post-yield regime, and off-state. It is possible to design the geometry of MR damper with a high dynamic force range using a suitable hydraulic model. The important part of pre-yield regime is a bypass gap, which is parallelly connected to the active zone of MR damper. The bypass gap causes a decline in F-v dependency at low piston velocity as was described in [46, 83]. The analytical hydraulic model of bypass gap was published in [46] but the model presented in this publication is strongly simplified and inaccurate. For this reason, the CFD model of bypass gap represents a more precise way. A numerical model of bypass gap and its experimental verification are sub-goals of this thesis. The hydraulic models of post-yield regime

are described in publications [10, 38, 84]. However, the important input into this model is the yield stress of MR fluid which must be obtained from the datasheet of MR fluid and the magnetostatic model. Unfortunately, in the whole range of publications, this step is omitted. The experimental verification of published hydraulic model of post-yield regime connected with magnetostatic model will be performed. This is one of sub-goals of this thesis. The last one is the off-state regime. The off-state hydraulic model is based on the post-yield hydraulic model. The important input into this model is viscosity of MR fluid.

4 AIM OF THE THESIS

The present dissertation thesis was closely connected with the project for European Space Agency: “Semi-active damping system FLPP3”. This project was solved in co-operation with the company Honeywell. The semi-actively control MR damper of strut appears to be an effective version to decrease the transmissibility of vibration isolation platform for space application, according to the state of the art. The performance of this system has a significant influence on the response time and the dynamic force range of MR damper. For ESA´s launch vehicle, it is important to achieve the semi-active control frequency up to 25 Hz. For effective control of this frequency, the response time of damping element about 4 ms is needed. The design of demonstrator of this type of MR damper is the main aim of this thesis.

In 2013, the only option of how to design the MR damper with the response time of 4 ms was to use the ferrite material for magnetic circuit, according to the state of the art. However, the design of MR damper with ferrite magnetic circuit exhibits a lot of design limitations, such as low strength (30 MPa), poor machinability, fragile behaviour, or low magnetic saturation (500 mT). The latter has a significantly influence on the dynamic force range. An important sub-aim of the present thesis was to find the method or material for the design of MR damper with short time response without the use of ferrite material. Another important sub-aim was to add new methods for the design of MR damper with short response time, e.g. the model of bypass gap, magnetostatic or transient magnetic model.

4.1 The aim of the thesis

The main aim of the submitted dissertation thesis is to design and tests a demonstrator of magnetorheological suspension damper with short response time for space application. A design of MR valve is fundamental for the design of the MR damper. The sub-aims of the thesis refer to the methods necessary to add for the design of semi-active control MR damper with short response time.

The sub-aims of the thesis are as follows:

- a method to decrease the response time of MR damper,
- magnetostatic, transient magnetic models and their experimental verification,
- a model of bypass gap and its experimental verification,
- experimental verification of published hydraulic models.

4.2 Scientific question and hypotheses

Scientific question 1:

It is possible to design a semi-actively controlled magnetorheological damper for space application, which has a response time of about 4 ms and a dynamic force range more than 4?

Hypotheses 1: The ferrite material for the magnetic circuit of the MR damper will allow designing an MR damper with a response time of approximately 4 ms.

Hypotheses 2: The dynamic force range of the MR damper cannot be achieved more than 4 because the ferrite material has low level of magnetic saturation.

Scientific question 2:
It is possible to design a magnetic circuit of MR damper from material with high magnetic saturation and low electric resistivity which achieved a short response time?

Hypotheses 3**:** The decrease of creation of eddy currents, which has significant effect on the response time, is possible by suitable structural modification which rapidly increases the electric resistivity in the flow path of eddy currents.

4.3 Thesis layout

The main aim of the present dissertation thesis was published in the impact journal Smart Materials and Structures (IF 2.909). The design and experiments related to the developed MR damper with short time response were published in the paper (**I.**).

The methods to decrease the response time of MR damper were searched for. The main limitation parameters of the response time are the eddy currents in the magnetic circuit of MR damper. The research was focused on the elimination of eddy currents in the magnetic circuit. In this area, a considerable progress has been achieved by using a suitable shaped groove (geometric modification) in the magnetic circuit of MR damper. This method allows for development of magnetic circuit of MR damper with a high dynamic force range and a low response time. The efficiency of this method can be increased by 3D metal printing (SLM). This method was patented (**II.**).

The transient magnetic model of MR damper and its experimental verification were published at the International Conference in Kuala Lumpur (**III.**). The paper passed the review process. This model is important for the design of MR damper for the specific response time.

The CFD model of bypass gap of MR damper and its experimental verification were published at the International conference in Svratka, Czech Republic. The paper passed the review process (**IV.**).

Impact journal Smart Material and Structures (Journal impact factor = 2.909)

I. KUBÍK, M.; MACHÁČEK, O.; STRECKER, Z.; ROUPEC, J.; MAZŮREK, I., 2017. Design and testing of magnetorheological valve with fast force response time and great dynamic force range. Smart Materials and Structures. 26(4), 47002. ISSN 0964-1726

Czech patent

II. KUBÍK M.; MACHÁČEK O.; STRECKER Z.; ROUPEC J.; MAZUREK I.; KOUTNY D.; PALOUŠEK D., 2017. Struktura jádra obsahujícího pruty z feromagnetického materiálu a způsob jejího vytvoření. Czech Republic, PV 2017-91. 2017.

Article in conference proceedings – (after review, Scopus)

III. KUBÍK, M.; MACHÁČEK, O.; STRECKER, Z.; ROUPEC, J.; MAZŮREK, I.

Transient magnetic model of magnetorheological damper and its experimental verification. The 4th International Conference on Mechantronics and Mechanical Engineering 2017

Article in conference proceedings – Web of Science

IV. KUBÍK, M.; MACHÁČEK, O.; STRECKER, Z.; ROUPEC, J.; MAZŮREK, I., 2016. Hydraulic resistance of magnetorheological damper viscous bypass gap. In: ZOLOTAREV I.; RADOLF V.;, ed. *22nd International Conference on Engineering Mechanics*. Svratka: Institute of Thermomechanics, Academy of Sciences of the Czech Republic, p. 330–334.

Full version of publication in attachment of the present thesis.

5 NEW METHODS FOR THE DESIGN SEMI-ACTIVE CONTROL MR DAMPER

In this chapter, new methods for the design of the semi-active control MR damper with short response time and high dynamic range are presented. The next sections are divided into the same sections as the methods in the state of the art section. According to the state of the art, these methods are presented in:

- In magnetic section,
  - magnetostatic model and its experimental verification (5.1.1),
  - transient magnetic model and its experimental verification (5.1.2),
  - elimination of eddy currents in the magnetic circuit (5.1.3).
- In hydraulic section,
  - CFD model of the bypass gap and its experimental verification (5.2.1),
  - experimental verification of published hydraulic models (5.2.2).

5.1 Magnetic section

In this section, the proposed magnetic models and their experimental verification are described; specifically, these are magnetostatic and transient magnetic models. Both magnetic models were verified on the MR damper geometry (see geometry the attachment 1). The next section also discusses the methods of elimination of eddy current in the magnetic circuit of MR damper.

5.1.1 Magnetostatic model of the MR damper and its experimental verification

A magnetostatic model is usually used for a design process of the MR damper. However, the accuracy of hydraulic models and a transient magnetic model are strongly influenced by the results of the magnetostatic model. The experimental verification of this model was an important step in designing the MR damper with short response time. The magnetostatic model allows to determine the magnetic flux density in the active zone of the MR damper, which is a fundamental input into the post-yield hydraulic model. The magnetostatic model was experimentally verified on the MR damper geometry (see dimensions in attachment 1).

Materials and methods

The geometry of the magnetic circuit of the MR damper was simplified in the magnetostatic model as 2D axisymmetric (Figure 31) and the software Ansys Electronics 17.1 was used. Low carbon steel 11SMn30 was set as the material for the magnetic circuit (Figure 31, green). The B-H curve of this material was experimentally determined (see attachment 2). The B-H curve of air or Lord MRF-132DG was set in the active zone (Figure 31, yellow). The coil was excited by the magnetomotive force (current x 120 A. turns). For discretization of geometry, 3584 elements and the nonlinear residual at 0.0001 were used in the model.

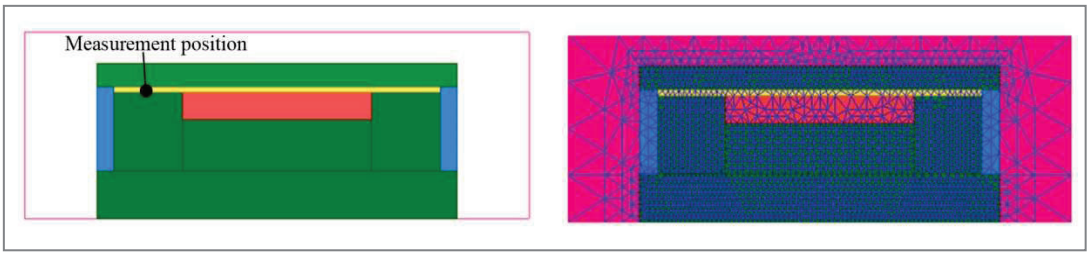

Figure 31 The geometry of MR damper in magnetostatic model; 11SMn30 (green), aluminum alloy (blue), copper (red), vacuum (white, yellow)

The magnetic flux density in the active zone was measured with the ultrathin Hall probe and the magnetometer F.W. Bell 5180. A precise position of the Hall probe was provided by the devices with a motion screw (Figure 32, middle and right). The coil was excitated by the laboratory source Manson SDP 2603. The current in the coil was measured with a current clamp Fluke i30. The measured data were acquired by Dewe 50 with a sampling frequency of 100 Hz and showen in the software DeweSoft. The verification of the magnetostatic model was only possible with an air in the active zone of the MR damper.

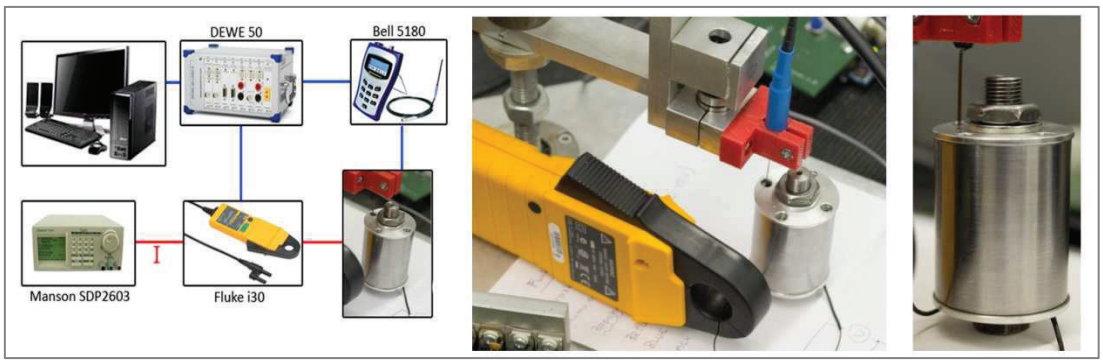

Figure 32 The measurement circuit (left), position Hall probe (middle, right)

The measurement methodology of the magnetic flux density in the active zone was as follows:

1) demagnetization of magnetic circuit before the experiment (zero remanent magnetisation),
2) increase in the electric current to 5 A,
3) decrease in the electric current to 0 A,
4) change of polarization of electric current,
5) increase in the electric current to 5 A,
6) decrease in the electric current to 0 A,
7) change of polarization of electric current,
8) increase in the electric current to 5 A,
9) decrease in the electric current to 0 A.

Results and discussion

Figure 33, left, shows the magnetic flux and Figure 33, right, the magnetic flux density from the magnetostatic model for current 2A.

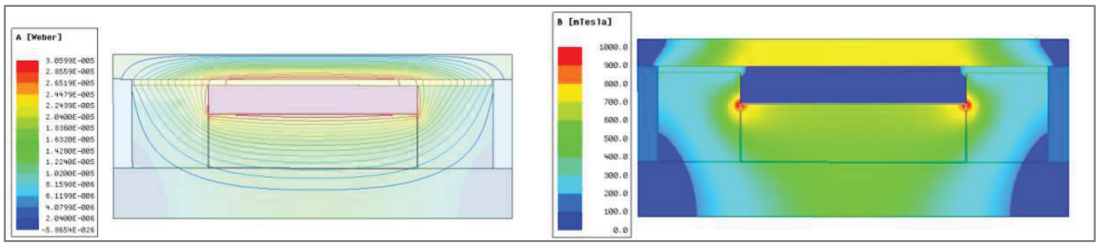

Figure 33 The magnetic flux at 2 A (left), magnetic flux density at 2A (right) with air

The magnetic flux density in the centre of the active zone with air (Figure 31) is important for experimental verification of magnetostatic model. Figure 34 shows a dependency of magnetic flux density and magnetic flux intensity in the centre of the active zone with air on the electric current from the magnetostatic model.

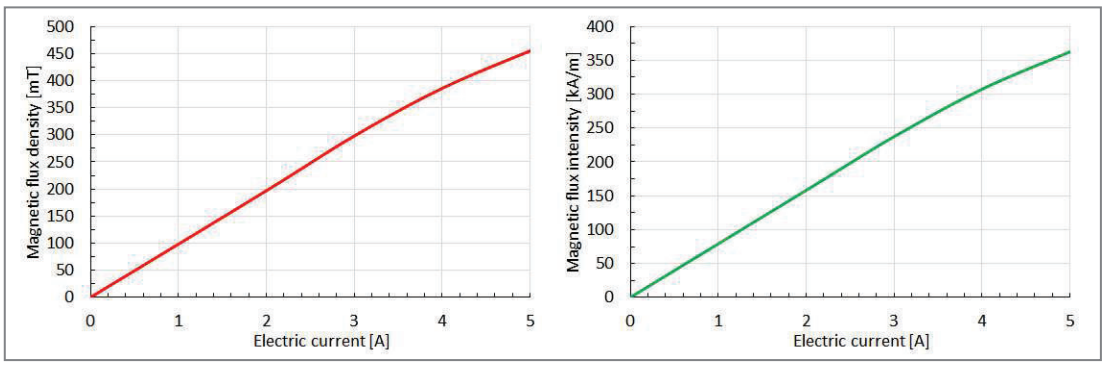

Figure 34 The magnetic flux density (left) and magnetic flux intensity (right) in the middle of active zone with air

The whole hysteresis magnetic curve (Figure 35, left) and a virgin magnetization curve (Figure 35, right) were measured.

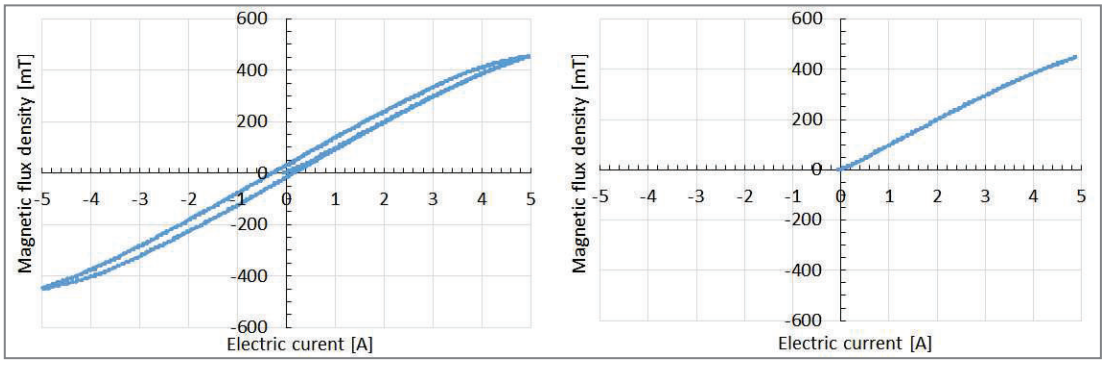

Figure 35 Hysteresis magnetic loop (left), virgin magnetization curve (right) from the experiment

A virgin magnetization curve (Figure 35, right) is important for verification of magnetostatic model. A comparison of the magnetostatic model with the experiment is illustrated in Figure 36.

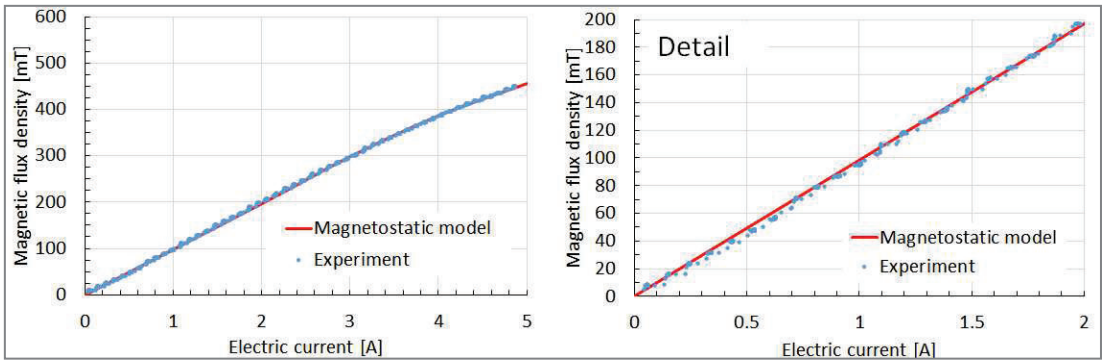

Figure 36 Comparison of the magnetostatic model and the experiment (left), the detail of a comparison of the magnetostatic model and the experiment (right)

The maximum difference between the magnetostatic model with air and the experiment was under 1 %. However, the accuracy of the magnetostatic model is strongly dependent on the accurancy of measurement of B-H curve. The magnetic circuit of the MR damper was composed of the same material as the testing sample for measurements of B-H curve (the same chemical composition). The magnetostatic model was experimentally verificated on the air in the active zone.

An important output of the magnetostatic model is the intensity of the magnetic field (magnetic flux density) in the active zone with the MR fluid. These value inputs represent as an essential parameter in the post-yield hydraulic model of the damper MR (yield stress) and fundamentally affect its accuracy. The MR damper was tested with Lord MRF-132DG. For this reason, the B-H curve of MRF-132DG was set in the active zone in the magnetostatic model [88]. The results obtained from the magnetostatic model with MRF-132DG are shown in Figure 37.

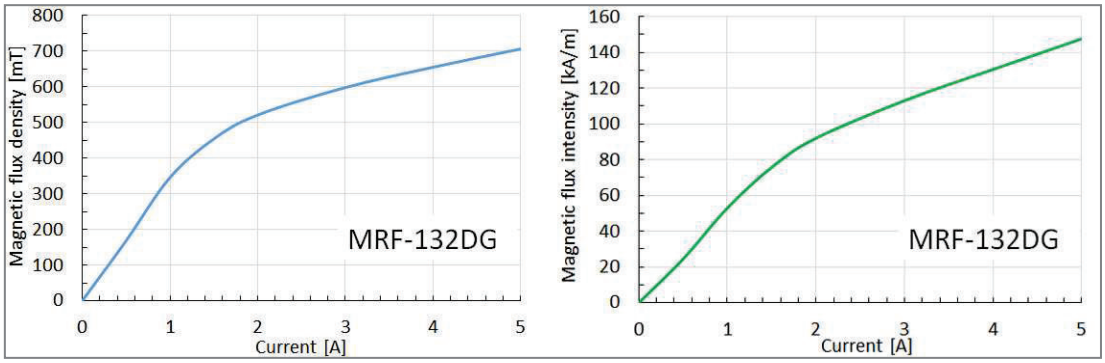

Figure 37 The magnetic flux density (left) and the magnetic flux intensity (right) in the active zone with MRF-132DG from the magnetostatic model

The yield stress in the active zone was determined from the datasheet of the MR fluid, and the magnetic flux density in the active zone was determined from a magnetostatic model. A dependency of the yield stress in the active zone of MR damper and the electric current on the coil can be seen in Figure 38.

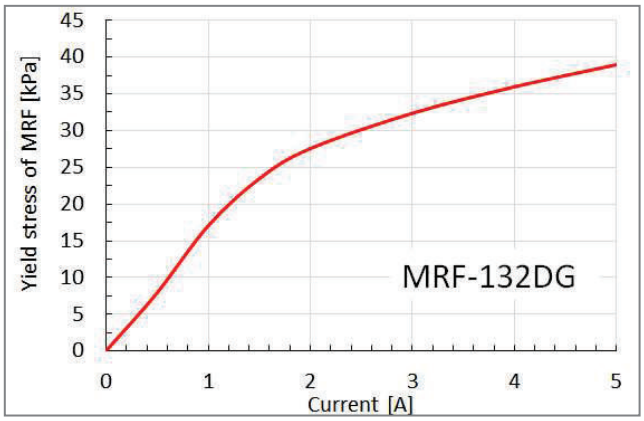

Figure 38 Dependency of the yield stress in the active zone on the electric current of the coil with MRF132DG

The presented geometry of the MR damper operates effectively up to the electric current of 1.5 A; after that the slope of yield stress is slightly increases, according to magnetostatic model.

5.1.2 Transient magnetic model and its experimental verification

The transient magnetic model allows determination of the response time of the magnetic field (the most important part of the response time of the MR damper).

Materials and methods

The model was created in the software Ansys Electronics 17.1. The geometry was simplified as 2D axisymmetric. A description of the model and experiment was published in the paper entitled "**Transient magnetic model of magnetorheological damper and its experimental verification**" (International Conference in Kuala Lumpur) [89].

Results and discussion

The verification of the transient magnetic model was possible only with air in the active zone where the maximum difference between the model and the experiment was 28 % (Figure 39, left) with air in the active zone. This difference is probably caused by inaccurately specified electrical conductivity given in the datasheet of the material manufacturer. The response time was dependent on the electric current. The response time of the magnetic field of MR damper with Lord MRF-132DG was determined by verification using the transient magnetic model (Figure 39, right). The response time of the magnetic field with the MR fluid was also dependent on the electric current in the coil. This is probably caused by a non-linear behaviour of the magnetic circuit material.

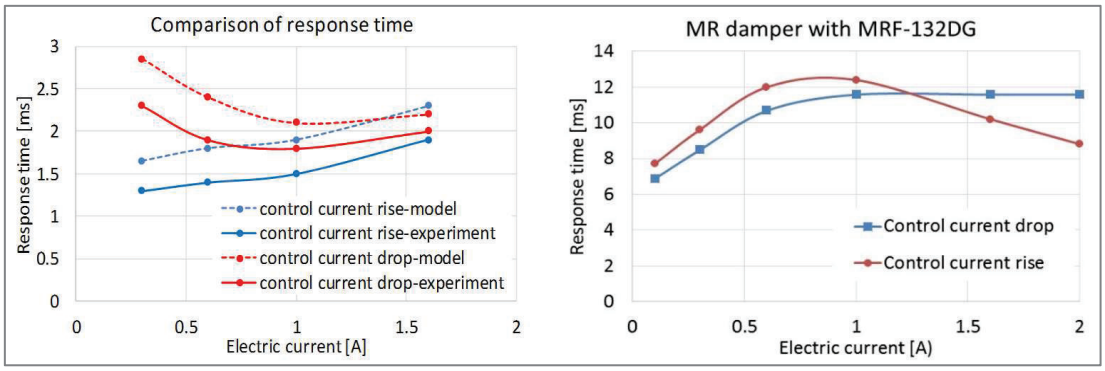

Figure 39 Dependency of the response time of the magnetic field on the electric current from the transient magnetic model with air (left), with MRF-132DG (right) [89]

The response time of the magnetic field from the transient magnetic model was compared with measurements of the response time of the MR damper published by Strecker [11] (Figure 40). The transient magnetic model uses the same geometry of the MR damper measured by Strecker [11]. The maximum difference between the transient model and the Strecker's measurement was 25 %. However, in the response time from the transient magnetic model does not refer to the response time of the MR fluid.

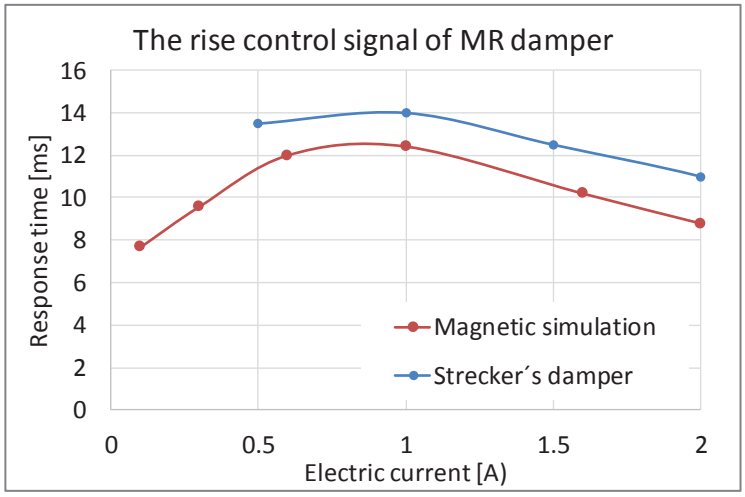

Figure 40 Comparison of the influence of response time of the magnetic field from the transient magnetic simulation (red) and the experimentally measured response time by Strecker [11] (blue) on the rise of control current

The experimentally verified transient magnetic model was used for determining the influence of the magnetic circuit material or the type of MR fluid on the response time of the magnetic field in the active zone. A more detailed description can be found in [89]. The 2D transient model can be simply extended to a 3D model.

5.1.3 Elimination of eddy currents in the magnetic circuit

From the point of view of high dynamic force range and short response time, a suitable material for the magnetic circuit should have a high magnetic saturation and a low electric conductivity. Unfortunately, the material with a low electric conductivity usually has a low magnetic saturation. **A selection of the material for**

the magnetic circuit is a trade-off between the magnetic saturation and the electric conductivity.

Therefore, the question has arisen: "Could the electric resistivity in the direction of eddy currents be increased by structural modification of any part of the magnetic circuit?". In this case, the material with a high magnetic saturation could be used; the response time would be reduced by the geometric adjustment. The option is to use a laminated magnetic circuit (sheet). However, this method is not suitable for the geometry of the MR damper. Another option was found in the analogy of a simple relationship for the electrical resistance R of the wire. In this equation, l is the length of the wire [mm], cross section of the wire is S [m^2] and the electric resistivity of the wire material is ρ [Ω·m].

$$R = \frac{l\rho}{S} \tag{3.1}$$

The higher the length l in the direction of flow path of eddy currents, the higher the electric resistance R in this direction. The area S has also important effect. The increase in the length of the eddy currents "path" is possible via appropriate grooves in the magnetic circuit. This method is demonstrated on the MR damper geometry, specifically on the yellow marked part (Figure 41). On the left in Figure 41, the magnetic flux in the MR damper can be seen. Figure 41 a) shows a direction of the eddy currents in the conventical MR damper. The flow path of the eddy currents is relatively short; therefore, suitable grooves can rapidly increase this path and also the electric resistivity, see Figure 41 b).

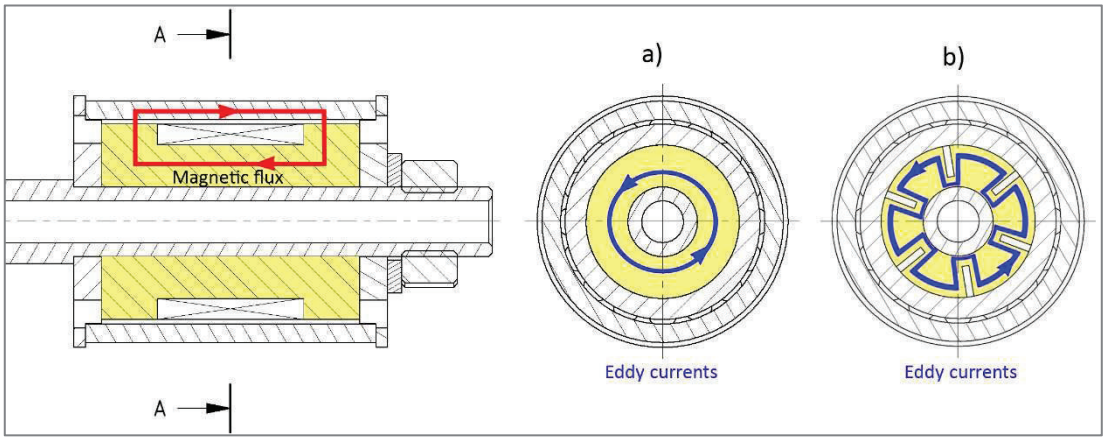

Figure 41 Direction of the magnetic flux (left), influence of the grooves on the path of the eddy currents (middle, right)

Materials and methods

Based on the verified magnetic transient analysis (3D analysis), a suitable geometry of the grooves of the MR damper was determined. A more detailed analysis of influence of grooves was dealt with Strmiska in diploma thesis [90]. The grooves were manufactured by electro erosive wire machining of the magnetic circuit parts (Figure 42). Forty-eight 0.3 mm wide grooves were manufactured. The magnetic circuit was made from the low carbon steel 11SMn30.

Figure 42 Manufactured grooves on the geometry of the MR damper

For the comparison of influence of the grooves on the response time, two identical magnetic circuits were manufactured from the same material. The first magnetic circuit was with the grooves while the other was without the grooves. Magnetic flux density was measured in the active zone with air with the ultrathin Hall probe and the magnetometer F.W. Bell 5180. The coil was energized by power supply Manson SDP 2603 and current controller (our design). Measurements of the response time of the magnetic circuit were based on the methodology in [91]. The response time of the magnetic circuit without grooves was measured using a rise in the control current.

Results and discussion

The measured response time of the magnetic field in the active zone was 1.69 ms (air). The course of the magnetic flux density over time is shown in Figure 43.

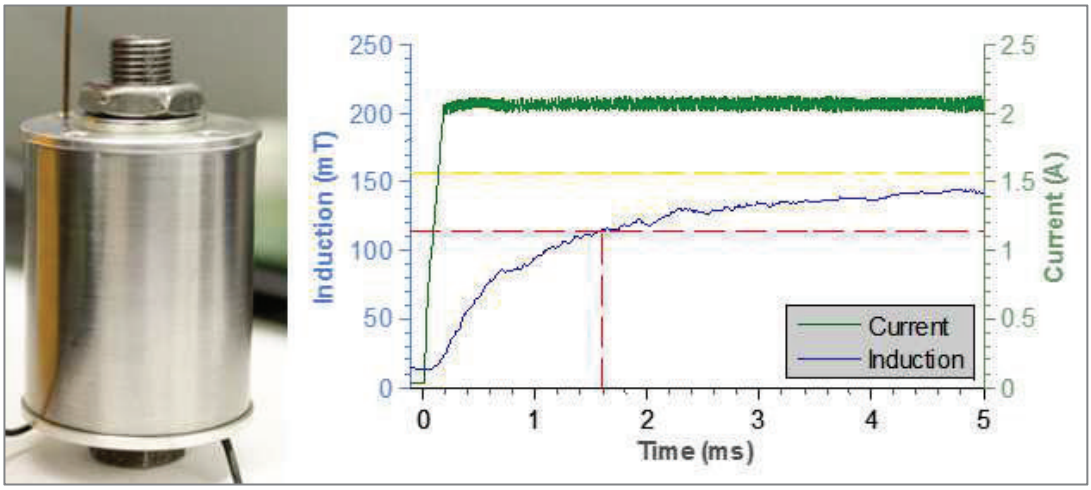

Figure 43 The response time on the air of the magnetic circuit without grooves

The response time of the magnetic circuit with the grooves was measured with a rise in the control current. The measured response time of magnetic field in the active zone was 0.36 ms (air), see Figure 44.

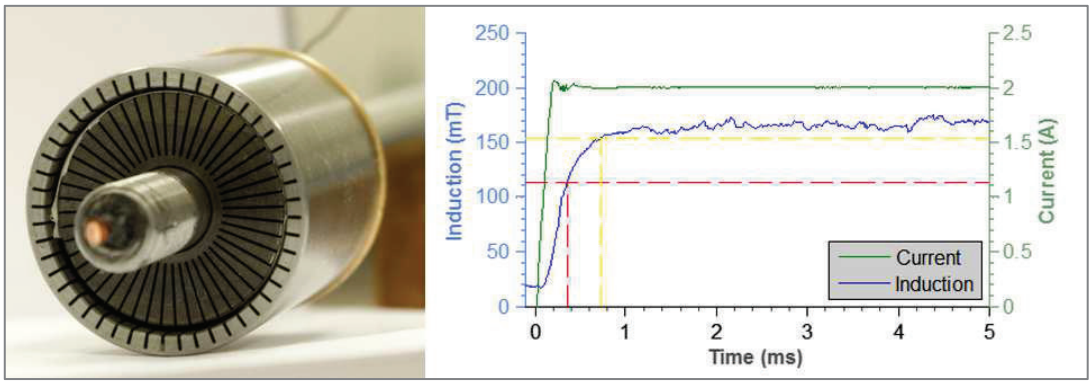

Figure 44 The response time on the air of the magnetic circuit with grooves

According to the obtained results, the response time of the magnetic circuit of the MR damper can be significantly reduced by suitable grooves on the magnetic circuit. The response time of the magnetic field in the active zone dropped 4.6 times using a grooving structure. The maximum magnetic flux density remained the same. The response time of MR damper with the grooved magnetic circuit and the MR fluid in the active zone was solved by the transient magnetic model at 1.7 ms.

It can be concluded that a grooving method is feasible. However, where is the limit for decrease in the response time and dimensions of the grooves? The thickness of grooves (number of grooves in the part) has a limit because of manufacturing technology. The author of this thesis proposed a different method of how to decrease the eddy currents, i.e. to manufacture a magnetic circuit with ferromagnetic rods oriented in the direction of the magnetic flux by SLM (Selective Laser Melting) – method of 3D print. The rods are interconnected only by a small connecting bridges. The principle will be described on the magnetic circuit in the shape of the toroid; the magnetic flux in the toriod can be seen in Figure 45 on the left and the eddy currents on the right.

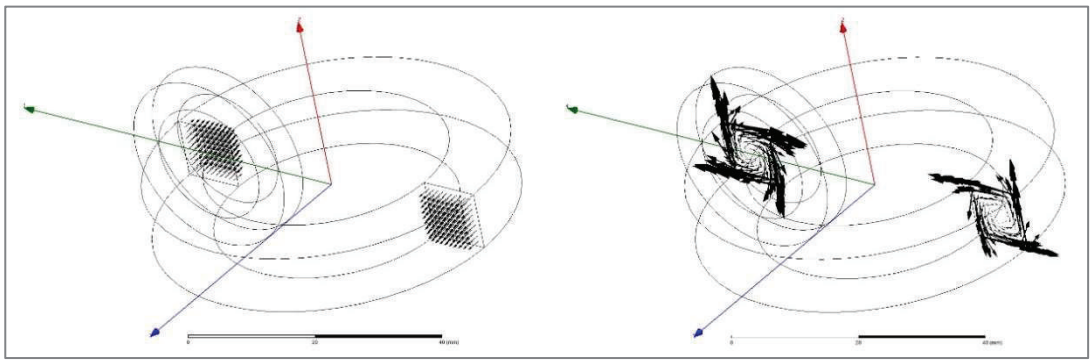

Figure 45 Magnetic flux (left), eddy currents (right) [92]

The ferromagnetic rods are oriented in the direction of magnetic flux and separated in the perpendicular direction by air or other material with a high electric resistivity. To ensure the integrity of the toroid, the connection bridges are designed. An example of the proposed design of the magnetic circuit is given in Figure 46.

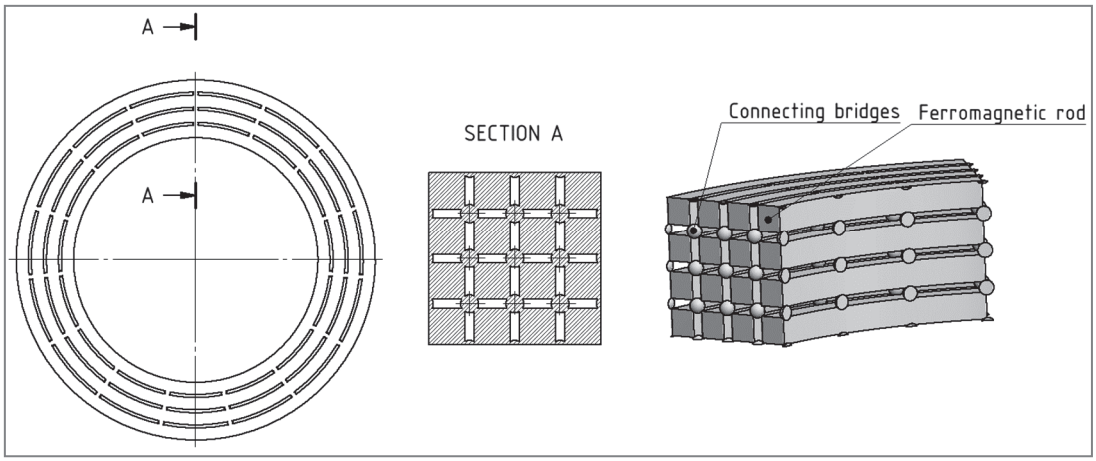

Figure 46 An example of the design of the magnetic circuit according to the patent manufactured by the 3D metal printing [92]

It is necessary to manufacture appropriately small (in millimeters) ferromagnetic rods and connecting bridges to achieve a proper efficiency of the magnetic circuit. Unfortunately, such magnetic circuit is very difficult to manufacture with the conventional technologies; however, the 3D metal print is usable. This method was patented under the title: "**The magnetic circuit containing rods of ferromagnetic material and the method of its manufacture**" [92]. A full version of the patent is described by the author of the patent, who is also the author of the present thesis, in the appendix.

5.2 Hydraulic section

In this section, the proposed CFD model of the bypass gap, the model of the post-yield regime and the off-state regime are experimentally verified. The CFD model of the bypass gap (pre-yield regime) and its experimental verification on the developed experimental test rig is described in the section 5.3.1. Yang hydraulic models of the post-yield and the off-state were experimentally tested on the geometry of the MR damper in sections 5.3.2 and 5.3.3.

5.2.1 Bypass gap in the MR damper (pre-yield regime)

A common design of the MR damper (without a bypass gap) has a step rise of the damping force at low piston velocities; the force-velocity dependency of MR damper is the same as that of friction damper. This causes an undesirable hardness, e.g. in the vehicle application; it may degrade a riding comfort. A parallel connection between the bypass gap and the active zone causes a decrease in the damping force at low piston velocity (Figure 47). A methodology for designing the bypass gap has not yet been published in the available literature. The analytical approach is very complicated and inaccurate.

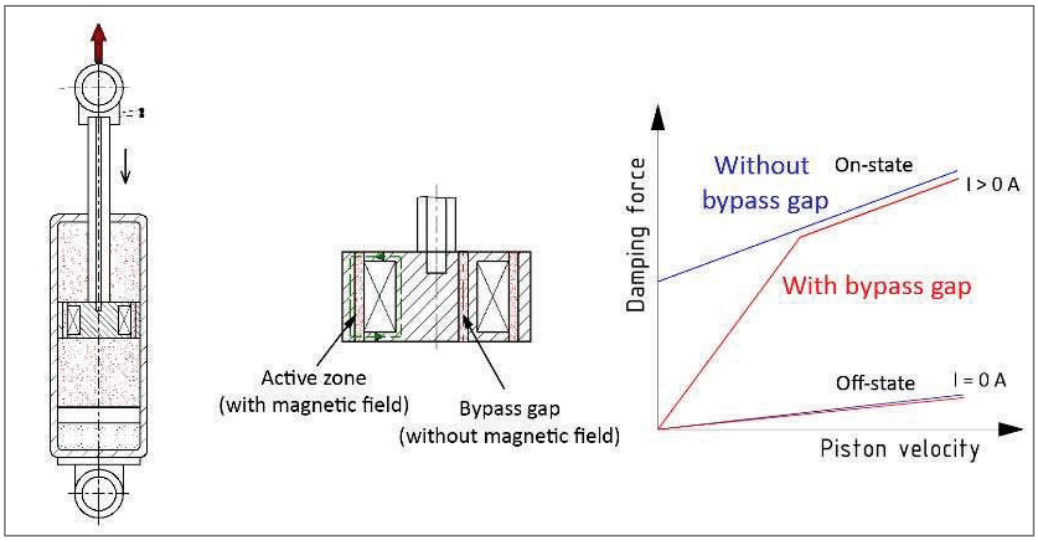

Figure 47 The bypass gap (left), damping force dependency on the piston velocity (right) [47]

Materials and methods

The CFD model of the bypass gap and its experimental verification on the developed test rig were published in the following paper:" **Hydraulic resistance of magnetorheological damper viscous bypass gap**" [47]. The CFD model was created in software Ansys CFX and the k-ε turbulent model was used. The fundamental input to the model was an apparent viscosity of MR fluid [93]. The experimental test rig was designed and manufactured for the testing of bypass gap (Figure 48). Different diameters and lengths of the bypass gap were tested.

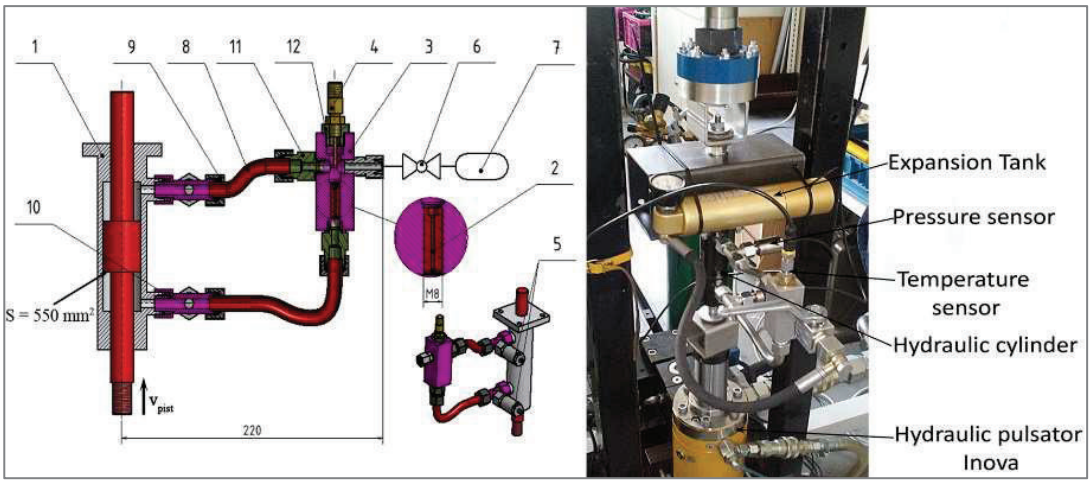

Figure 48 The experimental test rig [47]

The exact diameter of the bypass gap was measured with a microscope and a precision scale (Figure 49). The MRF-122EG and the MRF-140CG were tested.

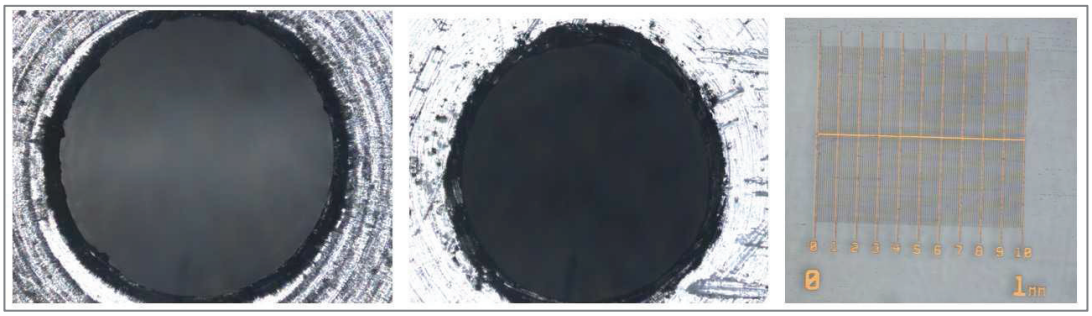

Figure 49 The diameter of the bypass gap from microscope (left, middle); precision scale (right)

Results and discussion

A comparison between the model and the experiment can be seen in Figure 50. The maximum difference between the experiment and the CFD model was 24 %. CFD model can be used for the design of the bypass gap in the magnetorheological damper; the achieved results were published at the conference listened in WOS.

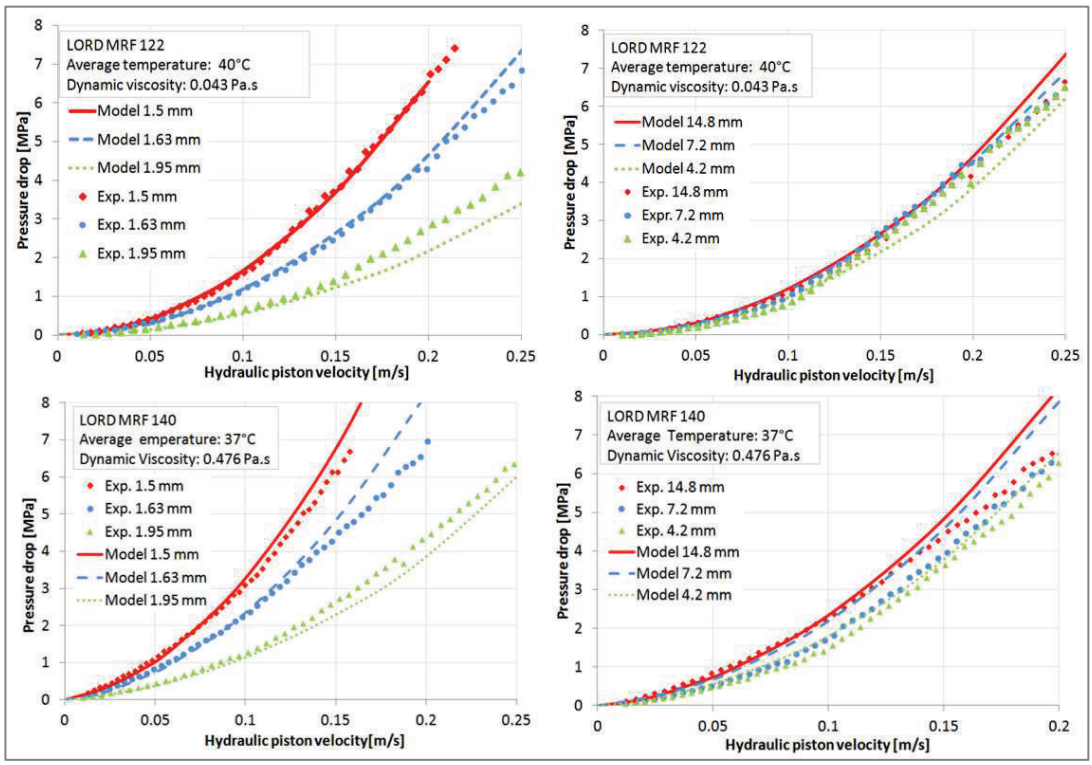

Figure 50 Comparison of the CFD model and the experiment for different diameters and lengths of the bypass gap and two types of MR fluid [47]

5.2.2 Post-yield regime

The Yang hydraulic model in section 2.4.4.2 was experimentally verified on the geometry of MR damper (attachment 1) with MRF-132DG.

Materials and methods

The tested MR damper (attachment 1) with MRF-132DG was placed into the test rig with a hydraulic pulsator (Figure 51). The load cell Interface 1730 ACK-50 kN was used for measurement of the damping force and the Messotron WLG150 sensor was used for stroke measurement. The MR damper was tested by a sweep method with

a constant stroke of 24 mm and frequency from 0.1 Hz to 4 Hz. A numerical derivation of displacement was used for determination of piston velocity.

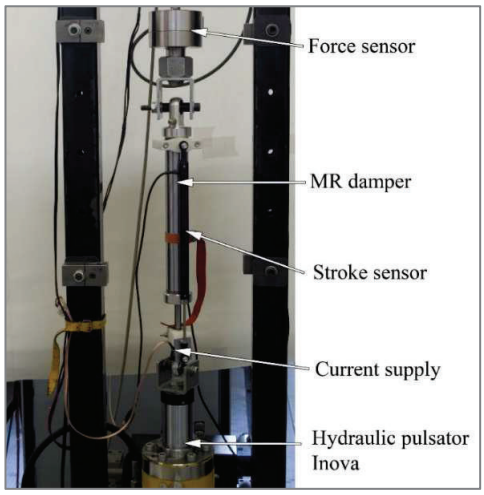

Figure 51 Measurement of circuit

The sampling frequency of 10 kHz was used for the data acquired from the experiment. The MR damper was tested in 0 A, 0.2 A, 0.4 A, 0.5 A, 1 A and 1.5 A.

Results and discussion

In the next part, the stroke, piston velocity and damping force dependency on the time are shown in Figure 52.

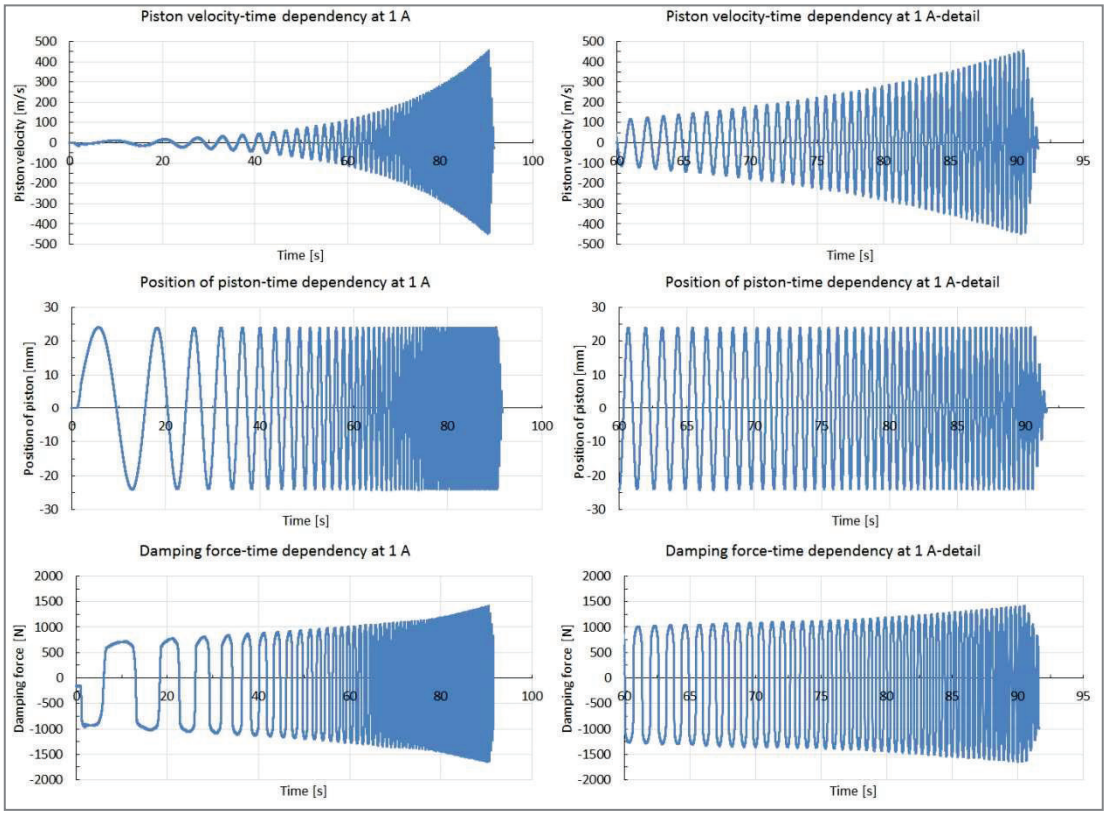

Figure 52 Measured data from the experiment

A dependency of the damping force on the piston velocity and the position of the piston are shown in Figure 53.

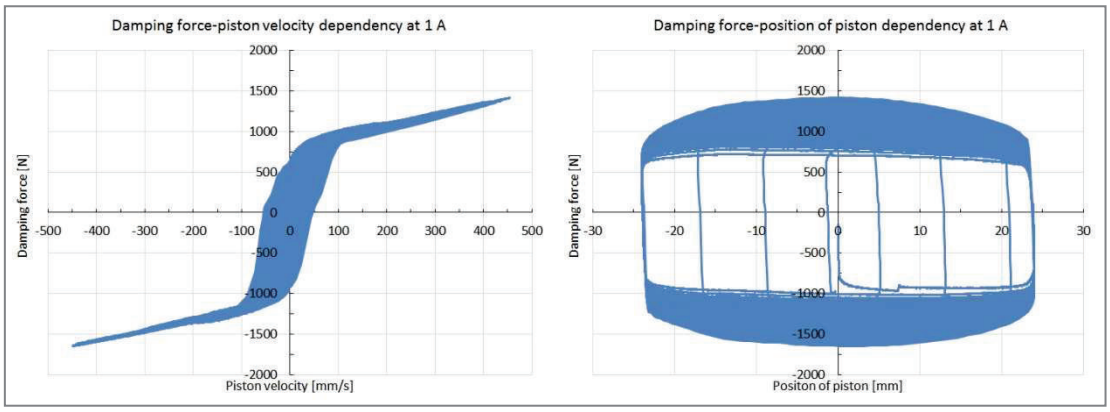

Figure 53 Damping force-piston velocity dependency (left); the damping force-position of piston dependency (right)

However, the measured F-v dependency of the MR damper has a hysteresis which is caused by elasticity of the hydraulic system. The effect of the hydraulic system elasticity was eliminated by choosing the measured data from the centre of the stroke. This method of data evaluation was programmed in Matlab. A comparison of raw (left) and evaluated (right) F-v dependency for current of 1A in the coil is plotted in Figure 54.

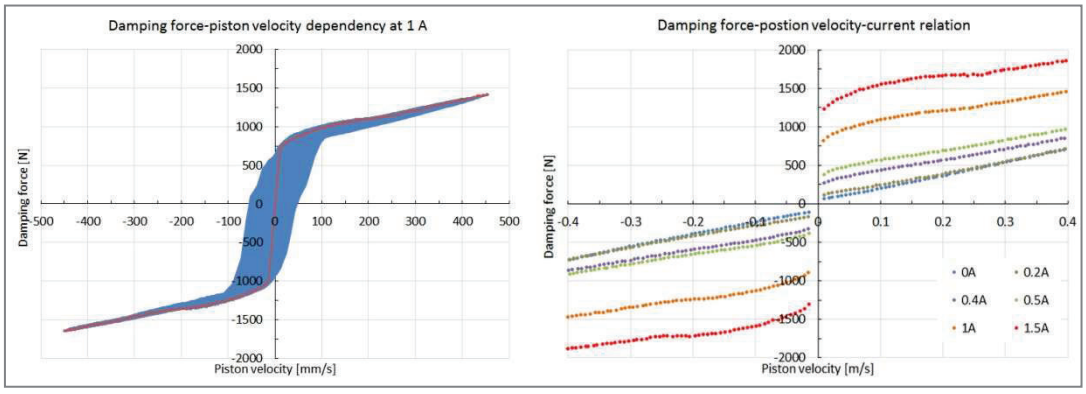

Figure 54 The measured F-v dependency at 1 A (blue) and F-v dependency for different current

The same method was used for determination of F-v dependency for the other currents (Figure 54 right). The measurement of sliding friction of the piston rod seal is important for a proper comparison of the model and the experiment. The friction force was determined by experiment at low piston velocity (0.01 m/s) as $F_f = 51\ N$ (Figure 55).

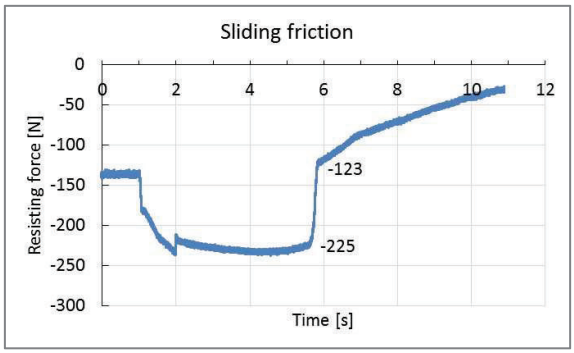

Figure 55 Sliding friction of the MR damper

The most important parameter influencing the accuracy of hydraulic model of MR damper is the yield stress in the active zone. The value of yield stress for different currents in the coil is based on the MR fluid datasheet and the results of magnetic flux density obtained by the magnetostatic model. Tab. 2 lists the results from the magnetostatic model for different currents on the coil.

Tab. 2 Results from magnetostatic model

Electrical current [A]	Magnetic flux intensity in the active zone [kA/m]	Yield stress in the active zone [kPa]
0.2	6.4	1.5
0.4	18	5.7
0.5	24	7.8
1	53	17
1.5	76	23.5

A comparison between the experiment and the model for currents of 0.2 A, 0.4 A, 0.5 A, 1 A and 1.5 A is shown in Figure 56.

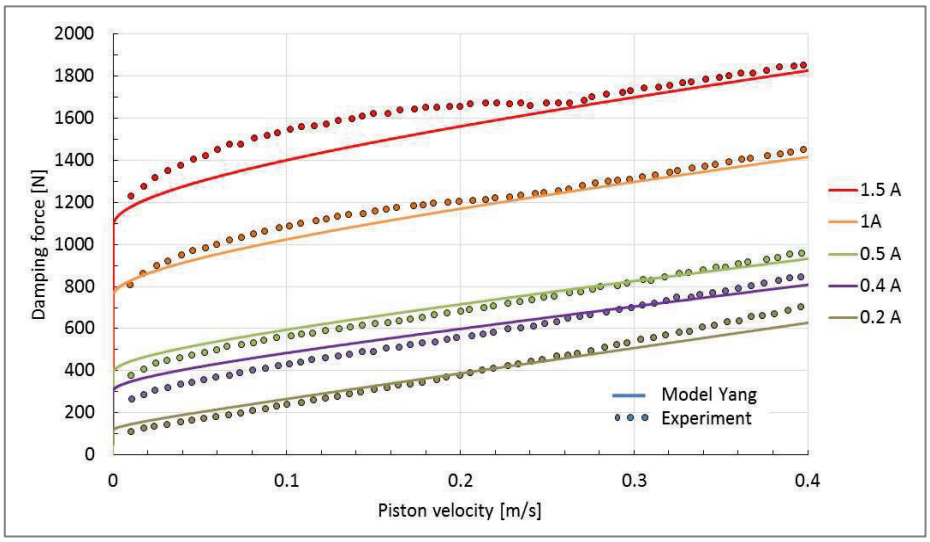

Figure 56 The comparison of the Yang hydraulic model and experiment

The maximum difference between the hydraulic model and the experiment is 21 %. I assume that the difference is caused by inaccurate dependency of yield stress and

magnetic flux density or inaccurate B-H curve of MR fluid. We do not have any information about methods of measuring yield stress or B-H curve presented in the datasheet of Lord MR fluids. However, for the design of MR damper, this accuracy of the model is sufficient.

However, a more sophisticated hydraulic model of the MR damper exists. Goldasz [38] published a bi-plastic Bingham model which included a pre-yield regime (very low piston velocity).

5.2.3 Off-state regime

The off-state regime of the MR damper was based on the hydraulic model by Yang.

Materials and methods

The most important parameter for the model is a dynamic viscosity of MR fluid at different temperatures. The temperature of the MR fluid in the hydraulic system was 30 °C. The dynamic viscosity for this temperature is 0.156 Pa.s, according to Kubík [93]. The presented measured data was obtained by method presented in previous section.

Results and discussion

A comparison between the hydraulic model and the experiment is shown in Figure 57. The maximum difference between the model and the experiment is 24 %. However, the accuracy is strongly dependent on the proper measurement of the MR fluid temperature. The accuracy of the model is also influenced by the developed of the velocity profile in the active zone or turbulent flow. The influence geometry of lids on pressured drop was neglected.

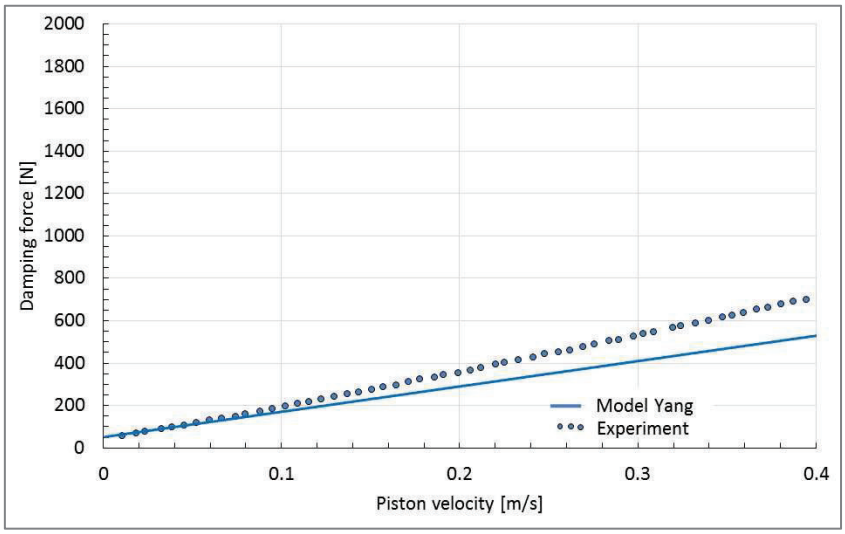

Figure 57 Comparison of the Yang model (full line) and the experiment (dots) for the off-state regime

6 MAGNETORHEOLOGICAL SUSPENSION DAMPER FOR SPACE APPLICATION

According to the state of art, a commonly used variant of the vibration isolation system for space application is based on the composite cone. Nevertheless, this cone is unsatisfactory for a wide range of space applications because of high transfer of vibration. For this reason, the systems based on damping flexure element or strut platform are used. The company Honeywell developed the vibration isolation platform ELVIS which is composed of D-Strut; this system was used in passive or active control version. The semi-active control of the damping element (control up to 25 Hz) in connection with a design concept of D-Strut seems to be a more effective vibration isolation system than the passive D-Strut of a similar weight. The MR damper appears to be a suitable candidate for semi-active control damping element.

The Honeywell company addressed Brno University of Technology with the offer to participate in the development of the semi-actively control D-Strut for the space applications. The use of a semi-actively controlled MR damper was planned with the framework of the project for the European Space Agency (ESA). It was necessary to experimentally demonstrate that a semi-active control of D-Strut system would bring a significant reduction in transfer of vibration to payload. As early as in 2014, the development of the magnetorheological suspension strut demonstrator (the project Semi-active Damping System FLPP3) started. The demonstrator of magnetorheological suspension damper (in the following section used abbreviation **m**agneto**r**heological **d**amper **strut**) for space application was designed according to specific requirements (chapter 6.1). This demonstrator was composed of bellows unit, the MR valve, and springs (chapter 6.2). Ing. Ondřej Macháček dealt with the development of bellows unit and the author of the present thesis also intensively contributed to the development of this unit. Tests of MR valve with short response time and the valve development were carried out by the author of this thesis (chapter 6.3) as its main goal; consequently, the results were published in the impact journal [91]. A vibration isolation test rig was developed for the tests of vibration isolation efficiency. The benefit of the MR semi-active damping control with the control algorithm was tested on the previously described test rig (chapter 6.4).

The **MR valve design**, described in chapter 6.3, was **created earlier** than the **methods in the chapter 5** were specified. Therefore, these methods were not used for the design of the MR valve. The time line of the project and development of the methods presented in the chapter 5 are shown in Figure 58.

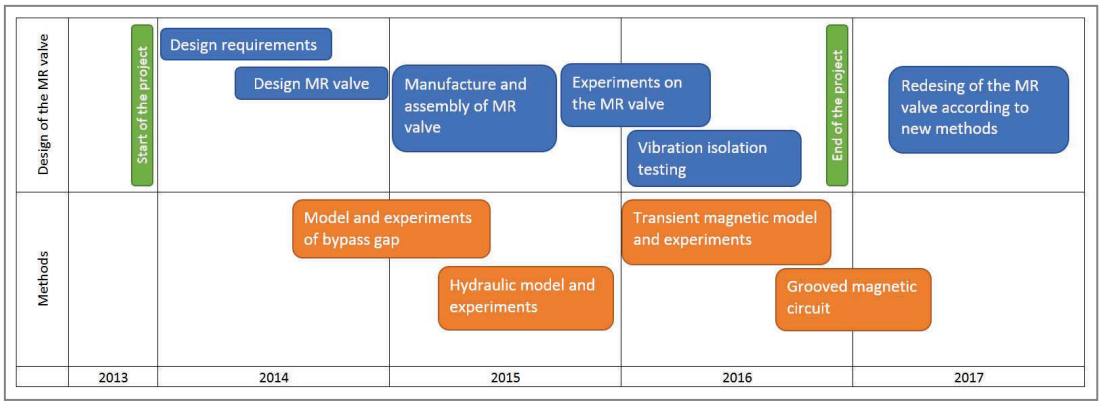

Figure 58 Time line of the project and development of method

6.1 Specific parameters for the development of the MRD-strut demonstrator

A vibration isolation system was developed for the launch vehicle Vega with the specific weight of 640 kg. The important parameter was a hermetically separated MR fluid from the surrounding environment. Another requirement was to ensure a semi-active control of frequencies up to 25 Hz. The effective control requires an average of 10 control intervals per cycle; therefore, it was necessary to change the damping force up to 250 Hz. From this frequency range, the required MR valve response time was 4 ms. The maximum required damping force of one strut in the system was 1500 N at the velocity of 0.08 m/s from the dynamic model of a vibration isolation platform, which will be similar to ELVIS. An even weight distribution of 640 kg over the eight struts (640/8 = 80 kg) was assumed. The resonant frequency of D-Strut system of 10 Hz was tuned.

6.2 The demonstrator of MRD-strut

The demonstrator of MRD-strut was based on the Honeywell D-Strut for the vibration isolation platform ELVIS (Figure 59). The resonant frequency of MRD-strut demonstrator was set to 10 Hz. This system uses bellows for the separation of the MR fluid from surroundings. The MRD-strut demonstrator is a three-parameter vibration isolation system where the damper element is semi-actively controlled. The demonstrator of MRD-strut allowed for a simple change of the stiffness springs, assembling and disassembling, a simple connection of measuring sensors, etc. The weight of this demonstrator was not an important requirement.

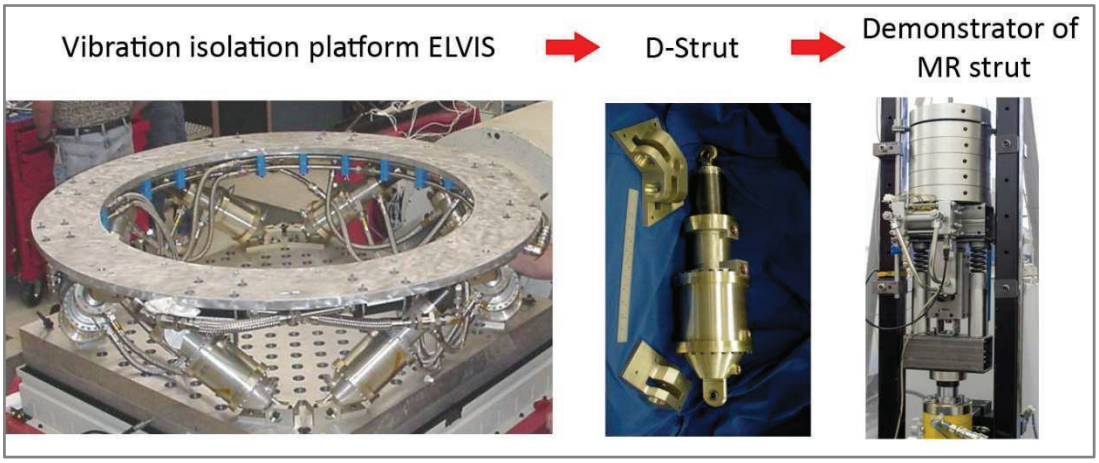

Figure 59 Demonstrator of the MRD-strut with the MR valve with short response time

The demonstrator of MRD-strut was composed of coil springs, bellows unit, MR valve and connection fittings. The stiffness of the springs can be set by a special threaded pipe. The spring is screwed into the pipe, which reduces the spring length (stiffness, Figure 61). The bellows unit was composed of two metal bellows made by Witzenmann company that are connected by the pipes to the MR valve (Figure 60, Figure 61 right).

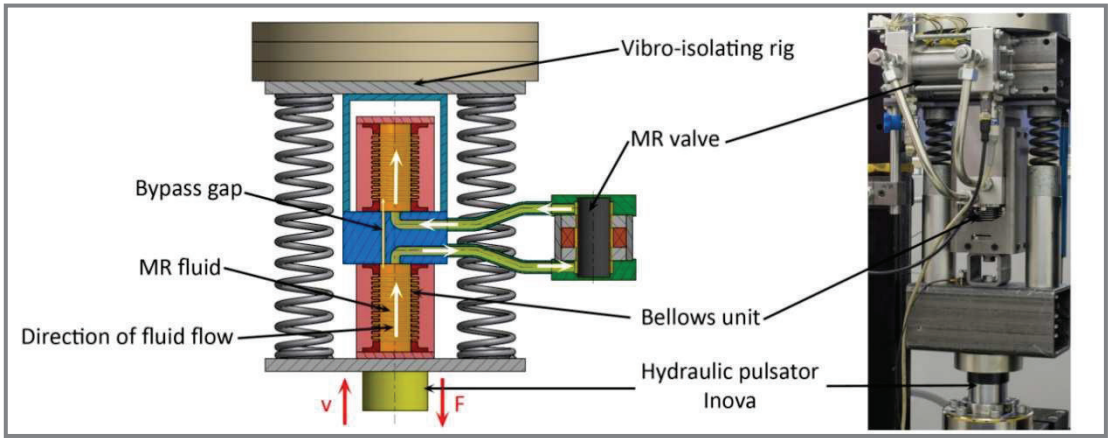

Figure 60 The demonstrator of the MRD-strut with the MR valve [92]

Compressing of primary bellows, the MR fluid flows through the MR valve to the secondary bellows that extends. The hydraulic resistance of the MR valve creates a pressure drop which leads to "inflating" of the bellows (volumetric stiffness). The bellows unit was a three-parameter vibration isolation system because of the stiffness K_B created by volumetric stiffness of bellows. The stiffness K_A was the stiffness of springs and axial stiffness of bellows. The three-parameter vibration isolation system was also important for the semi-actively controlled system because of its influence on transmissibility at higher frequencies (above 25 Hz) than that allowed by semi-active control.

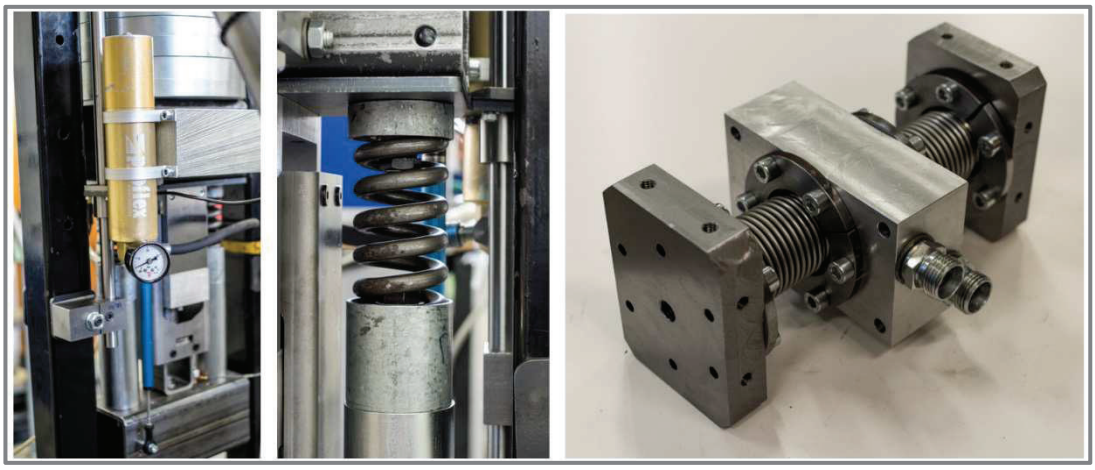

Figure 61 Location of the expanse tank (left), connection of the spring to the threaded pipe (middle), disassembled bellows unit (right)

6.3 Magnetorheological valve

As already mentioned, the MR valve design was based on the knowledge available in 2014. Some methods in chapter 5 were not used because they were not known at that time. The design and experiments of MR valve were published in the impact journal Smart Materials and Structures under the title: „**Design and testing of magnetorheological valve with fast force response time and great dynamic force range**".

Materials and methods

The MR valve design was composed of three coils (1), which were wound with opposite orientation, the ferrite magnetic circuit (2,3,5), outer tube (4), coil support (6), valve flange (8) and sealing (7, 9, 10). The magnetic circuit was made from Epcos ferrite N95 material as the ferrite material is the only material suitable for the MR valve design with short response time. The main disadvantage of this material was its poor machinability, low mechanical properties, and low level of magnetic saturation.

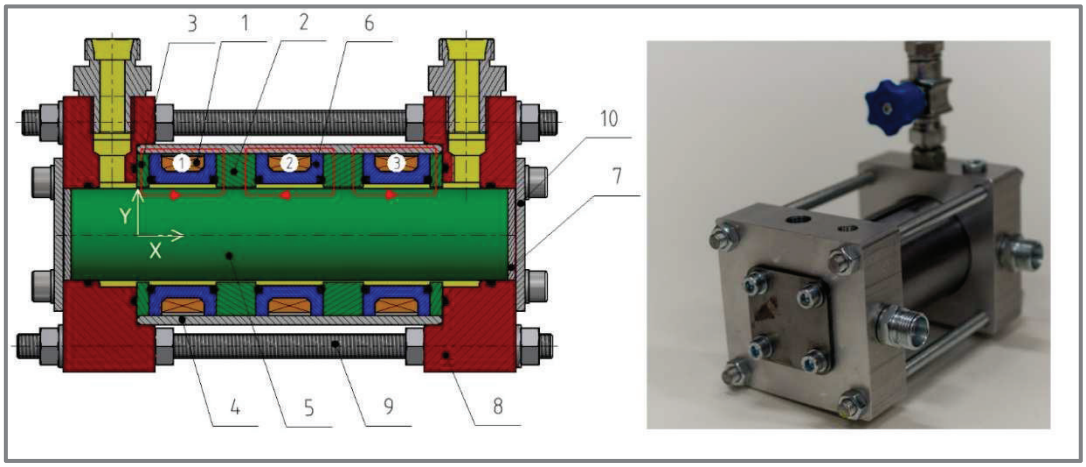

Figure 62 The developed MR valve; ferrite N95 (green), S235JR+C (grey), MR fluid (yellow), Aluminum (red), Ercatel POM (blue), copper (orange) and NBR (black) [94]

Machining of the ferrite parts can only be performed by grinding under special conditions. The round piece (5) was the most difficult part to produce; this part was prepared and machined by the company Epcos. Figure 63 shows the manufactured ferrite parts.

Figure 63 Ferrite core (left), ferrite rings (middle and right)

The expansion tank was connected to the MR valve through the hydraulic valve (Figure 61 left). The overpressure (4 bar) was set in the hydraulic system to prevent possible cavitation by the expansion tank. 230 ml of Lord MRF-122EG was used in the hydraulic system. The bypass gap of the MR valve was placed in the bellows unit. Important geometric, electric, and rheological parameters are published in [94]. Pressure, damping force, stroke, and temperature were measured during the experiment with several sensors as shown in Figure 64.

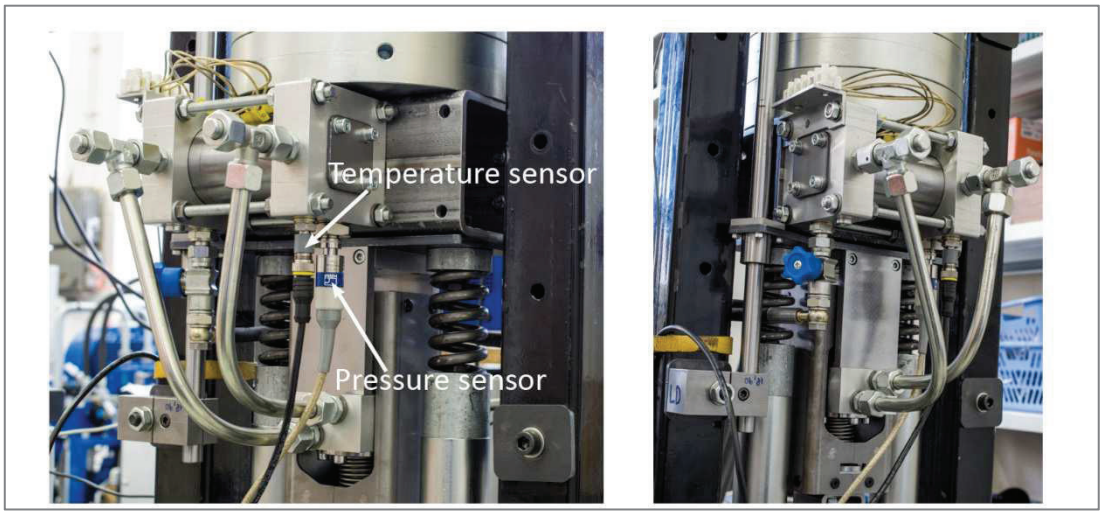

Figure 64 Position of the MR valve on the demonstrator of the MRD-strut; location of the pressure and the temperature sensor

The response time and force-velocity-current course were measured on the manufactured and assembled demonstrator of the MRD-strut with the MR valve. The F-v-I course was measured with the hydraulic pulsator Inova. The sweep method with constant stroke of 5 mm from 0.1 Hz to 8 Hz was used. The points from the centre of the stroke (zero compression of springs) were selected from the measured data as this is the method of how to eliminate the stiffness of the hydraulic system.

The response time of the damping force was measured on the developed system with the MR valve. The coils of the MR valve were supplied by the current controller which was controlled by the system Arduino. The electric current on the

coil was switched between the on-state and off-state with frequency of 2 Hz (Figure 65). The sampling frequency of measurement was 10 kHz.

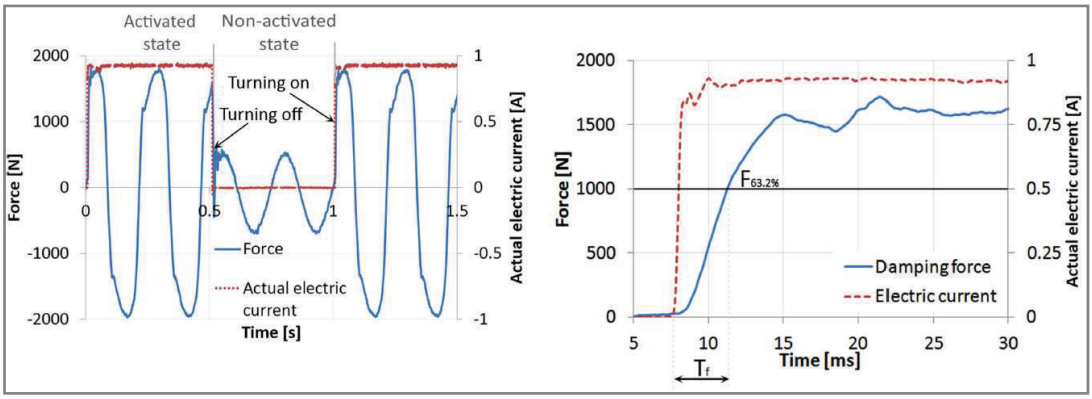

Figure 65 Measurement methodology of the response time [94]

Results and discussion

The hydraulic model presented in [92] was compared with the experiment (Figure 66). The maximum difference between the model and the experiment was 18 %.

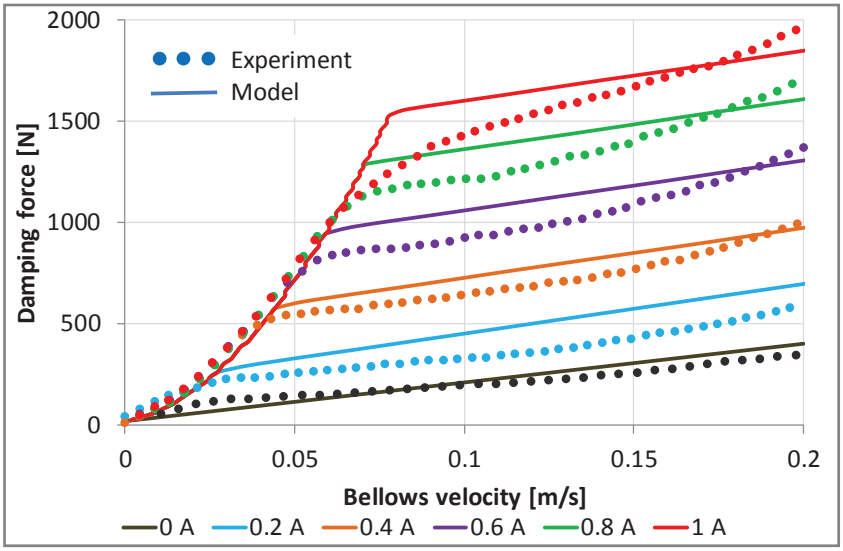

Figure 66 F-v-I course of the demonstrator MR strut with the MR valve; the comparison of hydraulic model and experiment [94]

From the measured data and the model, a dynamic force range of the MRD-strut was determined. According to the experiment, the developed system with the MR valve achieves a maximum dynamic force range 8.

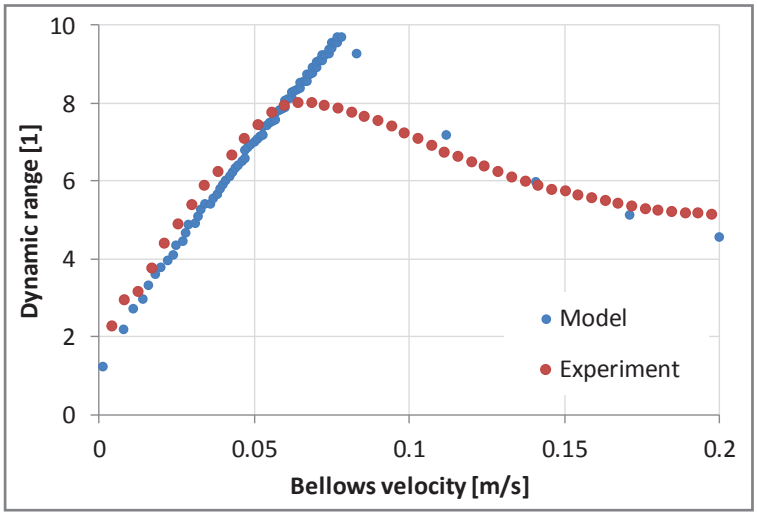

Figure 67 Dynamic force range of the developed system with the MR valve [94]

The response time was evaluated as a rise or drop of 63.3 % steady state damping force. More details about the methodology of measurement of response time is in the publication [94]. The evaluated data from the measurement of response time dependency on bellows velocity can be seen in Figure 68.

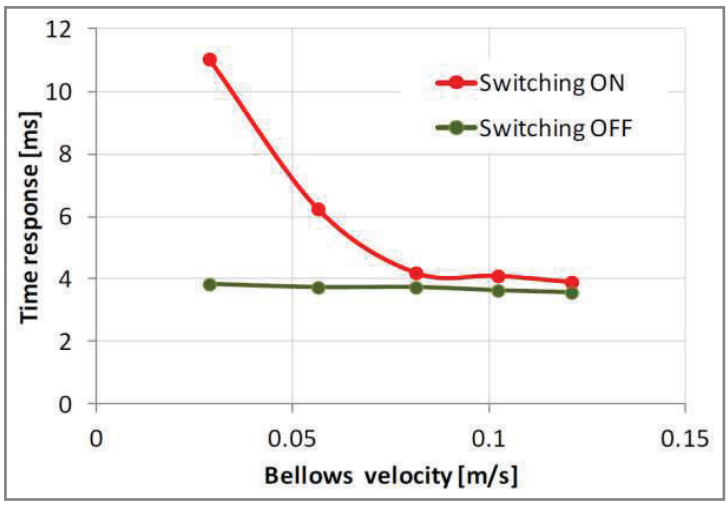

Figure 68 The response time of the developed demonstrator of the MRD-strut with the MR valve in the current of 1A [94]

The response time of developed system with the MR valve achieved the response time of approximately 4.1 ms for bellows velocity higher than 0.08 m/s. For lower velocity of bellows and a rise control signal, response times were higher. The influence of piston velocity on the response time is probably caused by no zero stiffness of the hydraulic system. The response time 4.1 ms is primarily caused by the outer tube where eddy currents could be generated.

6.4 Vibration isolation efficiency of developed system with MR valve

Materials and methods

The developed MRD-strut with the MR valve was placed to the vibration isolation rig, see in Figure 69. The payload weight was set on 75 kg plus the weight of the parts connected to the MR valve. The bellows unit was excited by the hydraulic pulsator with constant acceleration of 1 g in the range from 3 Hz to 50 Hz over 60 sec.

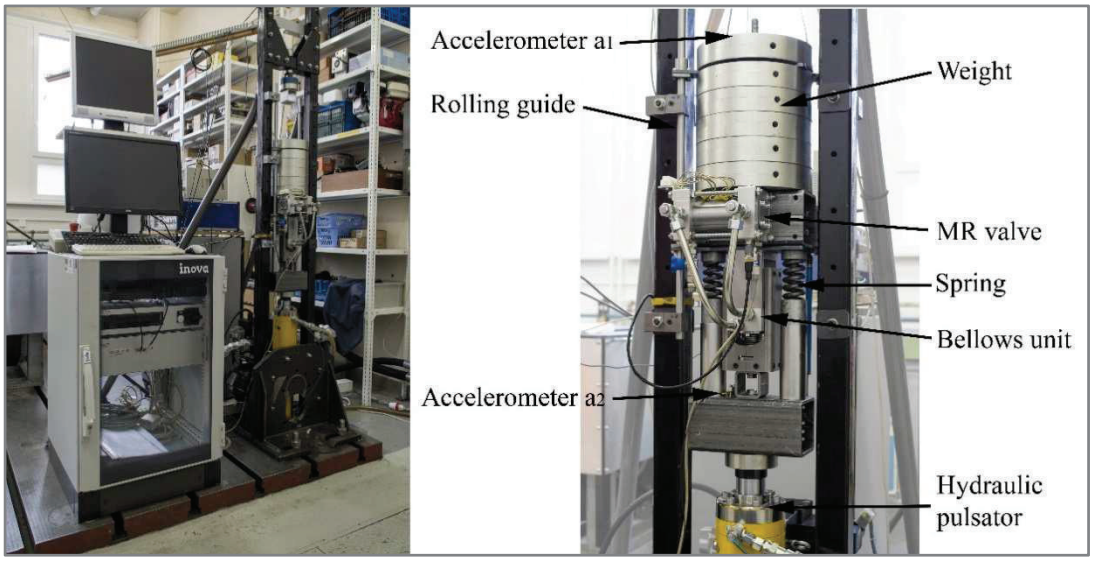

Figure 69 Vibration isolation rig with demonstrator of MRD strut with MR valve (left), description of demonstrator (right)

The acceleration of the hydraulic pulsator a_2 (base) and the weight a_1 (payload) were measured with a piezoelectric sensor Bruel and Kjaer 4507B (Figure 69, Figure 70). The data from the accelerometer were acquired by Dewe 50 and software Dewesoft.

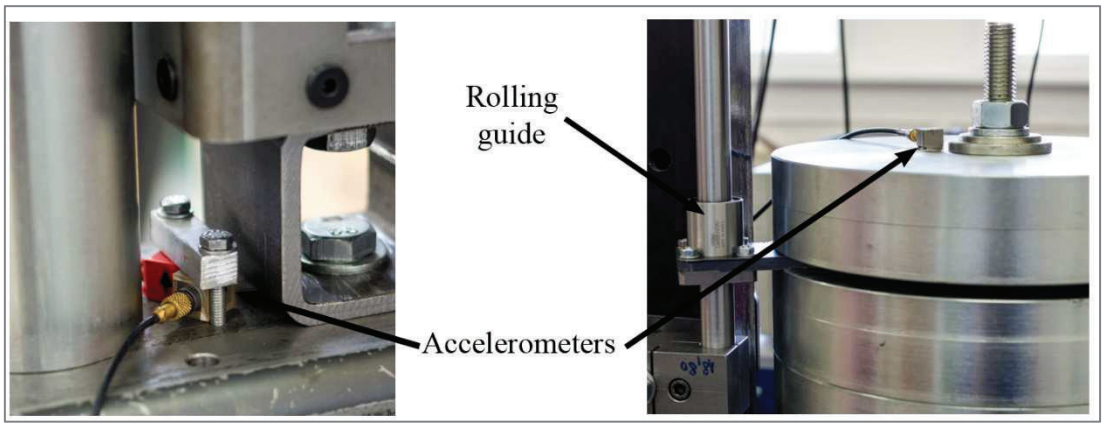

Figure 70 The location of accelerometers

Two mathematical channels were created by the FFT analysis of the base acceleration and FFT analysis of payload acceleration.

Results and discussion

By dividing these mathematical channels, the acceleration transmissibility of the tested system was created, see Figure 71.

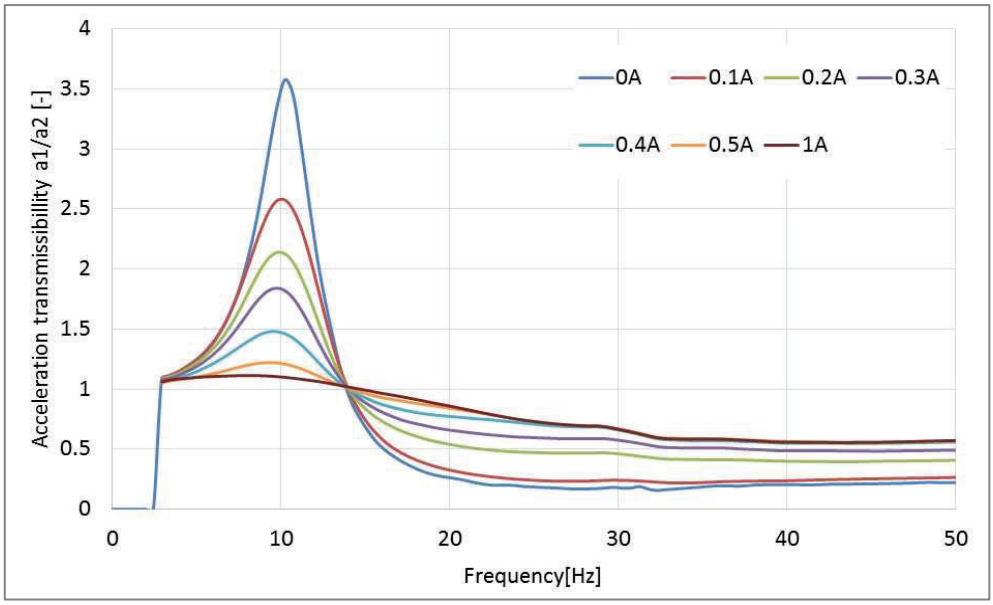

Figure 71 Acceleration transmissibility of the MRD-strut demonstrator in the passive variant for different electric currents

An increase in the electric current caused a decrease in acceleration transmissibility at the resonant frequency and an increase in the acceleration transmissibility at the isolation frequency. The semi-active control algorithm LQR was used for the control of the damping force. However, the company Honeywell did not give their consent to the publication of a more detailed description of the control algorithm. A comparison of the passive variant (maximum and minimum damping) and the semi-active variant with the control algorithm LQR is illustrated in Figure 72.

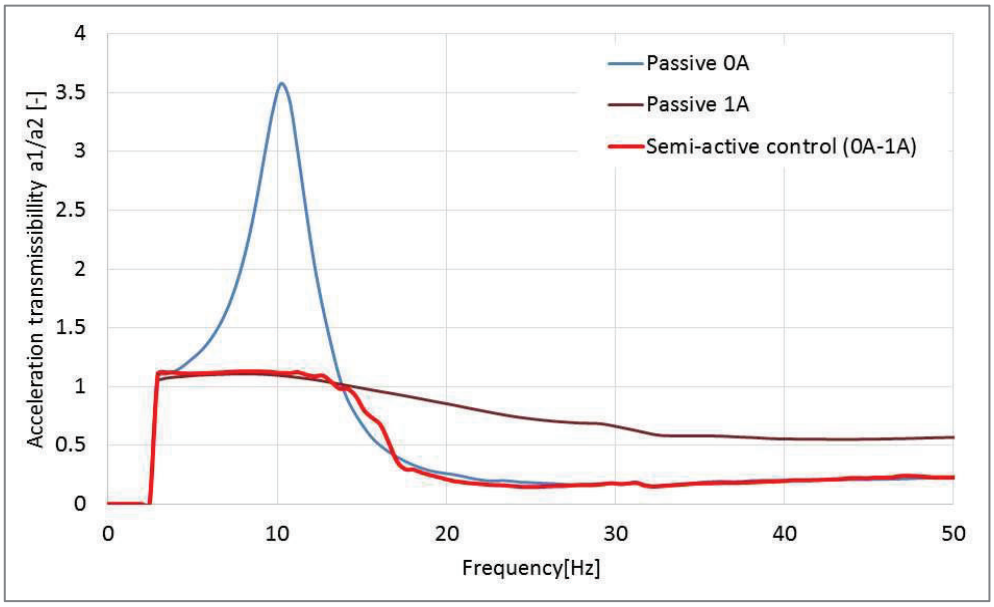

Figure 72 Comparison of the passive and the semi-active variant of the vibration isolation system

The acceleration transmissibility from the semi-active control at the resonant frequency is similar to the acceleration transmissibility from maximum damping (1 A), while at the isolation frequency, it is similar to minimum damping (0 A). The system was tested **only on the sweep excitation signal** with the constant acceleration amplitude. A significant benefit of the semi-active control was demonstrated.

The results of the project were very well rated in ESA. The project is expected to continue in 2017 and will be focused on the development of the MR strut with the aim to achieve the TR6 level. In the next project, a design of the MR valve will be modified according to the new knowledge available.

6.5 Preliminary concept of the MRD valve with application of new methods

A preliminary concept of the MR valve for space with application of new methods can be seen in Figure 73. A magnetic circuit is made from Fe-Co alloy (Vacoflux 27 and Vacoflux 18 HR) and a grooving method for designing a magnetic circuit is used. The material Vacoflux achieves the yield strength about 250 MPa. The thickness of the grooves is 0.3 mm. The covers are made from Al alloy.

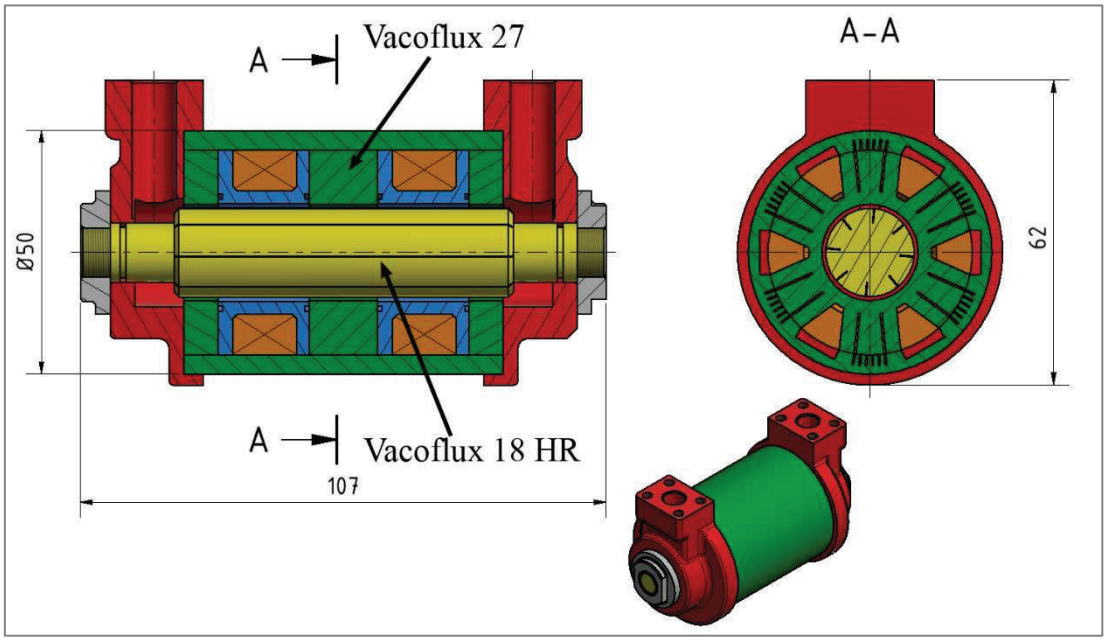

Figure 73 A proposed concept of the MR valve for space with application of new methods; Vacoflux 27 (green), Vacoflux 18 HR (yellow), Al alloy (red) and steel (grey).

The grooves in the core (Figure 73, yellow part) are filled with plastic material. The position of grooves in the magnetic circuit is shown in Figure 74.

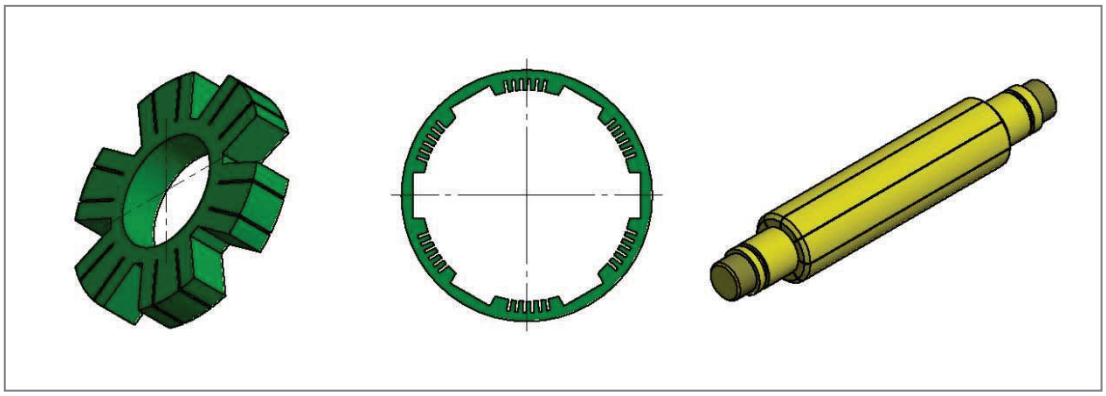

Figure 74 Position of grooves in the magnetic circuit of MR valve

The response time of this MR valve was estimated to 1.4 ms. The damping force of 1600 N at 0.1 m/s and dynamic force range 10 will be achieved in the MR valve according to the hydraulic model. The weight of this valve is 1.04 kg.

7 CONCLUSION

7

The present thesis deals with the development of the MR damper with short response time for space application. Vibration and shock loads during the shipment of launch vehicle may cause destruction of sensitive equipment of the satellites. Therefore, satellites must be designed to high dynamic level, which rapidly increases the cost and weight of satellites. Other method is used to the vibration isolation system which is between the launch vehicle propulsion and the payload. An interesting candidate for vibration isolation system for space application is a semi-active control vibration isolation system which contains a magnetorheological damper (valve) with short response time. The design process of MR damper with short response time suffers from a number of limitations. Some methods for design of MR damper with short response time doesn't exists.

The main aim of the present thesis was to develop a demonstrator of the MR suspension damper with short response time for space application. The original design and results were published in scientific paper. The magnetic circuit of this damper was manufactured from the ferrite material which allows for short response time of the MR damper. The measurement of F-v-I and response time were performed on the manufactured demonstrator. A designed MR damper achieved the dynamic force range 8 (eight) and the response time of 4.1 ms according to the experiment.

New methods for design of MR damper with short response time were published as sub-aims of the thesis. First sub-aim of thesis was to find a method to decrease the response time of the MR damper. A grooving method of magnetic circuit (shape approach) of the MR damper and the magnetic circuit containing rods of the ferromagnetic material with bridges were presented as a new method allowing for decrease in the response time of the MR damper. The decrease in the response time of the MR damper to 1.7 ms occurred when steel or similar material were used (high magnetic saturation). This method was patented under the title: "The magnetic circuit containing rods of ferromagnetic material and the method of its manufacture".

Second sub-aim was magnetostatic, transient magnetic models and their experimental verification. A magnetostatic model and its experimental verification on the geometry of the MR damper were presented in this work with a difference between the model and the experiment under 1 %. The output of this model is an important input into the post-yield hydraulic model. The transient magnetic model and its experimental verification were presented in this thesis with a difference between the model and the experiment 28 %. The transient magnetic model allows to design (material selection, geometry etc.) the MR damper for specific response time of magnetic field. The shape of B-H curve of the material magnetic circuit influences the dependency of the response time of magnetic field on the electric current of the MR damper according to the transient magnetic model.

Third sub-aim was hydraulic models of the MR damper and their experimental verification. The CFD hydraulic model of the bypass gap (pre-yield regime) of the MR damper was presented. The experimental test rig was developed for testing the bypass gap. A different diameter and length of the bypass gap were tested and compared with the experiment. The maximum difference between the model and the experiment was 24 %. The Yang hydraulic model of the post-yield regime and the off-state was compared with the experiment on the geometry of the

MR damper (attachment). The maximum difference between the model and the experiment was 21% for the post-yield regime and 24 % for the off-state, respectively.

The current thesis contains the original results extending the knowledge in the area of magnetorheological damper. The main contribution of the thesis can be summarized as follows:

- Experimental verification of the transient magnetic model of the magnetic circuit of the MR damper [89]. This model allows to design MR damper with specific response time of magnetic field.
- New method for the elimination of the eddy currents in the magnetic circuit of the MR damper [92]. This method allows to design MR damper with short response time and high dynamic force range.
- A unique design of the MR damper with short response time for space application was published [94].

Regarding the scientific questions, the obtained knowledge can be summarized in the following concluding remarks:

- Experiments conducted using ferrite material for magnetic circuit is possible to design MR damper with response time near 4 ms (**hypothesis H1 was confirmed**).
- Multi-coil configuration of MR damper allows for dynamic force range higher than 4 when the ferrite material is using (**hypothesis H2 was falsified)**.
- The grooving method of magnetic circuit or magnetic circuit containing rods of ferromagnetic material allow to design magnetic circuit of MR damper from material with high magnetic saturation and low electric resistivity which achieved a short response time. Those methods increase path of eddy currents (**hypothesis H3 was confirmed**).

The presented methods allow for a design of the MR damper with response time of magnetic field under the response time of the MR fluid itself. Now, a limiting parameter for the response time of the MR damper is the MR fluid itself. Next research will be targeted at the development of MR fluid with a lower response time than that commercially available.

8 LIST OF PUBLICATION AND PATENTS

8.1 Papers published in journals with impact factor

KUBÍK, M.; MACHÁČEK, O.; STRECKER, Z.; ROUPEC, J.; MAZŮREK, I., 2017. Design and testing of magnetorheological valve with fast force response time and great dynamic force range. Smart Materials and Structures. 26(4), 47002. ISSN 0964-1726
(**Journal impact factor = 2.909, quartile Q1)**

KLAPKA, M.; MAZŮREK, I.; MACHÁČEK, O.; KUBÍK, M., 2016. Twilight of the EUSAMA diagnostic methodology. MECCANICA, p. 1-12. ISSN: 0025-6455.
(**Journal impact factor = 1.83, quartile Q2**)

STRECKER, Z.; MAZŮREK, I.; ROUPEC, J.; MACHÁČEK, O.; KUBÍK, M.; KLAPKA, M. Design of magnetorheological damper, with short time response. JOURNAL OF INTELLIGENT MATERIAL SYSTEMS AND STRUCTURES, 2015, roč. 26, č. 14, s. 1951-1958. ISSN: 1045- 389X.
(**Journal impact factor = 1.975, quartile Q2**)

ROUPEC, J.; BERKA, P.; STRECKER, Z.; MAZŮREK, I.; KUBÍK, M.; MACHÁČEK, O.; ANDANI, M., 2017. A novel method for measurement of MR fluid sedimentation and its experimental verification. Smart Materials and Structures.
(**After review**, **Journal impact factor = 2.909**, **quartile Q1)**

8.2 Papers in conference proceedings (Scopus or WOS)

KUBÍK, M.; MACHÁČEK, O.; STRECKER, Z.; ROUPEC, J.; MAZŮREK, I. Transient magnetic model of magnetorheological damper and its experimental verification. The 4th International Conference on Mechantronics and Mechanical Engineering 2017

ROUPEC, J.; KUBÍK, M.; MAZŮREK, I.; STRECKER, Z. Problems of FEM Analysis of Magnetic Circuit. In Mechatronics 2013 - Recent Technological and Scientific Advances. London: Springer, 2013. s. 299-305. ISBN: 978-3-319-02294-9.

STRECKER, Z.; ČÍPEK, P.; ROUPEC, J.; MACHÁČEK, O.; KUBÍK, M. Testing of Car Suspension With Fast MR Damper, Controlled by Modified Groundhook Algorithm. In Engineering Mechanics 2016. Engineering mechanics 2014. First edition. Prague: Institute of Thermomechanics Academy of Sciences of the Czech Republic, v.v.i., 2016. s. 526-529. ISBN: 978-80-87012-59-8. ISSN: 1805-8248.

KUBÍK, M.; MACHÁČEK, O.; STRECKER, Z.; ROUPEC, J.; MAZŮREK, I. Hydraulic resistance of magnetorheological damper viscous bypass gap. In Engineering Mechanics 2016. Engineering mechanics 2014. first edition. Praha: Institute of Thermomechanics Academy of Sciences of the Czech Republic, 2016. s. 330-333. ISBN: 978-80-87012-59-8. ISSN: 1805-8248.

ROUPEC, J.; MAZŮREK, I.; STRECKER, Z.; KUBÍK, M.; MACHÁČEK, O. Temperature dependence of magnetorheological fluid yield stress and Bingham

viscosity. In Engineering Mechanics 2016. Engineering mechanics 2014. Praha: Academy of Science of the Czech Republic, v.v.i., 2016. s. 498-501. ISBN: 978-80-87012-59-8. ISSN: 1805-8248.

MACHÁČEK, O.; KUBÍK, M.; MAZŮREK, I.; STRECKER, Z.; ROUPEC, J. Frictionless Bellows Unit Connected with the Magnetorheological Valve. In ENGINEERING MECHANICS 2016. First edition, 2016. Praha: Institute of Thermomechanics Academy of Sciences of the Czech Republic, 2016. s. 354-357. ISBN: 978-80-87012-59- 8.

8.3 Papers in conference proceedings

KUBÍK, M.; MAZŮREK, I. Design of semi- active magnetorhelogical valve. In The Latest Methods of Construction Design. Springer International Publishing, 2014. s. 51-56. ISBN: 978-3-319-22761- 0.

STRECKER, Z.; ROUPEC, J.; KUBÍK, M.; FRIEDEL, D. Experimental evaluation of MR damper time response on modified Groundhook algorithm efficiency. In Engineering Mechanics 2014. 1st. 2014. s. 600-603. ISBN: 978-80-214-4871- 1.

KUBÍK, M.; MAZŮREK, I.; ROUPEC, J. Decreasing of sliding friction in hydraulic piston damper. In Engineering mechanics 2015. Prague: 2015. s. 170-171. ISBN: 978-80-86246-42- 0.

KUBÍK, M.; MACHÁČEK, O.; STRECKER, Z.; MAZŮREK, I. FEM model of magnetic circuit and its verifivation. In Book of Proceeding of 56th International Conference of Machine Design Departments. Nitra: Publishing Center SUA Nitra, 2015. s. 99-104. ISBN: 978-80-552-1377- 4.

8.4 Patent

KUBÍK M.; MACHÁČEK O.; STRECKER Z.; ROUPEC J.; MAZUREK I.; KOUTNY D.; PALOUŠEK D., 2017. Struktura jádra obsahujícího pruty z feromagnetického materiálu a způsob jejího vytvoření. Czech Republic, PV 2017-91. 2017.

9 LITERATURE

[1] JOHNSON, Conor D, Paul S WILKE and Scott C PENDLETON. SoftRide Vibration and Shock Isolation Systems that Protect Spacecraft from Launch Dynamic Environments 10 Hz 70 Hz. 2006, pp. 89–102.

[2] JOLLY, Mark R, Jonathan W BENDER, J David CARLSON and Lord DRIVE. Properties and Applications of Commercial Magnetorheological Fluids. *Journal of Intelligent Material Systems and Structures*. 1999, vol. 10, no. 1, pp. 5–13.

[3] RABINOW, Jacob. The Magnetic Fluid Clutch. *Transactions of the American Institute of Electrical Engineers*. 1948, vol. 67, no. 2, pp. 1308–1315. ISSN 0096-3860.

[4] KORDONSKY, W.I. Elements and Devices Based on Magnetorheological Effect. *Journal of Intelligent Material Systems and Structures*. 1993, vol. 4, pp. 65–69.

[5] KORDONSKY, W.I. Magnetorheological valve and devices incorporating magnetorheological elements. 1995.

[6] ACHEN, Albert, James TOSCANO, Robert MARJORAM, Ken St CLAIR, Bill MCMAHON, Alexander GOELZ and Shigeru SHUTTO. Semi-Active Vehicle Cab Suspension Using Magnetorheological (Mr) Technology. *Proceedings of the JFPS International Symposium on Fluid Power*. 2008, vol. 2008, pp. 561–564.

[7] ROUPEC, Jakub. *Mezní a degradační procesy magnetoreologických tlumičů odpružení*. B.m., 2011. Brno University of Technology.

[8] *BWI group*. 2013. Available at: http://www.bwigroup.com/en/

[9] WEBER, Felix, Hans DISTL and Peter HUBER. Design, implementation and field test of the adaptive damping system of the Franjo Tudjman Bridge nearby Dubrovnik, Croatia. *IABSE Symposium* .... 2007, no. November 2015. ISSN 22213783.

[10] YANG, G, Spencer JR, D CARLSON and K SAIN. Large-scale MR fluid dampers: modeling and dynamic performance considerations. *Engineering Structures*. 2002, vol. 24, pp. 309–323.

[11] STRECKER, Z., J. ROUPEC, I. MAZUREK, O. MACHACEK, M. KUBIK and M. KLAPKA. Design of magnetorheological damper with short time response. *Journal of Intelligent Material Systems and Structures*. 2015, vol. 26, no. 14, pp. 1951–1958. ISSN 1045-389X.

[12] *Advanced Mechanical engineering solution*. Available at: http://www.amesweb.info

[13] PIERSOL, Allan G and Thomas L PAEZ. *Harris' shock and vibration handbook*. 2010. ISBN 9780071633437.

[14] CARLSON, J. David. *Electric/Magnetic Controlling Vibration with Magnetorheological Fluid Damping*. 2002. Available at: http://www.sensorsmag.com/sensors/electric-magnetic/controlling-vibration-with-magnetorheological-fluid-damping-999

[15] *Shoxs seats*. Available at: http://www.nauticexpo.com/prod/shoxs/product-49138-403729.html

[16] *Letecká doprava budoucnosti*. Available at: http://vtm.e15.cz/letecka-doprava-budoucnosti-setrim-setris-setrime

[17] HARRIS, C. M. *Shock and Vibration Handbook, 2nd ed.* 1977. ISBN 0071370811.
[18] VERVOORDELDONK, Michiel J, Theo A M RUIJL and Rob M G RIJS. Development of a novel active isolation concept. 2004.
[19] STRIBERSKY, Anton, Andreas KIENBERGER and Günther WAGNER. Design and Evaluation of a Semi-Active Damping System for Rail Vehicles. 2017, vol. 3114, no. June.
[20] LAU, Y K and W H LIAO. Design and analysis of magnetorheological dampers for train suspension. 2005, vol. 219, pp. 261–276.
[21] SACHS, ZF. *Suspension Components and Systems*. 2010. Available at: http://www.interservice.bg/sites/default/files/fahrwerkkomponentenundsystemefrnutzfahrzeuge.pdf
[22] ZHANG, Hailong, Enrong WANG, Fuhong MIN, Rakheja SUBASH and Chunyi SU. Skyhook-based semi-active control of full-vehicle suspension with magneto-rheological dampers. *Chinese Journal of Mechanical Engineering*. 2013, vol. 26, no. 3, pp. 498–505. ISSN 1000-9345.
[23] LIU, Y, T P WATERS and M J BRENNAN. A comparison of semi-active damping control strategies for vibration isolation of harmonic disturbances. *Journal of Sound and Vibration*. 2005, vol. 280, nos. 1–2, pp. 21–39. ISSN 0022-460X.
[24] LIU, Yuyou. *SEMI-ACTIVE DAMPING CONTROL FOR VIBRATION ISOLATION OF BASE DISTURBANCES*. B.m., 2004. University of Southampton.
[25] ŠIKA, Zbyněk. *Aktivní a poloaktivní snižování mechanického kmitání strojů*. B.m., 2004. České vysoké učení technické v Praze.
[26] ESLAMINASAB, N. and M.F. GOLNARAGHI. The effect of time delay of the semi-active dampers on the performance of on-off control schemes. In: *International Mechanical Engineerong congress and Exposition*. 2007.
[27] ESA. Ariane 5 User ' s Manual. 2011, no. 5.
[28] CAMARASA PATRICK, DEMERVILLE TONY, Plagne Alain. Shock attenuation system for spacecraft and adaptor. In: *European Conference on Spacecraft Structures*. 2005.
[29] *Ariane 5 receives payloads for launch next week*. Available at: www.spaceflightnow.com
[30] ROUPEC, J, I MAZUREK, Z STRECKER and M KLAPKA. The behavior of the MR fluid during durability test. *Journal of Physics: Conference Series*. 2013, vol. 412, no. 1, p. 12024. ISSN 1742-6588.
[31] HAUSWIRTH, Rainer. Viscous isolation and damping strut utilizing a fluid mass effect. US 20050217954 A1. 2008. USA. Available at: doi:
[32] COBB, Richard G, Jeanne M SULLIVAN, Alok DAS, L PORTER, T Tupper HYDE, Torey DAVIS, Zahidul H RAHMAN and John T SPANOS. Vibration isolation and suppression system for precision payloads in space. 1999, vol. 8, pp. 798–812.
[33] HINDLE, Tim. Design Study for Small Satellite Softride Launch Vibration Isolation System. 2005, no. 5.
[34] RUEBSAMEN, Dale T. Summary of launch vibration isolation system. no date.
[35] DAVIS, Lawrence P. Three parameter viscous damper and isolator.

US005332070A. 1994. US.
[36] COLLETTE, Christophe, Stef JANSSENS and Kurt ARTOOS. Review of Active Vibration Isolation Strategies. 2011, no. 4, pp. 1–8.
[37] DAVIS, Porter, Dave CUNNINGHAM and John HARRELL. Advanced 1.5 Hz passive viscous isolation system. In: *35th Structures, Structural Dynamics, and Materials Conference*. B.m.: American Institute of Aeronautics and Astronautics, 1994, Structures, Structural Dynamics, and Materials and Co-located Conferences. Available at: doi:
[38] GOŁDASZ, Janusz and Bogdan SAPIŃSKI. *Insight into Magnetorheological Shock Absorbers*. Cham: Springer International Publishing, 2015. ISBN 978-3-319-13232-7.
[39] CARLSON, J.David and Mark R JOLLY. MR fluid, foam and elastomer devices. *Mechatronics*. 2000, vol. 10, no. 4, pp. 555–569. ISSN 09574158.
[40] GRUNWALD, A. and A.G. OLABI. Design of magneto-rheological (MR) valve. *Sensors and Actuators A: Physical*. 2008, vol. 148, no. 1, pp. 211–223. ISSN 09244247.
[41] GUOHUI, Yang, Fengchen TU, Quan YANG, Caichun HE and Lida WANG. 2012 International Conference on Future Energy, Environment, and MaterialsExperimental Study and Design on Automobile Suspension Made of Magneto-Rheological Damper. *Energy Procedia*. 2012, vol. 16, pp. 417–425. ISSN 1876-6102.
[42] GUDMUNDSSON, Ketill Heidar. *Design of a Magnetorheological Fluid for an MR Prosthetic Knee Actuator with an Optimal Geometry*. B.m., 2011. University of iceland.
[43] SHAFER, Alex S. and Mehrdad R. KERMANI. Design and validation of a magneto-rheological clutch for practical control applications in human-friendly manipulation. *Proceedings - IEEE International Conference on Robotics and Automation*. 2011, pp. 4266–4271. ISSN 10504729.
[44] NGUYEN, T. M., C. CIOCANEL and M. H. ELAHINIA. A Squeeze-Flow Mode Magnetorheological Mount: Design, Modeling, and Experimental Evaluation. *Journal of Vibration and Acoustics*. 2012, vol. 134, no. 2, p. 21013. ISSN 07393717.
[45] JOLLY, M. R., J. W. BENDER and J. D. CARLSON. Properties and Applications of Commercial Magnetorheological Fluids. *Journal of Intelligent Material Systems and Structures*. 1999, vol. 10, no. 1, pp. 5–13. ISSN 1045-389X.
[46] SOHN, Jung Woo, Jong-Seok OH and Seung-Bok CHOI. Design and novel type of a magnetorheological damper featuring piston bypass hole. *Smart Materials and Structures*. 2015, vol. 24, no. 3, p. 35013. ISSN 0964-1726.
[47] KUBÍK, M.; MACHÁČEK, O.; STRECKER, Z.; ROUPEC, J.; MAZUREK, I. Hydraulic resistance of magnetorheological damper viscous bypass gap. *In Engineering Mechanics 2016*. 2016, vol. 1, pp. 330–333.
[48] HU, G., M. LONG, M. HUANG and W. LI. Design, Analysis, Prototyping, and Experimental Evaluation of an Efficient Double Coil Magnetorheological Valve. *Advances in Mechanical Engineering*. 2015, vol. 6, pp. 403410–403410. ISSN 1687-8132.
[49] WU, Guangbin, Zhimin FENG, GANG ZHANG and Zhenning HOU. Experimental study on response time of magnetorheological damper. In: *2011*

2nd International Conference on Artificial Intelligence, Management Science and Electronic Commerce (AIMSEC). B.m.: IEEE, 2011, p. 3968–3972. ISBN 978-1-4577-0535-9.

[50] GONCALVES, Fernando D, Mehdi AHMADIAN and J D CARLSON. Investigating the magnetorheological effect at high flow velocities. *Smart Materials and Structures*. 2005, vol. 15, pp. 75–85. ISSN 0964-1726.

[51] GUAN X, GUO P, Ou J. Study of the time response of MR dampers. In: *Second international conference on smart materials and nanotechnology in engineering,*. 2009.

[52] MASS, J and D GUTH. Experimental investigation of the transient behaviour of MR fluids. *ASME 2011 conference smart materials, adaptive structures and inteligent systems*. 2011.

[53] IYENGAR, Vardarajan R and Alexander ALEXANDRIS. Wear Testing of Seals in Magneto-Rheological Fluids©. *Tribology Transactions*. 2004, vol. 47, no. 1, pp. 23–28. ISSN 1040-2004.

[54] HEIPL, Oliver and Hubertus MURRENHOFF. Friction of hydraulic rod seals at high velocities. *Tribiology International*. 2015, vol. 85, pp. 66–73. ISSN 0301-679X.

[55] LUN, Saiman. Dual seal rod guide assembly with low friction disc. 2010.

[56] A., Hart John. MR rod guide assembly and MR damper having same. 2009.

[57] *Dampers Show Flexibility in Retrofit of London's Millennium Bridge*. Available at: http://www.designworldonline.com/dampers-show-flexibility-in-retrofit-of-londons-millennium-bridge/

[58] *Witzenmann*. Available at: http://www.witzenmann.cz/cs/index.jsp

[59] *FerroTec company*. Available at: http://www.ferrotec.com.sg/ferrofluid.ferrotec/products/ferrofluid/vfFerrofluid.html

[60] MATUSZEWSKI, Leszek and Zbigniew SZYDŁO. The application of magnetic fluids in sealing nodes designed for operation in difficult conditions and in machines used in sea environment. 2008, vol. 15, no. 3, pp. 49–58. ISSN 12332585.

[61] KORDONSKI, W. I. and S. R. GORODKIN. Magnetorheological Fluid-Based Seal. *Journal of Intelligent Material Systems and Structures*. 1996, vol. 7, no. 5, pp. 569–572. ISSN 1045-389X.

[62] LLOYD H. DIXON, Jr. Eddy Current Losses in Transformer Windings and Circuit Wiring. In: . 2010.

[63] *Vacuum schmelze*. Available at: http://www.vacuumschmelze.de

[64] SHOKROLLAHI, H and K JANGHORBAN. Soft magnetic composite materials (SMCs). 2007, vol. 189, pp. 1–12.

[65] HOGANAS. *Material data_Somaloy*. Available at: https://www.hoganas.com/globalassets/media/sharepoint-documents/BrochuresanddatasheetsAllDocuments/SomaloyMaterialData_November_2016_1806HOG.pdf

[66] SCHOPPA, Andreas, Patrice DELARBRE, Elmar HOLZMANN and Maximilian SIGL. Magnetic Properties of Soft Magnetic Powder Composites at Higher Frequencies in Comparison with Electrical Steels. no date, pp. 3–7.

[67] DIPL, Nils Bornemann and Stefan TILLER. Soft Magnetic Composites (SMC) Sintered Soft Magnetic Materials. no date.

[68] *TDK Epcos*. Available at: https://en.tdk.eu/
[69] *Eddy curent*. Available at: https://en.wikipedia.org/wiki/Eddy_current
[70] *Transformer*. Available at: http://www.electronicshub.org/transformer-types/
[71] OLIVER, Michael L. and William C. KRUCKEMEYER. Magneto-rheological damping valve using laminated construction. 6,481,546. 2002. US.
[72] GOLINELLI, Nicola and Andrea SPAGGIARI. Design of a novel magnetorheological damper with internal pressure control. *Frattura et Integrita Strutturale*. 2015, vol. 32, pp. 13–23.
[73] NGUYEN, Q H, S B CHOI, Y S LEE and M S HAN. An analytical method for optimal design of MR valve structures. no date.
[74] YU, Chengbin Du and Faxue Wan and Guojun. A magnetic flux leakage study of a self-decoupling magnetorheological damper. *Smart Materials and Structures*. 2011, vol. 20, no. 6, p. 65019. ISSN 0964-1726.
[75] LIAO C.R, Zhao D. X. A design methodology for a magnetorheological fluid damper based on a multi-stage radial flow mode. no date.
[76] WANG, D. H. and W. H. LIAO. Magnetorheological Fluid Dampers: A Review of Parametric Modelling. *Smart Materials and Structures*. 2011, vol. 20, p. 23001. ISSN 0964-1726.
[77] YAZID, I I M, S A MAZLAN, T KIKUCHI, H ZAMZURI and F IMADUDDIN. Magnetic circuit optimization in designing Magnetorheological damper. *Smart Structures and Systems*. 2014, vol. 14, no. 5, pp. 869–881.
[78] GOLDASZ, Janusz. Electro-mechanical analysis of a magnetorheological damper with electrical steel laminations. 2013, no. 2, pp. 8–12.
[79] TAKESUE, N., J. FURUSHO and Y. KIYOTA. Analytic and experimental study on fast response MR-fluid actuator. *2003 IEEE International Conference on Robotics and Automation*. 2003.
[80] ZHENG, Jiajia, Yancheng LI, Zhaochun LI and Jiong WANG. Transient multi-physics analysis of a magnetorheological shock absorber with the inverse Jiles–Atherton hysteresis model. *Smart Materials and Structures*. 2015, vol. 24.
[81] CARLSON, J. D. What Makes a Good MR Fluid? *Journal of Intelligent Material Systems and Structures*. 2002, vol. 13, nos. 7–8, pp. 431–435. ISSN 1045-389X.
[82] FOISTER, Robert T., Thomas W. NEHL, William C. KRUCKEMEYER and Oliver RAYNAULD. Magnetorheological (mr) piston assembly with primary and secondary channels to improve mr damper force. 2009. Available at: http://www.google.tl/patents/US20110100775
[83] LISENKER, Ilya, Randall L. HOFMANN and Michael W. HURTT. Magnetorheological piston and damper assembly. 2005. Available at: http://www.google.com.sv/patents/US6874603
[84] STERNBERG, Alan, Ren?? ZEMP and Juan Carlos DE LA LLERA. Multiphysics behavior of a magneto-rheological damper and experimental validation. *Engineering Structures*. 2014, vol. 69, pp. 194–205. ISSN 01410296.
[85] ZEKERIYA, Parlak, Tahsin ENGIN and İsmail ÇALLI. Optimal design of MR damper via finite element analyses of fluid dynamic and magnetic field. *Mechatronics*. 2012, vol. 22, pp. 890–903.

[86] HU, Guoliang, Ming LONG, Ming HUANG and Weihua LI. Design , Analysis , Prototyping , and Experimental Evaluation of an Efficient Double Coil Magnetorheological Valve Design , Analysis , Prototyping , and Experimental Evaluation of an Efficient Double Coil Magnetorheological Valve. 2015, vol. 2014, no. AUGUST.

[87] GUO, C., X. GONG, L. ZONG, C. PENG and S. XUAN. Twin-tube- and bypass-containing magneto-rheological damper for use in railway vehicles. *Proceedings of the Institution of Mechanical Engineers, Part F: Journal of Rail and Rapid Transit*. 2013, vol. 229, no. 1, pp. 48–57. ISSN 0954-4097.

[88] LORD. *LORD Corporation*. Available at: http://www.lord.com/

[89] KUBÍK, M.; MACHÁČEK, O.; STRECKER, Z.; ROUPEC, J.;NOVÁK, P.; MAZUREK, I. Transient magnetic model of magnetorheological damper and its experimental verification. In: *The 4th International Conference on Mechantronics and Mechanical Engineering*. 2017.

[90] STRMISKA TOMÁŠ. *Návrh magnetického obvodu rychlého magnetoreologického tlumiče bez použití feritů*. B.m., 2017. Brno University of Technology.

[91] KUBÍK, Michal, Ondřej MACHÁČEK, Zbynek STRECKER, Jakub ROUPEC and Ivan MAZŮREK. Design and testing of magnetorheological valve with fast force response time and great dynamic force range. *Smart Materials and Structures*. 2017, vol. 26, no. 4.

[92] KUBÍK;, M. MACHÁČEK O.; STRECKER Z.; ROUPEC J.;MAZUREK I.; KOUTNY D.; PALOUŠEK D.; Struktura jádra obsahujícího pruty z feromagnetického materiálu a způsob jejího vytvoření. PV 2017-91. 2017. Czech Republic.

[93] KUBÍK, Michal and I. KUBÍK, M.; MACHÁČEK, O.; STRECKER, Z.; ROUPEC, J.; MAZUREK. Dynamic viscosity of commercially available magnetirheological fluids. In: *23nd International Conference on Engineering Mechanics*. 2017.

[94] KUBÍK, M.; MACHÁČEK, O.; STRECKER, Z.; ROUPEC, J.; MAZŮREK, I. Design and testing of magnetorheological valve with fast force response time and great dynamic force range. *Smart Materials and Structures*. 2017, vol. 26, no. 4, p. 47002. ISSN 0964-1726.

LIST OF FIGURES

ATTACHMENT 1 – THE GEOMETRY OT THE MR DAMPER

A design of tested MR damper is based on the Delphi MR damper. The tested MR damper is composed of outer tube (1), coil core (2), coil (3), flanges (4), piston rod (5), washer 10 (7), nut M10 (8), floating piston (9), seal Hennlich S16 (10) and Teflon guide (11). The flange (4) has 16 holes with diameter of 4 mm which allows for the MR fluid to flow to the active zone. The coil contains 120 turns.

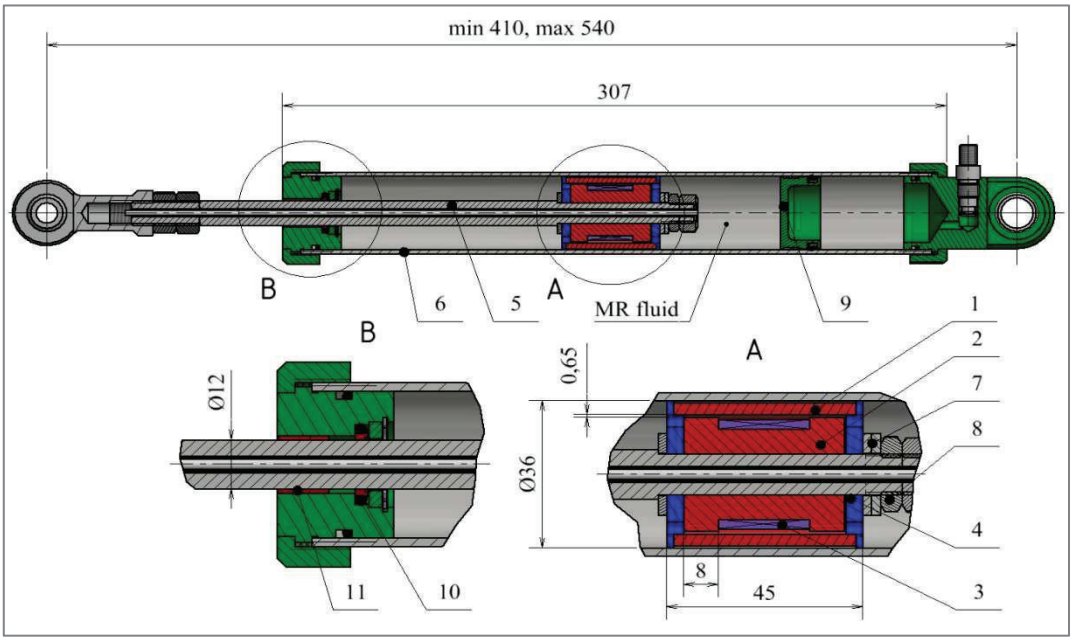

Figure 75 Geometry of MR damper; 11SMn30 (red), bronze (blue), carbon steel (gray), copper (purple).

The coil core (2) and the outer tube (1) were manufactured from 11SMn30 (red, Figure 75). The B-H curve of this material was experimentally determined. The flanges were manufactured from bronze because of its good sliding properties. The flanges guide the piston in the hydraulic tube. The piston rod and the hydraulic tube were manufactured from carbon steel with higher content of carbon than 11SMn30 due to the strength of this material (gray, Figure 75). The coil power supply is provided by the wire which is sealed in the hollows of piston rod (**Figure 76**).

Figure 76 The design of MR damper

ATTACHMENT 2 – EXPERIMENTAL MEASUREMENT OF THE B-H CURVE OF SELECTED LOW CARBON STEEL

A small difference in the chemical composition or machining influences the slope of B-H curve (relative permeability) and magnetic saturation. Each melt material of low carbon steel has a different B-H curve due to a different chemical composition. The available low carbon steels usable for the magnetic circuit of MR damper were tested. Low carbon steel 11 SMn30, S235JR+C and prure iron (Behanit) were tested.

A tested bar sample had a diameter of 10 mm and length of 100 mm. Five different samples were prepared (Tab. 3). Bar samples were tested in JHO (Figure 77). Magnetic flux intensity was measured with a tangencial Hall probe on the surface of tested sample. The experiment was carried out by ing. Zdeněk Roubal, Ph.D. at the Faculty of Electrical Engineering and Communication.

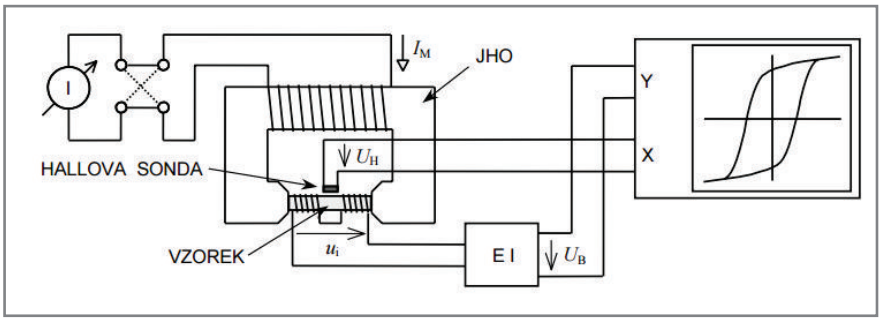

Figure 77 Methodology of measurement of B-H curve

The samples were tested up to the magnetic flux intensity of 4500 A/m. The measurement period was 40 seconds. A chemical composition and description of tested samples are listened in Tab. 3.

Tab. 3 Samples

Sample number	Material	%C	%Mn	%Si	%P	%S	Machining
1	11SMn30+C	0.1	1.21	0.04	0.056	0.283	Yes
2	11SMn30+C	0.1	1.18	0.03	0.035	0.297	No
3	S235JR+C	0.09	0.41	0.084	0.01	0.03	Yes
4	S235JR+C	0.13	0.52	0.099	0.007	0.012	No
5	Behanit	0.01	0.2	0.01	0.006	0.001	Yes

A comparison of the B-H curves of tested samples is given in Figure 78. The highest relative permeability was achieved with pure iron (sample 5_Behanit). The lowest relative permeability was achieved by the sample 4_ S235JR+C. The sample 4 had the highest content of carbon.

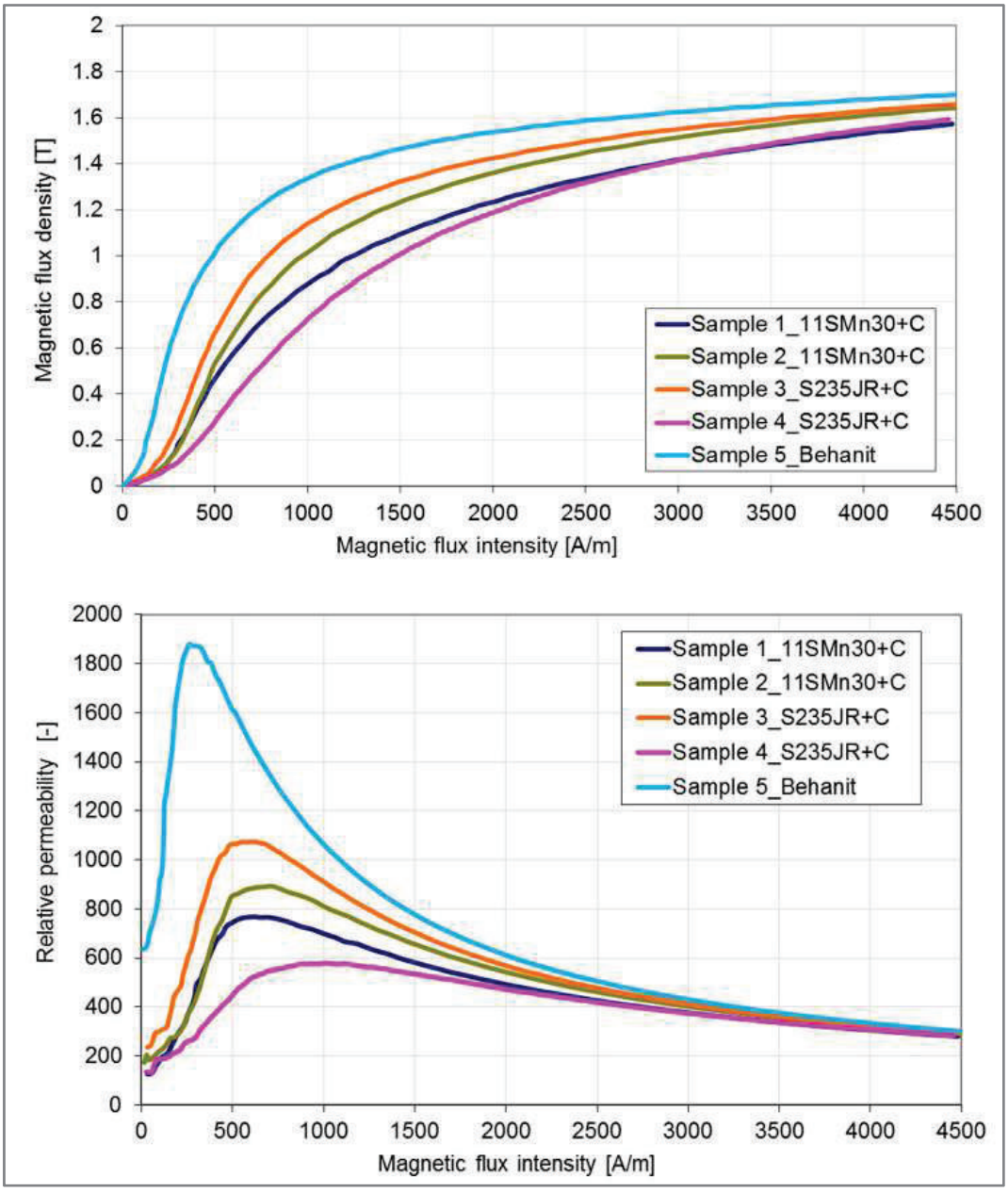

Figure 78 Experimentally measured the B-H curve of samples of low carbon steel

The influence of content of carbon in low carbon steel was tested (Figure 79). The higher the content of the carbon, the lower the relative permeability. However, the magnetic saturation is slightly different.

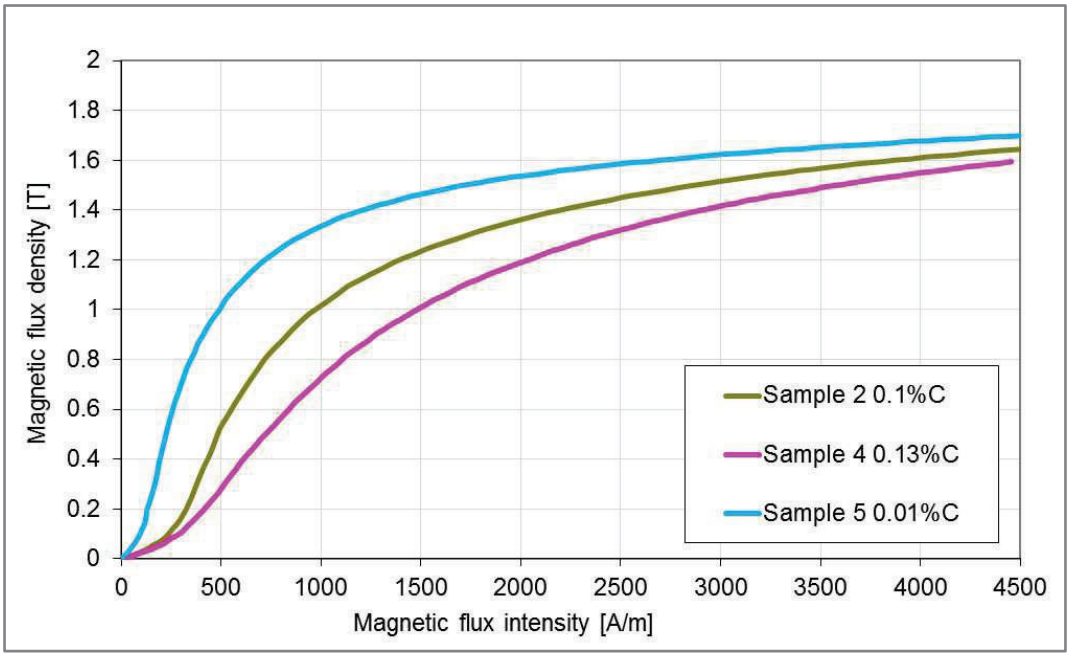

Figure 79 Influence of the content of carbon to the magnetic properties of low carbon steel

The influence of the machining on the magnetic properties was tested; machining has no influence on the initial relative permeability. However, with machining (heat treatment), the maximum relative permeability and the magnetic saturation are decreasing.

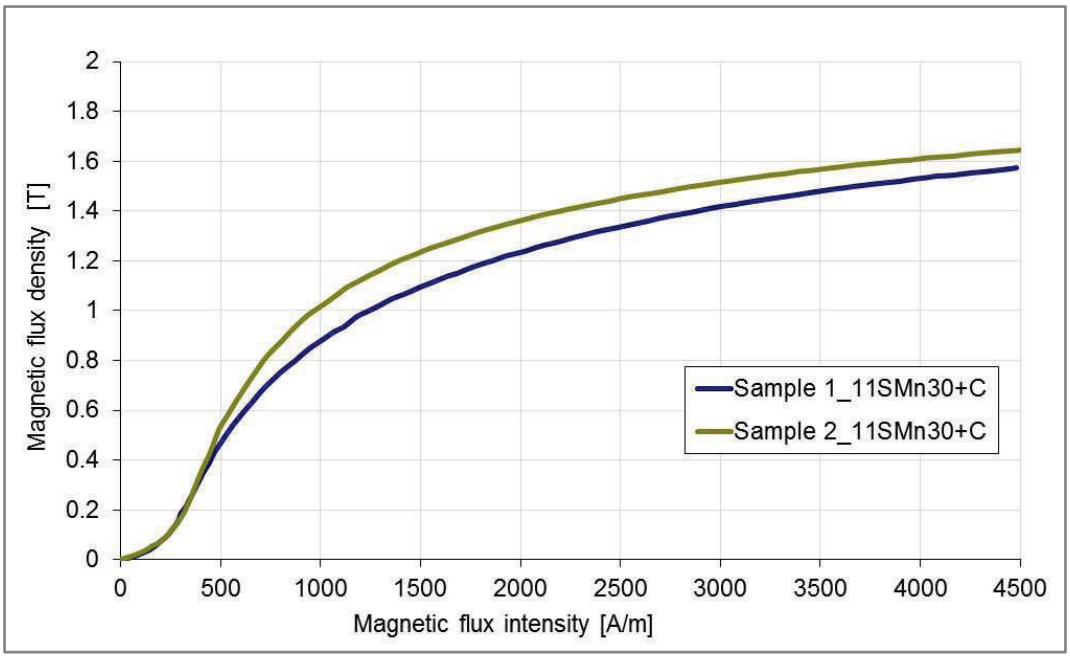

Figure 80 Influence of the machining of the magnetic properties of low carbon steel

These experiments provide the basic information on the changes of magnetic properties due to the chemical composition and machining. These data are not adequately described for the low carbon steel in the available literature.